

AN EPIDEMIOLOGICAL MODEL OF MALARIA ACCOUNTING FOR ASYMPTOMATIC CARRIERS

JACOB B. AGUILAR AND JUAN B. GUTIERREZ *

ABSTRACT. Asymptomatic individuals in the context of malarial disease refers to subjects who carry a parasite load but do not show clinical symptoms. A correct understanding of the influence of asymptomatic individuals on transmission dynamics will provide a comprehensive description of the complex interplay between the definitive host (female *Anopheles* mosquito), intermediate host (human) and agent (*Plasmodium* parasite). The goal of this article is to conduct a rigorous mathematical analysis of a new compartmentalized malaria model accounting for asymptomatic human hosts for the purpose of calculating the basic reproductive number (\mathcal{R}_0), and determining the bifurcations that might occur at the onset of disease free equilibrium. A point of departure of this model from others appearing in literature is that the asymptomatic compartment is decomposed into two mutually disjoint sub-compartments by making use of the naturally acquired immunity (NAI) of the population under consideration. After deriving the model, a qualitative analysis is carried out to classify the stability of the equilibria of the system. Our results show that the dynamical system is locally asymptotically stable provided that $\mathcal{R}_0 < 1$. However this stability is not global, owing to the occurrence of a sub-critical bifurcation in which additional non-trivial sub-threshold equilibrium solutions appear in response to a specified parameter being perturbed. To ensure that the model does not undergo a backward bifurcation, we demand that an auxiliary parameter denoted $\Lambda < 1$ in addition to the threshold constraint $\mathcal{R}_0 < 1$. The authors hope that this qualitative analysis will fill in the gaps of what is currently known about asymptomatic malaria and aid in designing strategies that assist the further development of malaria control and eradication efforts.

Dedicated to my mother Jacqueline Donna

1. INTRODUCTION

Malaria is one of the most lethal and complex parasitic diseases in the world [48]. Throughout human history, malaria has burdened most regions of our planet and has had a profound impact in human history and evolution; e.g. it has been credited for contributing to the decline of the Roman Empire [53, p. 14]. In 2015, the World Health Organization (WHO) reported the occurrence of approximately 214 million new cases of malaria (range: 149–303 million), which resulted in 438 thousand disease-induced deaths (range: 236–635 thousand) [48]. It was estimated that 70% of these fatalities were experienced by children under the age of five.

The life-cycle of the *Plasmodium* parasite can be broken down into two separate subcycles: the asexual cycle, occurring in humans (intermediate host) and the sexual cycle in mosquitoes (definitive host), in which maturity is reached. The **sexual cycle** begins when a susceptible mosquito feeds on the blood of an infectious human, ingesting sexual forms of the *Plasmodium* parasite previously developed in the human body, known as *gametocytes*. While in the midgut lumen of the mosquito, these *gametocytes* fuse to form diploid *zygotes*, which grow into elongated *ookinetes*. The motile *ookinetes* burrow into the outer membrane of the mosquito midgut and form ellipsoid shaped *oocysts*. Eventually, the *oocysts* rupture releasing thousands of haploid forms called *sporozoites* [52]. These *sporozoites* accumulate in the salivary glands of the mosquito, causing it to become infectious.

The **asexual cycle** begins when an infectious mosquito bites the host and injects saliva with anti-coagulant agents that keep the wound open thus allowing a blood meal, and simultaneously injecting *sporozoites* into the skin [16]. The *sporozoites* travel through the blood vascular system to the liver where they invade the cells of the liver, known as *hepatocytes*. Inside the human, a *Plasmodium* infection goes through two cycles: a initial liver (hepatic, or exo-erythrocytic) stage lasting a few days, followed by a blood (erythrocytic) stage that lasts until the hosts clears naturally the infections, receives treatment, or dies. The **hepatic stage** begins in the *hepatocytes*, where a proportion of the *sporozoites* undergo a process called *pre-erythrocytic or hepatic schizogony*, in which they multiply asexually to produce thousands of haploid daughter cells, known as *merozoites*. During

* JGUTIERR@UGA.EDU

this process, *schizonts* are formed, causing the *hepatocytes* to rupture. This allows the *merozoites* to enter the bloodstream. The **erythrocytic stage** begins when free-floating *merozoites* invade *erythrocytes* in a matter of minutes. Inside the *erythrocyte*, parasites enter the ring stage in which some mutate into an enlarged ring-shaped form called *trophozoites* that mature into *schizonts*, causing the cell to burst and releasing more *merozoites* into the bloodstream. In the case of *P. falciparum*, this process of invasion and rupture of RBCs occurs synchronously every 48 hours. At this point in the subcycle, a small portion of the *merozoites*, for reasons currently unknown, morph into *gametocytes*, or sexual forms; however, no sexual reproduction occurs inside the host [14].

The infected human host is now ready to infect new susceptible mosquitos, thus completing the *Plasmodium* life cycle. It is worth mentioning that the blood stage parasites are responsible for most clinical symptoms associated with the disease [14]. The periodic rupturing of the RBCs results in the release of various debris and waste products, which in turn activate the immune system and cause symptoms such as chills, fatigue, pain, and fever. The average duration for the infection of an RBC is dependent on the *Plasmodium* species. *P. falciparum* has the interesting pathological effect of sequestration, which occurs when infected RBCs containing mature forms of the parasite, i.e. *trophozoites* and *schizonts*, adhere to the walls of small diameter blood vessels, e.g. the endothelium of capillaries and venules [20]. As a result of sequestration, the microcirculation is reduced and in some cases inflammatory processes take place. One of the common complications of this sequestration is cerebral malaria, which might cause patients to sustain brain injury resulting in long-term neuro-cognitive impairment [44].

A human host is called asymptomatic when it is a carrier for the *Plasmodium* parasite, but displays no clinical symptoms. Asymptomatic carriers contribute to *gamete* circulation by providing a hidden reservoir for the parasite to take refuge. As pointed out in [38, 2012], asymptomatic infections often go undetected, resulting in a major source of *gametocytes* for local mosquito vectors. Accordingly, asymptomatic carriers contribute to the persistence of malaria transmission within their localized populations [6]. Frequent exposure to the *Plasmodium* parasites leads to naturally acquired immunity to the symptoms of the disease, but not necessarily to the parasite and as a result it creates asymptomatic carriers in a given population [61]. Asymptomatic malaria infections have been reported in various high and intermediate transmission areas, such as Kenya and Nigeria [6, 25]. Recently, asymptomatic infections have been reported in relatively low endemic areas, such as Colombia and the Amazonian region of Brazil [15, 18]. There is much evidence that asymptomatic malaria infections play a fundamental role in malaria transmission, cf. [42]. Disease transmission dynamics are greatly affected by the amount of asymptomatic carriers in a given population over a specified time interval. Indeed, a positive correlation between high transmission and high asymptomatic prevalence has been reported in Nigeria, Senegal, Gabon and the Amazonian regions of Brazil [4, 19, 21, 25].

In accordance with [8, 1980], we define malaria immunity as the state of resistance to the infection brought about by all processes which are involved in destroying the plasmodia or limiting their multiplication. *Natural innate immunity* is an intrinsic property of the host. This type of immunity is characterized by an immediate inhibitory response to the introduction of the parasite which is independent of any previous infection. There are two types of acquired immunity, namely: *active acquired immunity* and *passive acquired immunity*. *Active acquired immunity* is defined as an enhancement of the host's defense mechanism due to previous contact with the pathogen. *Passive acquired immunity* is characterized by either the mother to child transfer of protective antibodies in the pre or post natal developmental periods or by the injection of such antibodies. In this work we are focused on *Active acquired immunity*, more specifically a type of immunity that is acquired through means of exposure.

Humans experience various kinds of *Active acquired immunity* which provide different kinds of protection. Making use of the definitions in [23, 2009], we define protection to be objective evidence of a lower risk of clinical disease, indicated by the absence of fever, i.e. the oral temperature does not exceed the threshold 37°C [13], with parasitemia. *Anti-disease immunity* is conferred protection against clinical disease; which affects the overall risk and extent of morbidity associated with a given parasite density. *Anti-parasite immunity* is conferred protection against parasitemia; which affects the parasite density. *Premunition* provides protection against new infections by maintaining a generally asymptomatic parasitemia, [35, 36, 54]. In this article, we make use of a kind of *premunition* called naturally acquired immunity (NAI). In holoendemic regions across sub-Saharan Africa most people are continuously infected by *P. falciparum* while the majority of infected adults rarely experience observable disease. As reported in [23, 2009], this valid protection against infection is NAI corresponding to *P. falciparum*.

Mathematical models of malaria transmission have been studied by various authors, for a survey we refer the reader to [45, 2011]. Asymptomatic malaria has also been previously modeled and studied. Filipe et al. [28, 2007]

presented an asymptomatic malaria model that was formed by inserting a state-invariant control parameter ϕ which stands for the proportion of human infections that develop disease. After letting $1/h$ denote the mean latent period in humans, they proceeded to define the progression rates from the exposed to the symptomatic and asymptomatic classes to be the products $h\phi$ and $h(1-\phi)$, respectively. Additionally, asymptomatic humans were included in the recovered compartment.

In this article we depart from the previous models of asymptomatic malaria by creating explicitly different compartments for symptomatic (Y) and asymptomatic (A) subjects, which in addition to susceptibles (S), exposed (E), and recovered (R) yields the acronym *SEYAR*. Another important point of departure with respect to previous models of asymptomatic malaria is that in the *SEYAR* model the progression rates (4) to symptomatic and asymptomatic are nonlinear functions of the time-dependent exposed proportion. Therefore, the *SEYAR* model does not fall into a sub-class of such models currently appearing in literature. Moreover, we do not include the asymptomatic humans in the recovered compartment. This allows an effective isolation of the effect that asymptomatic carriers have on the disease transmission dynamics. The derivation of the *SEYAR* model (4) hinges on a specific decomposition of the infected human compartment into two mutually disjoint sub-compartments accounting for asymptomatic and symptomatic carriers. This decomposition is accomplished by making use of a nonlinear exposure dependent NAI function, which is the solution to the initial-value problem (1) derived in Section 2. Although there is much in the literature, the proper inclusion of asymptomatic carriers into the epidemiological modeling of malaria warrants a formal mathematical understanding.

This manuscript provides a new malarial model accounting for asymptomatic human hosts in terms of the NAI of the population under consideration and is organized as follows: Section 1 presents a summary of the state of the art, Section 2 presents the model formulation, Section 3.1 covers the issue of well-posedness of the initial value problem and provides an analysis of the total population dynamics, Section 3.2 contains a rigorous study of the local asymptotic stability of disease-free equilibrium (DFE) for the model with a mathematical and epidemiological interpretation of the reproductive threshold, Section 3.3 introduces a mathematical framework to formally address the impact of the asymptomatic class on the reproductive threshold, Section 3.4 is focused on nonlinear stability analysis and provides a classification parameter in which its size determines the type of bifurcation undergone by the dynamical system, Section 4.1 provides a unified derivation of many static quantities widely used in malaria epidemiology, Section 4.2 incorporates generalized control measures into the dynamical system, Section 4.3 introduces a modification of the model including relapse rates, Section 5.1 is focused on a sensitivity analysis of the reproductive threshold arising from the model, Section 5.2 consists of numerical results corresponding to the following three high transmission sites: Kaduna in Nigeria, Namawala in Tanzania, and Butelgut in Papua New Guinea, Section 6 consists of a summary of the results contained in Sections 2-5.2 and a discussion regarding future direction and extensions, Section 7 contains formal proofs of the lemmas and theorems contained in Sections 2-4.2, Section 7.5 is a summary of the main stability theorems used in the investigation of the local asymptotic stability of the equilibrium solutions studied in Sections 3.2 and 3.4, and Section 7.6 contains tables of numerical rates corresponding to the high transmission sites studied in Section 5.2.

2. METHODS: MODEL FORMULATION

The formulation of the *SEYAR* model for the spread of malaria in the human and mosquito populations begins with dividing the total host-vector population into two compartments, denoted by $N_H(t)$ and $N_M(t)$, which stand for the total population sizes of the humans and mosquitoes, respectively, at a given time t . From this point on, whenever implied by the context of the discussion, the time t dependency is suppressed to avoid a cluttering of the notation. Assuming a homogeneously mixed host population, we further decompose the compartments into the following five epidemiological classes: susceptible human S , exposed human E , symptomatic human Y , asymptomatic human A , and recovered human R . So that, $N_H = S + E + Y + A + R$. For simplicity of exposition the state variable is identified with its corresponding class. For example, when we are considering a human from class A , it is understood that A is a function and not a class, in general. A point of departure from the usual *SEIR* models, as studied in [22, 40, 41, 51, 59], resides in the mutually disjoint partitioning of the infected compartment into two sub-compartments, labeled asymptomatic A and symptomatic Y , i.e. $I = Y \cup A$ where $Y \cap A = \emptyset$. For the mosquito population we have the following three classes: susceptible mosquito M_S , exposed mosquito M_E and infected mosquito M_I . Accordingly, the total mosquito population is given by $N_M = M_S + M_E + M_I$.

A fundamental step in the accurate modeling of any infectious disease resides in the formulation for the force of infection, i.e. the probability per unit time for a susceptible to become infected. As mentioned in [28], it is

known that the infection rates between human and mosquito populations depend on numerous factors, including: the man-biting rate of the mosquito σ (which is the number of bites per mosquito), transmission probabilities (to be later defined), and the number of infectious and susceptible of each species involved. Furthermore, we assume that the average number of mosquito bites suffered by humans depends on the total sizes of their respective populations in the community. As a result, the number of bites per human is $\sigma \frac{N_M}{N_H}$. Therefore, the force of infection from mosquitoes to humans λ_{SE} is defined to be the product of the number of bites per human, the transmission probability β_M from a mosquito in the class M_I to a human in class S and the probability that a mosquito is infectious $\frac{M_I}{N_M}$, i.e.

$$\lambda_{SE} = \omega_M = \sigma \frac{N_M}{N_H} \beta_M \frac{M_I}{N_M} = \sigma \beta_M \frac{M_I}{N_H}.$$

Although asymptomatic carriers do not get clinically ill, they still harbor low levels of *gametocytes* in their bloodstreams and are able to pass the infection onto mosquitoes, [64]. When a mosquito from class M_S bites a human from class Y , the force of infection ω_Y is defined as the product of the number of bites per mosquito σ , the transmission probability β_Y from a human in Y to a mosquito in M_S and the probability that a human is in the symptomatic class $\frac{Y}{N_H}$. When a mosquito from the class M_S bites a human from class A , the corresponding force of infection ω_A is the product of the number of bites per mosquito σ , the transmission probability β_A from a human in A to a mosquito in M_S and the probability that a human is in the asymptomatic class $\frac{A}{N_H}$. As pointed out in [37], the parasites carried by asymptomatic hosts can be more infectious than those of symptomatic hosts. One could assume that a typical asymptomatic carrier has a higher NAI level than a symptomatic, so that $\beta_A \leq \beta_Y$, or visa versa. However, from a mathematical standpoint this assumption is unnecessary and will not be made. Accordingly, the force of infection from humans to mosquitoes ν_{SE} is defined to be the sum of the forces of infection corresponding to the humans in classes Y and A , i.e.

$$\nu_{SE} = \omega_Y + \omega_A = \sigma \left(\beta_Y \frac{Y}{N_H} + \beta_A \frac{A}{N_H} \right).$$

Let $\nu_{EI} = \tau$, where τ is the mean duration of the definite host latent period, i.e. the reciprocal of the *Plasmodium* incubation period corresponding to mosquito species being studied.

Remark 2.1. *It is worth pointing out that the progression rate ν_{SE} is equal to the sum of the human to mosquito infection forces ω_Y and ω_A , while λ_{SE} is equal to the singular force of infection from mosquitoes to humans, denoted as ω_M . The decomposition of the human infected compartment results in two different infection forces corresponding to the asymptomatic and symptomatic carriers. However, no decomposition is applied for the infected mosquito compartment.*

At a given time $t \in \mathbb{R}_+$ an individual's experience of malaria is dependent upon the degree of naturally acquired immunity that he or she has gained. Effective anti-parasitic immunity is achieved only after many frequent infections, [10, 32, 43]. This important epidemiological observation, in combination with the discussion regarding naturally acquired immunity (NAI) in Section (1), implies that the rate of progression λ_{EA} from the exposed class E to asymptomatic class A depends on the proportion of human individuals receiving sufficient protection from the average NAI accumulated in the population with respect to natural exposure. Let $u(t)$ denote the proportion of the human population fully protected by NAI. Since naturally acquired immunity to the *Plasmodium* parasite is acquired and accumulates over time in response to frequent exposure. The rate that this proportion of protected individuals changes depends on the the rate that the human population is being exposed, up to a threshold value. To uncover this exposure dependency, firstly let the lower and upper protected proportion thresholds be given by u_{low} and u_{high} , respectively. It should be noted that $0 < u_{low} < u_{high} < 1$. An increase or decrease in the protected proportion u corresponds to an increase or decrease in the exposed proportion $\frac{E}{N_H}$. Let $\varepsilon := \frac{E}{N_H}$, upon assuming that the initial NAI protected proportion is given by the lower threshold $u(0) := u_{low}$, these epidemiological principles lead to the following initial value problem (IVP) being posed

$$(1) \quad \begin{cases} \dot{u} = (u_{high} - u)\dot{\varepsilon}, \\ u(0) = u_{low}. \end{cases}$$

By making use of the integrating factor $L = e^{\int_0^t \dot{\varepsilon}(s)ds} := e^\varepsilon$, it follows that

$$\begin{aligned} \dot{(Lu)} &= L\dot{\varepsilon}u_{high}, \\ Lu &= e^{\varepsilon_0}u_{low} + (L - e^{\varepsilon_0})u_{high}, \\ u &= L^{-1}e^{\varepsilon_0}u_{low} + (1 - L^{-1}e^{\varepsilon_0})u_{high}, \\ u &= e^{\varepsilon_0 - \varepsilon}u_{low} + (1 - e^{\varepsilon_0 - \varepsilon})u_{high}. \end{aligned}$$

Upon rearranging terms and invoking a slight abuse of notation, to emphasize the exposure ε dependency of u , the solution is represented by the following equation

$$(2) \quad u(\varepsilon) = e^{\varepsilon_0 - \varepsilon}(u_{low} - u_{high}) + u_{high}.$$

In the above, the symbol $\varepsilon_0 := \varepsilon(0)$ stands for the initial exposed proportion of the human host population. Care should be taken to ensure that the progression rate is mathematically well-defined and epidemiological sensible, i.e. a singularity should not arise and it should be non negative. Provided that \mathbf{x} is such that $\varepsilon \in C^1(\mathbb{R}_+)$, then clearly the progression rate will not experience a singularity. However, assuming that the initial exposed proportion is zero for some time t_0 , a subtle complication arises for existence times such that the human population is extinct, i.e. $N_H(t_0) = 0$. If the state variable E is positive, then clearly N_H is positive and thus non-zero, so ε will not undergo a singularity. However, in the case that E is zero for such existence times, then it is possible that N_H may simultaneously be equal to zero, thus forcing a singularity to arise. Therefore, the following piecewise function $\tilde{\varepsilon}$ is defined to remedy this subtle issue and ensure that the proportion of exposed humans is taken to be zero in the case that the human population is extinct

$$\tilde{\varepsilon} := \begin{cases} \frac{E}{N_H}, & \text{if } N_H \neq 0, \\ 0, & \text{if } N_H = 0. \end{cases}$$

Time dependency is implicit in the above function definition. It is worth emphasizing that the above function holds for any time (intervals or discrete values) such that $N_H = 0$. Mathematically speaking, if \mathbf{x} is such that $\varepsilon \notin C^1(\mathbb{R}_+)$, the only complication occurs for $t \in \mathbb{R}_+$ such that $N_H = E = 0$. In this case, a singularity arises in the composite function $u = (u \circ \varepsilon)$. In order to account for this, epidemiological unreasonable, minor issue, ε is extended to its infimum value by the above function definition. From this point on, an abuse of notation is invoked in which an identification of ε with its continuous extension is made. In other words, for all practical purposes, we take $\tilde{\varepsilon} = \varepsilon$.

Besides the trivial singularity issue covered above, care must be taken to ensure the non-negativity of the nonlinear progression rate u . As a result, the solution to the IVP (1) implicitly imposes an additional constraint upon the initial data of the *SEYAR* model (4). The constraint is listed below in lemma (1), which is proven in Appendix (7).

Theorem 2.1. *(Initial Data Constraint for the SEYAR Model)* Let ϑ be defined as follows

$$(3) \quad \vartheta := \ln \left(\frac{u_{high}}{u_{high} - u_{low}} \right).$$

To ensure the non-negativity of u , the initial data is required to satisfy the inequality $E_0 \leq \vartheta N_0$.

Let the eight dimensional vector of functions $\mathbf{x} = (S, E, Y, A, R, M_S, M_E, M_I)^T$ be such that $\varepsilon \in C^1(\mathbb{R}_+)$ and ϑ be defined as in Lemma (2.1) above. It directly follows that u is trapped in the compact sub-interval T_u , defined in Section 3.2. Therefore, the following bounds are established

$$\begin{aligned} \text{ess inf}_{t \in \mathbb{R}^+} \|u\| &= u_{low}, \\ \|u\|_\infty &= u_{high}. \end{aligned}$$

After placing all the above together, the nonlinear progression rate u is well-defined in a mathematical and epidemiological sense. It is worth mentioning that due to the constructive assumptions mentioned above, the vector of functions $(\varepsilon, u(\varepsilon))$ is trapped in the unit rectangle $(0, 1) \times (0, 1)$, for all $t \in \mathbb{R}_+$.

Define $\lambda_{EA} = \gamma u(\varepsilon)$ where γ is the mean duration of the human latent period, i.e. the time that elapses before the presence of a disease is manifested by symptoms. It is a direct consequence that $\lambda_{EY} = \gamma(1 - u(\varepsilon))$,

so that $\lambda_{EA} + \lambda_{EY} = \gamma$. Since the naturally acquired immune proportion will grow in response to exposure, the rate of progression from the exposed class E to asymptomatic class A should increase, warranting the choice of λ_{EA} . Furthermore, on time intervals such that the exposure rate increase without bound, i.e. $\varepsilon \rightarrow +\infty$, it follows that $u(\varepsilon) \rightarrow \|u\|_\infty := u_{high}$. In this case the progression rate $\lambda_{EA} = \gamma u_{high}$ is maximized. This is consistent with the observation that the average amount of asymptomatic human hosts in a population should increase after frequent exposure over a sufficient time period. When the exposed proportion is equal to zero over a prescribed time interval, it follows that $u = e^{\varepsilon_0}(u_{low} - u_{high}) + u_{high}$ over the interval. This quantity is a sum consisting of the upper threshold and a negative scaled difference of the lower and upper thresholds. If this infimum is achieved, then the progression rate λ_{EA} will be minimal. This is due to the fact that if there is little exposure, then there is little NAI developed in the population, so that the rate of progression from E to Y will be maximal, i.e. $\lambda_{EY} = \gamma(1 - \text{ess inf}_{t \in \mathbb{R}^+} \|u\|) = \gamma(1 - u_{low})$. Furthermore, the progression rate from E to Y should decrease to the smaller threshold value $\lambda_{EY} = \gamma(1 - \|u\|_\infty) = \gamma(1 - u_{high})$, as the exposure rate increases. Listed below is the flow diagram for the *SEYAR* model (4).

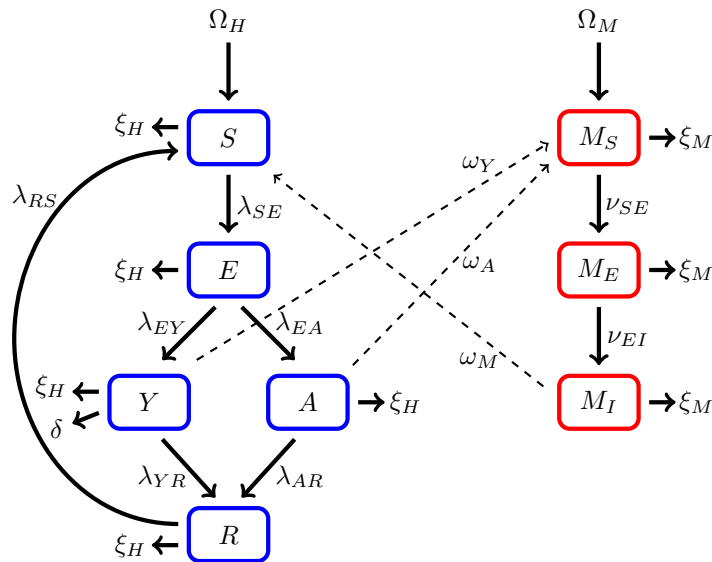


FIGURE 1. Schematic diagram of the malaria model including an asymptomatic compartment

In Figure 1, the solid lines represent progression from one compartment to the next, while the dotted stand for the human-mosquito interaction. Humans enter the susceptible compartment either through birth or migration and then progress through each additional compartment subject to the rates described above. These assumptions give rise to the following *SEYAR* model IVP (4) describing the dynamics of malaria disease transmission in the human and mosquito populations

$$\begin{cases} \dot{S} = \Omega_H + \lambda_{RS}R - \left(\sigma \beta_M \frac{M_I}{N_H} + \xi_H \right) S, \\ \dot{E} = \sigma \beta_M \frac{M_I}{N_H} S - (\gamma + \xi_H)E, \\ \dot{Y} = \gamma(1 - u(\varepsilon))E - (\xi_H + \delta + \lambda_{YR})Y, \\ \dot{A} = \gamma u(\varepsilon)E - (\lambda_{AR} + \xi_H)A, \\ \dot{R} = \lambda_{AR}A + \lambda_{YR}Y - (\lambda_{RS} + \xi_H)R, \\ \dot{M}_S = \Omega_M - \left(\xi_M + \sigma \beta_Y \frac{Y}{N_H} + \sigma \beta_A \frac{A}{N_H} \right) M_S, \\ \dot{M}_E = \sigma \left(\beta_Y \frac{Y}{N_H} + \beta_A \frac{A}{N_H} \right) M_S - (\xi_M + \tau) M_E, \\ \dot{M}_I = \tau M_E - \xi_M M_I, \\ (S_0, E_0, Y_0, A_0, R_0, M_{S_0}, M_{E_0}, M_{I_0})^T \in \mathbb{R}_+^8 \text{ such that } E_0 \leq \vartheta N_0, \end{cases}$$

where u and ϑ are defined by equations (2) and (3), respectively. For convenience, the model parameters are summarized in Table 1 below. All of the parameters are strictly positive, with exception for the disease induced death rate δ , which is allowed to be non-negative.

TABLE 1. Model Parameters

Parameter	Description	Dimension
Ω_H	Recruitment rate of humans	humans \times time $^{-1}$
Ω_M	Recruitment rate of mosquitoes	mosquitoes \times time $^{-1}$
ξ_H	Natural mortality rate of human	time $^{-1}$
ξ_M	Natural mortality rate of mosquito	time $^{-1}$
β_A	Probability of disease transmission from asymptomatic human to a susceptible mosquito	time $^{-1}$
β_Y	Probability of disease transmission from symptomatic human to a susceptible mosquito	time $^{-1}$
β_M	Probability of disease transmission from infected mosquito to susceptible human	time $^{-1}$
γ	The intermediate host mean latent period	time $^{-1}$
τ	The definitive host mean latent period	time $^{-1}$
δ	Disease-induced death rate for humans	time $^{-1}$
σ	Biting rate of mosquito	time $^{-1}$
λ_{AR}	Asymptomatic human recovery rate	time $^{-1}$
λ_{YR}	Symptomatic human recovery rate	time $^{-1}$
λ_{RS}	Temporary immunity loss rate in humans	time $^{-1}$
$u(\varepsilon)$	Exposure dependent NAI protected proportion	time $^{-1}$
u_{low}, u_{high}	Lower and upper NAI protected thresholds	time $^{-1}$

Remark 2.2. The parameter value labeled ϕ in Figure 6 on [28, p. 2575] corresponds to the term $(1 - u_{low})$ in the SEYAR model formulation, where the baseline value is assumed to be 0.5. The naturally acquired immune proportion will increase or decrease, depending on the rate that the human population is being exposed. Hypothetically, as the rate of exposure increases or decreases, this proportion should grow or shrink up to a threshold value. This epidemiological behavior is quantified by the solution to the IVP (1). Assuming $u_{low} = 0.5$, as above, and that it is possible for at most ninety percent of the population to acquire sufficient protection through means of natural exposure, i.e. $u_{high} = 0.9$. Then, the initial exposed proportion ε_0 can be assumed to take any value in the interval $\left[0, \ln\left(\frac{u_{high}}{u_{high} - u_{low}}\right)\right] = [0, \ln(\frac{9}{4})] \approx [0, 0.81]$. In other words, one can assume at most 81% of the human population to be initially exposed. On the other hand, if one modifies the above assumptions so that the initial naturally acquired immune proportion is $u_{low} = 0.5$, then $\varepsilon_0 \in [0, \ln(\frac{9}{8})] \approx [0, 0.12]$, so that at most 12% of the human population can be assumed to be initially exposed.

3. MODEL ANALYSIS

3.1. Well-Posedness and Feasible Region. Although assuming that $\Phi \in C^1$ provides sufficient regularity to ensure that system (4) is well-posed, this work is primarily concerned with the stability of the system near equilibrium points. This requires additional regularity assumptions on the vector field Φ in order to invoke a variation of the Center Manifold Theorem, cf. [11]. Consequently, from now on it is necessary to assume that $\Phi \in C^2 \subset C^1$, i.e. it is at least twice-continuously differentiable. Moreover, to be reasonable in an epidemiological sense, the functions under consideration should possess a bounded first derivative, i.e. they should be members of the class $C_b^1(\mathbb{R}_+)$. From this point on, the model is studied in the more regular (smaller) function space $C^2(\mathbb{R}_+^8) \cap C_b^1(\mathbb{R}_+^8)$. In light of the mathematical and epidemiological well-posedness of the IVP (1) and structure of the underlying vector field, the additional C^2 regularity will be inherited by the solution \mathbf{x} .

To this end, let $\mathbf{x} = (S, E, Y, A, R, M_S, M_E, M_I)^T$, so that x_i is the i^{th} component of the 8-dimensional vector $\mathbf{x} \in C^2(\mathbb{R}_+^8) \cap C_b^1(\mathbb{R}_+^8)$ and rewrite (4) in the following compact form:

$$(4) \quad \begin{cases} \dot{\mathbf{x}}(t) = \Phi(\mathbf{x}(t)), \\ \mathbf{x}(0) = \mathbf{x}_0. \end{cases}$$

Theorem 3.1 (Existence Theory of the SEYAR Model). *There exists a sufficiently regular unique solution \mathbf{x} to the SEYAR model IVP (4) that can be continued to a maximal time interval. Additionally, \mathbf{x} depends continuously on the initial data \mathbf{x}_0 and model parameters involved.*

The dynamics of the total population are given by the following decoupled system

$$(5) \quad \begin{cases} \dot{N}_H = \Omega_H - \xi_H N_H - \delta Y, \\ \dot{N}_M = \Omega_M - \xi_M N_M. \end{cases}$$

Due to the non-homogeneous term δY , the asymptotic behavior of the human population is more delicate. For the human population, we have the following theorem which provides a tighter lower bound on the attracting region for the model. In the absence of infection, the long-time behavior of N_H is trivial, i.e. the total human population converges to the equilibrium population density, as in the mosquito population. In the case of an infectious disease, one would expect the population to converge to a smaller quantity, as there is a disease induced death rate δ adding to the natural death rate ξ_H . In this case, the long-time population size will be smaller, as it has to account for the additional disease-induced deaths suffered by symptomatic individuals. Listed below is the theorem concerning the feasible region of model (4).

Theorem 3.2. (Feasible Region of the SEYAR Model) *Let (N_H, N_M) be the solution of system (5) emanating from Theorem 3.1, with corresponding initial data $(N_H(0), N_M(0)) \geq 0$. Define the following compact sub-space*

$$\Gamma := \left\{ \mathbf{x} \in C^2(\mathbb{R}_+^8) \cap C_b^1(\mathbb{R}_+^8) : N_H \in \left[\frac{\Omega_H - \delta \|Y\|_\infty}{\xi_H}, \frac{\Omega_H}{\xi_H} \right], N_M = \frac{\Omega_M}{\xi_M} \right\}.$$

Then, Γ is a forward invariant attractor for system (5).

Mathematically speaking, Theorem (3.2) reduces the complexity of the analysis involved regarding the long-term dynamics of the system by allowing the replacement of a potentially unbounded (epidemiologically unreasonable) space with the smaller (epidemiologically reasonable) compact sub-space Γ . If we let $L_t = e^{\xi_H t}$ denote an exponential multiplier, then the solution for the total dynamics of the human population is given by

$$N_H(t) = L_{-t} N_H(0) + \frac{\Omega_H}{\xi_H} (1 - L_{-t}) - \delta L_{-t} * Y(t).$$

The instantaneous rate of occurrence of death, i.e. the force of mortality ξ_H is assumed to be constant. As a result, the probabilities of living and dying up to t days are given by $e^{-\xi_H t}$ and $(1 - e^{-\xi_H t})$, respectively. Assuming that $N_H(0) = 0$, the above solution says that the total population $N_H(t)$ at time t is given by the weighted product of the carrying capacity $\frac{\Omega_H}{\xi_H}$ and the distribution of humans that are left after those that have died due to natural causes $(1 - e^{-\xi_H t})$, minus a weighted average of humans that have died due to symptomatic infections. The later quantity is captured by the non-homogeneous forcing term $-\delta L_{-t} * Y(t)$, given by a convolution with the inverse multiplier. Since convolution is a smoothing operation, this emphasizes the fact that we are subtracting a "smoothing average" over past time of the humans which have died from symptomatic infections. A straight-forward calculation yields the following differential inequality

$$\dot{N}_H \leq 0, \quad \text{if } N_H \geq \frac{\Omega_H}{\xi_H}.$$

From an epidemiological view point, the above inequalities imply that if the total population N_H breaches its carrying capacity, then the weighted average of fatal symptomatic infections must increase to stabilize the population back to a healthy level.

Remark 3.1. (Tighter Lower Bound on the Feasible Region) *The main feature of the above analysis is that it provides a tighter lower bound for the feasible region corresponding to the dynamical system. In an epidemiological setting, one can define the term $\delta \|Y\|_\infty$ to be the maximum disease-impact on the human population. In previous variants of malaria models appearing in literature, e.g. SIR, SIER, SIERS, etc., the quantity 0 is listed as the lower bound, however this is unreasonable since the populations under consideration usually do not go extinct, unless $\Omega_H = \delta \|Y\|_\infty$. If the maximum impact the disease is capable of having on the population is less than the recruitment rate, then their will always be accumulation over long-time. For other members of the SIR model class, the lower bound would be the same except with Y replaced by I . In the case of an infectious disease, there will be additional disease induced deaths, so that the total human population will not converge to the equilibrium population density. In reality, the total human population will converge to a quantity trapped in the interval $\left(\frac{\Omega_H - \delta \|Y\|_\infty}{\xi_H}, \frac{\Omega_H}{\xi_H} \right)$.*

3.2. Reproductive Threshold and Disease-Free Equilibrium. This section is focused on deriving a threshold value that characterizes the stability of the underlying dynamical system (4). This value, called the reproductive threshold, provides a way to estimate the reduction in transmission intensity required to eliminate malaria through vector-based control [58]. The basic reproductive number \mathcal{R}_0 corresponding to a given model is a threshold value which represents the average amount of new infections produced by a typical infectious individual in a completely susceptible population, at a disease-free equilibrium. This quantity is equal to the reproductive threshold for a class of simplified population models. However, in the case of more complicated dynamical systems \mathcal{R}_0 is a threshold which determines whether the disease will eventually, over long time, die out or persist and become an epidemic. Thus, in theory this threshold value does not necessarily represent the average number of secondary infections in a given population. This fact does not undermine the extreme importance of this threshold, as we will see that the size of this particular value has grave repercussions for the region under consideration.

Disease-Free Equilibrium (DFE) points are solutions of a dynamical system corresponding to the case where no disease is present in the population. Define the diseased classes to be E, Y, A, M_E and M_I . Notice that R is not considered to be a diseased class, as the asymptomatic class A has been effectively removed, cf. [51]. As a result, individuals in the R compartment are considered to be temporarily immune but not infectious. After determining the DFE of system (4), this threshold value is used to address its local asymptotic stability. Upon equating the right-hand side of (4) to zero and solving, we arrive at the following unique DFE

$$\mathbf{x}_{dfe} = \left(\frac{\Omega_H}{\xi_H}, 0, 0, 0, 0, \frac{\Omega_M}{\xi_M}, 0, 0 \right)^T.$$

Lemma 1. (Local Asymptotic Stability of the DFE for the SEYAR Model) Define the following quantity

$$(6) \quad \mathcal{R}_0 := \sqrt{\frac{\sigma^2 \tau \gamma \Omega_M \xi_H \beta_M}{\xi_M^2 (\gamma + \xi_H) (\tau + \xi_M) \Omega_H} \left(\frac{\beta_A U_{low}}{\lambda_{AR} + \xi_H} - \frac{\beta_Y (U_{low} - 1)}{\lambda_{YR} + \xi_H + \delta} \right)},$$

where $U_{low} := e^{\varepsilon_0} (u_{low} - u_{high}) + u_{high}$. Then, the DFE \mathbf{x}_{dfe} for the SEYAR model (4) is locally asymptotically stable provided that $\mathcal{R}_0 < 1$ and unstable if $\mathcal{R}_0 > 1$.

Lemma (1) is proven by utilizing the next generation method covered in [63]. The threshold value (6) has major epidemiological implications on the underlying dynamical system (4). To gain a deeper insight into the qualitative information encoded in this important quantity, we decompose it in the form of an epidemiological meaningful product in order to analyze each factors contribution

$$\begin{aligned} \mathcal{R}_0 &= \sigma \sqrt{\frac{\Omega_M}{\Omega_H}} \sqrt{\frac{\tau}{\tau + \xi_M}} \sqrt{\frac{\gamma}{\gamma + \xi_H}} \sqrt{\frac{\xi_H}{\xi_M}} \sqrt{\frac{\beta_M}{\xi_M}} \sqrt{\frac{\beta_A U_{low}}{\lambda_{AR} + \xi_H} - \frac{\beta_Y (U_{low} - 1)}{\lambda_{YR} + \xi_H + \delta}}, \\ &:= \sigma \prod_{i=1}^6 \sqrt{r_i}. \end{aligned}$$

Due to the above lemma and in an epidemiological setting it is desirable to have the reproductive threshold below unity. Listed below is the size contribution and biological description for each of the factors. The first factor is σ , which stands for the man-biting rate. This factor is usually much less than unity due to the fact that female anopheline mosquitoes generally transmit fewer than 100 sporozoites per bite, [50]. As malaria is a mosquito borne disease, the agent *Plasmodium* will spread at a much slower rate provided less vectors are introducing it into human hosts. Owning to the monotonicity of the square root function, it is sufficient focus on the size of each r_i .

- i The term $r_1 = \frac{\Omega_M}{\Omega_H}$ is the ratio of the mosquito and human recruitment rates. Clearly, this quotient is greater than unity due to fact that in any given population there will be more mosquitoes than human hosts. As the human and mosquito recruitment rates rank high on the sensitivity hierarchy of many epidemic models appearing in the literature, it is no surprise that this term is problematic with respect to the overall size of the threshold.
- ii The term $r_2 = \frac{\tau}{\tau + \xi_M}$ is the mosquito latent period τ divided by itself plus the mosquito mortality rate ξ_M . This quantity is bounded above by one and is monotonically decreasing with respect to ξ_M . It follows that larger the mosquito death rate is, the smaller r_2 will be.

- iii The first fully human-dependent term $r_3 = \frac{\gamma}{\gamma + \xi_H}$, is comprised of the human latent γ period divided by itself plus the human mortality rate ξ_H . As in the case of r_2 , this quantity is always less than one and monotonically decreases with respect to the human mortality rate. This is consistent with the fact that the fewer hosts there are for the parasite to invade, the less infectives will arise. However, since increasing ξ_H is not practical, this term offers no control over \mathcal{R}_0 .
- iv The term $r_4 = \frac{\xi_H}{\xi_M}$ is the ratio of the human and mosquito death rates. This particular quantity is always less than one as the mosquito death rate is much higher than the human death rate.
- v The term $r_5 = \frac{\beta_M}{\xi_M}$ is the ratio of the mosquito to human transmission probability β_M and the mortality rate of the mosquito population ξ_M . This quantity will be less than one provided $\beta_M < \xi_M$, i.e. the transmission probability is less than the death rate. In the case of a population with a relatively high vector transmission probability, then the vector death rate must be large enough to make r_5 less than one. This implies a restriction on the size of β_M . It will be shown in Section 3.4 that if β_M breaches a certain threshold, then sub-threshold endemic equilibria can emerge.
- vi The second fully human-dependent term is given by the following equation

$$r_6 = \frac{\beta_A U_{low}}{\lambda_{AR} + \xi_H} - \frac{\beta_Y (U_{low} - 1)}{\lambda_{YR} + \xi_H + \delta}.$$

The quantity, r_6 is a difference of ratios consisting of asymptomatic and symptomatic vital dynamics, along with transmission, recovery and disease-induced death rates; weighted with a distribution consisting of the lower and upper NAI-rate threshold of the human population scaled by an exponentiation of the initial exposure rate. For simplicity of exposition, we assume that the initial exposed proportion is zero, i.e. $\varepsilon_0 = 0$, so that $U_{low} = u_{low}$. If the initial exposed proportion is not equal to zero, then initially, $U_{low} < u_{low}$ and the reproductive threshold will be larger under parameter configurations to be specified shortly. Under such a configuration, upon initial exposure there will be more symptomatic individuals, but as exposure increases, less humans will die as naturally acquired immunity will begin to develop in the overall population. However, the following discussion is unaffected by this minor detail. As a result, the human-dependent factor is taken to be

$$r_6 = \frac{u_{low} \beta_A}{\lambda_{AR} + \xi_H} - \frac{(u_{low} - 1) \beta_Y}{\lambda_{YR} + \xi_H + \delta}.$$

Denote the low and high thresholds be such that $u_{low} > 0$ and $u_{high} < 1$, respectively and define the following compact sub-interval $T_u := [u_{low}, u_{high}] \subset (0, 1)$ consisting of various NAI protected proportions corresponding to a given population. When subjected to a certain parameter restriction, the sizes of the quantities $u_{low} = u(0)$ and r_6 are inversely related, i.e. the larger u_{low} is, the smaller r_6 will be; resulting in a relatively smaller \mathcal{R}_0 . Hence, an additional way to control the size of \mathcal{R}_0 arises, provided the parameters are such that this inequality restriction, to be mentioned below, holds. However, as we will see, if the parameters are such that this inequality reversed, then they are directly related.

Let $C_0 := \sigma \prod_{i=1}^5 \sqrt{r_i}$, $C_1 := \frac{\beta_A}{\lambda_{AR} + \xi_H}$ and $C_2 := \frac{\beta_Y}{\lambda_{YR} + \xi_H + \delta}$ and define $T \subset \mathbb{R}^+ \cup \{+\infty\}$ to be an ordered subset of the non-negative extended real numbers. In addition, let u solve equation (2) and denote $\{u(t) \in T_u | t \in T\}$ to be the set of NAI protected proportions experienced by a population over a prescribed, possibly infinite, time interval indexed with t and consider the following function

$$\mathcal{R}_0(u(t)) := C_0 \sqrt{(C_1 - C_2)u(t) + C_2}.$$

As a result, the type of monotonicity obeyed by $\mathcal{R}_0(u(t))$ is dependent on the sign of the non-zero combination of parameters $C_1 - C_2$. These observations motivate the following definition which classifies the configuration space of the model based on how the asymptotic dynamics of the corresponding population responds with respect to the NAI accumulated in response to the rate of exposure.

Definition 1. (*Configuration Space*) The SEYAR model (4) is said to possess a *Y-dominant configuration* if $C_1 - C_2 > 0$ and an *A-dominant configuration* provided that $C_1 - C_2 < 0$. Upon the trivial case that $C_1 - C_2 = 0$, the system is said to have a *Null-configuration*. Additionally, we refer to a system possessing such a configuration as either *A-*, *Y-* or *Null-configured*. A given human population is called *A-Y-*, or *Null-dominate* provided that its corresponding configuration is.

It is worth mentioning that although r_6 is always positive, the combination of parameters $C_1 - C_2$ need not be. The positiveness of r_6 is a result of how the transmission probabilities are weighted by the NAI protected proportion. If the system is *Null-configured*, then $\mathcal{R}_0(u(t)) := C_0 \sqrt{C_2}$ and it is locally asymptotically stable

provided that $C_0 < 1$ and $\beta_Y < \lambda_{YR} + \xi_H + \delta$, i.e. a high vector death rate and the symptomatics are recovering or dying out at a faster rate than they are transmitting. Consider the case of an *A-dominant configuration*, i.e.

$$(7) \quad \frac{\beta_A}{\beta_Y} < \frac{\lambda_{AR} + \xi_H}{\lambda_{YR} + \xi_H + \delta}.$$

As mentioned in Section 2, in the formulation of the *SEYAR* model (4) we do not assume an ordering on the asymptomatic and symptomatic transmission probabilities β_A and β_Y , respectively. However, under the assumption that asymptomatic carriers transmit at a lower rate than that of symptomatic, the left hand side of the above inequality is less than unity. Moreover, if we additionally assume that asymptomatic individuals recover faster than symptomatic, provided the disease induced death rate δ and recovery rates are such that $\lambda_{AR} > \lambda_{YR} + \delta$, then the right hand side of the above inequality is greater than unity and inequality (7) is satisfied. In an epidemiological setting, such a configuration corresponds to holoendemic regions across sub-Saharan Africa [2] in which the majority of people are continuously infected by *P. falciparum*, but only a small proportion display clinical symptoms. The high level of naturally acquired immunity present in the population allows them to live their daily lives feeling healthy despite a relatively high blood-parasite density, [23].

Analytically speaking, in the case of an *A-dominant configuration*, provided that the mosquito mortality rate ξ_M can be made large enough so that the term C_0 compromised of fractional multipliers is sufficiently small, then $\mathcal{R}_0(u_t)$ achieves its maximum $\mathcal{R}_0(u_{low})$ at the low NAI threshold u_{low} and decreases to its infimum $\mathcal{R}_0(u_{high})$ as the high NAI threshold u_{high} is approached. Moreover, since the ordered set T is a subset of a separable metric space, we can extract an ordered countable subset and form the partition $\{u_{low} = u(t_1) < \dots < u(t_n) < u(t_{n+1}) < \dots < u_{high}\}$ of the compact sub-interval T_u . In this case, the corresponding values of $\mathcal{R}_0(u(t))$ obey the following descending order $\{\mathcal{R}_0(u_{low}) > \dots > \mathcal{R}_0(u(t_n)) > \mathcal{R}_0(u(t_{n+1})) > \dots > \mathcal{R}_0(u_{high})\}$. This is consistent with the fact that as a given population acquires natural immunity through exposure, the disease will start to spread at a slower rate. Conversely, if the system has a *Y-dominant configuration*, i.e. $C_1 - C_2 > 0$, then the monotonicity is reversed.

In mathematical terminology, provided $\sigma < 1$, one can always find a large enough ξ_M to make $C_0 < 1$. In this case, the factor that will cause \mathcal{R}_0 to breach unity is r_6 . From an epidemiological standpoint, regardless of the size of vector transmission probability β_M or man-biting rate σ , if enough mosquitoes are dying to significantly slow the disease transmission dynamics, then $C_0 < 1$ and, as a result, the size of the reproductive threshold \mathcal{R}_0 will be determined by r_6 which depends on the human immune systems response to the *Plasmodium* parasite. This attest to the fact that in such vector transmitted diseases, the reproductive threshold will lower in response to vector elimination up to a point and the factor allowing the disease to persist under such low vector activity lies in the intricate relationship between the parasite and host. This delicate relationship is captured by the term r_6 .

Remark 3.2. (*Verification of the Reproductive Threshold*) A verification of the reproductive threshold \mathcal{R}_0 (6) arising from Lemma (1) above is provided utilizing Maple software in the electronic supplementary material.

3.3. The Impact of the Asymptomatic Class on the Reproductive Threshold. It would be informative to investigate how the reproductive threshold arising from the *SEYAR* model behaves in the case that the long time dynamic effects of asymptomatic carriers are not taken into account. The natural parameter space of the *SEYAR* model corresponding to the reproductive threshold is

$$\Theta := \{(\Omega_H, \Omega_M, \xi_H, \xi_M, \beta_A, \beta_Y, \beta_M, \gamma, \tau, \delta, \sigma, \lambda_{AR}, \lambda_{YR}, U_{low}) \in \mathbb{R}_{>0}^{14}\},$$

where $\mathbb{R}_{>0}^n := \{x \in \mathbb{R}^n : x_i > 0 \text{ for } i = 1, \dots, n\}$. The set Θ consists of all possible positive, epidemiologically reasonable, parameter values for the *SEYAR* model in which the reproductive threshold depends upon. Although the disease induced death rate δ is allowed to be non-negative, the analysis presented in this section is unaffected by this minor detail. Under this formalization, neglecting the disease transmission and recovery rates of asymptomatic human hosts on the reproductive threshold formally corresponds to restricting the model to the following *A-nullified* parameter configuration space $\tilde{\Theta}$, defined as

$$\tilde{\Theta} := \{(\Omega_H, \Omega_M, \xi_H, \xi_M, \beta_Y, \beta_M, \gamma, \tau, \delta, \sigma, \lambda_{YR}, U_{low}) \in \mathbb{R}_{>0}^{12} : \beta_A = \lambda_{AR} = 0\}.$$

Consider a typical element $\Theta_0 \in \Theta$ listed below

$$\Theta_0 = (\Omega_{H_0}, \Omega_{M_0}, \xi_{H_0}, \xi_{M_0}, \beta_{A_0}, \beta_{Y_0}, \beta_{M_0}, \gamma_0, \tau_0, \delta_0, \sigma_0, \lambda_{AR_0}, \lambda_{YR_0}, U_{low_0}).$$

In a similar fashion, the dual element $\tilde{\Theta}_0 \in \tilde{\Theta}$ corresponding to the symptomatic class Y is given by

$$\tilde{\Theta}_0 = \left(\Omega_{H_0}, \Omega_{M_0}, \xi_{H_0}, \xi_{M_0}, \beta_{Y_0}, \beta_{M_0}, \gamma_0, \tau_0, \delta_0, \sigma_0, \lambda_{YR_0}, U_{low_0} \right).$$

It is worth mentioning that the dual element $\tilde{\Theta}_0$ is comprised of the same fixed parameter configuration as described by Θ_0 , but with the asymptomatic progression rates specified above set equal to zero. To emphasize the asymptotic dynamic influence of the asymptomatic class A on the reproductive threshold \mathcal{R}_0 (6) arising from the *SEYAR* model (4), subject to a given fixed parameter configuration, the following notation is employed $\mathcal{R}_A := \mathcal{R}_0|_{\Theta_0}$. By denoting $\mathcal{R}_Y := \mathcal{R}_0|_{\tilde{\Theta}_0}$, the size relationship between the two quantities \mathcal{R}_A and \mathcal{R}_Y is captured below in the following theorem.

Theorem 3.3. *(Impact of the Asymptomatic Class on the Reproductive Threshold)* *Let \mathcal{R}_0 be the threshold quantity (6) arising from Lemma (1) and consider the following fixed parameter configuration vectors $\Theta_0 \in \Theta$ and $\tilde{\Theta}_0 \in \tilde{\Theta}$, corresponding to the *SEYAR* model (4), defined as above. Denote $\mathcal{R}_A := \mathcal{R}_0|_{\Theta_0}$ and $\mathcal{R}_Y := \mathcal{R}_0|_{\tilde{\Theta}_0}$, then it follows that $\mathcal{R}_Y < \mathcal{R}_A$.*

One should observe that the above inequality is strict. Therefore, neglecting to account for asymptomatic carriers results in an underestimation of the reproductive threshold. To demonstrate the theoretical estimate provided in Theorem (3.3), the numerical values of \mathcal{R}_A and \mathcal{R}_Y , along with the Entomological Inoculation Rate (*EIR*) and parameter configuration space classifications, introduced via definition (1) in Section 3.2 are presented in Table 5 of Section 5.2 below. These numerical values correspond to the following three high transmission sites: Kaduna in Nigeria, Namawala in Tanzania, and Butelgut in Papua New Guinea. The parameter values associated with each site are listed in Section 7.6.

Previously, it was shown that \mathcal{R}_0 can be written in the following form

$$(8) \quad \mathcal{R}_0 = \sigma \prod_{i=1}^6 \sqrt{r_i},$$

where each term $\sqrt{r_i}$ is defined as in Section 3.2. Care needs to be taken when arbitrarily substituting zero parameter values into the reproductive threshold \mathcal{R}_0 (8). Clearly, if the man-biting rate $\sigma = 0$ or mosquito to human transmission probability $\beta_M = 0$, then it follows that $\mathcal{R}_0 = 0$. These quantities effectively nullifying the reproductive threshold stands to epidemiological reason and corresponds to the following scenarios, respectively: (i) no mosquitoes are biting humans, and (ii) they are not transmitting the disease. Furthermore, if both the asymptomatic β_A and symptomatic β_Y transmission probabilities are equal to zero, then the reproductive threshold will be identically zero, as infected humans are not transmitting the disease to susceptible mosquitoes.

However, it is implied that while one (or possibly all) of such parameter values may be equal to zero, the other parameter values in which the threshold depends on will be such that it is well-defined. This problem is primarily due to the inclusion of vital dynamics for the human and mosquito populations into the dynamical system (4). For example, if one lets the human recruitment rate $\Omega_H = 0$ or the mosquito mortality rate $\xi_M = 0$, then a singularity occurs and \mathcal{R}_0 ceases to be well-defined. Although, the mosquito mortality rate being equal to zero in unreasonable in an epidemiological sense, as all mosquitoes experience death, it is informative to study how this parameters size effects \mathcal{R}_0 , as in general it is desirable to increase such a parameter when introducing control measures into the system. Moreover, it is worth mentioning from a mathematical standpoint, as it attests to the subtle fact that after including vital dynamics into a given compartmentalized infectious disease model, one can not expect to obtain qualitative information about the reproductive threshold in the absence of vital dynamics by simply setting the corresponding terms equal to zero. To properly study the asymptotic behavior of such models without vital dynamics included, one would have to go back to the original model derivation and not include them from the beginning, then proceed to calculate the threshold arising from the modified system.

The formal approach corresponding to the configuration space presented above ensures that this does not happen and adds another level of mathematical precision to the analysis presented in this work. Some other noteworthy consequences of the above formal approach related to the configuration space of the *SEYAR* model (4) are listed below.

i Consider the following fixed parameter configuration vector $\Theta_1 \in \mathbb{R}_{>0}^{13}$, defined by

$$\Theta_1 := \left(\Omega_{H_0}, \Omega_{M_0}, \xi_{H_0}, \beta_{A_0}, \beta_{Y_0}, \beta_{M_0}, \gamma_0, \tau_0, \delta_0, \sigma_0, \lambda_{AR_0}, \lambda_{YR_0}, U_{low_0} \right).$$

Then, by equation (8) and the fact that the square root function is uniformly continuous on $[0, +\infty)$, (so that the limit can be taken inside), it follows that

$$\begin{aligned}\lim_{\xi_M \rightarrow +\infty} \mathcal{R}_0 \Big|_{\Theta_1} &= \sigma \sqrt{r_1^0 r_3^0 r_6^0} \cdot \sqrt{\lim_{\xi_M \rightarrow +\infty} \frac{\tau_0 \xi_{H_0} \beta_{M_0}}{\xi_M^2 (\tau_0 + \xi_M)}}, \\ &= \sigma \sqrt{r_1^0 r_3^0 r_6^0} \cdot 0, \\ &= 0,\end{aligned}$$

where the superscripts appearing above each appropriate i^{th} term denote that fact that these quantities are fixed and thus invariant under the limit operation.

Due to the equivalency of the $\epsilon - \delta$ and sequential definitions of limits, there exist a natural number $\xi_{M_{n_0}} \in \mathbb{N}$ such that for all $\xi_{M_n} \geq \xi_{M_{n_0}}$, it follows that $\mathcal{R}_0 \in [0, 1)$. This qualitative observation can be interpreted as follows: provided a scenario such that all of the associated model parameters are fixed epidemiologically reasonable quantities, if control measures sufficient to increase the vector death rate are introduced into the model, then the corresponding reproductive threshold arising from the model will be lowered and eventually fall below unity. This is consistent with the discussion in Section 3.2.

ii In a similar fashion, consider the following fixed vectors $(\Theta_2, \Theta_3) \in \mathbb{R}_{>0}^{13} \times \mathbb{R}_{>0}^{13}$, defined as follows

$$\Theta_2 := \left(\Omega_{H_0}, \xi_{H_0}, \xi_{M_0}, \beta_{A_0}, \beta_{Y_0}, \beta_{M_0}, \gamma_0, \tau_0, \delta_0, \sigma_0, \lambda_{AR_0}, \lambda_{YR_0}, U_{low_0} \right)$$

and

$$\Theta_3 := \left(\Omega_{M_0}, \xi_{H_0}, \xi_{M_0}, \beta_{A_0}, \beta_{Y_0}, \beta_{M_0}, \gamma_0, \tau_0, \delta_0, \sigma_0, \lambda_{AR_0}, \lambda_{YR_0}, U_{low_0} \right).$$

Then it follows that

$$\begin{aligned}\lim_{\Omega_M \rightarrow +\infty} \mathcal{R}_0 \Big|_{\Theta_2} &= \sigma \prod_{i=2}^6 \sqrt{r_i^0} \cdot \sqrt{\lim_{\Omega_M \rightarrow +\infty} \frac{\Omega_M}{\Omega_{H_0}}}, \\ &= +\infty,\end{aligned}$$

and

$$\begin{aligned}\lim_{\Omega_H \rightarrow 0^+} \mathcal{R}_0 \Big|_{\Theta_3} &= \sigma \prod_{i=2}^6 \sqrt{r_i^0} \cdot \sqrt{\lim_{\Omega_H \rightarrow 0^+} \frac{\Omega_{M_0}}{\Omega_H}}, \\ &= +\infty.\end{aligned}$$

As pointed out in Section 3.2, the factor r_1 is always greater than unity. The above analysis demonstrates how \mathcal{R}_0 behaves with respect to the human and mosquito recruitment rates. As we will see in Section 5.1, if a given population, e.g. the three sites from which the parameter values are taken for this work, has a relatively small human recruitment rate and relatively large mosquito recruitment rate, then the factor r_1 will dramatically contribute to the size of \mathcal{R}_0 . For example, in the case of the Kaduna site $r_1 \approx 14762941.18$. The fractional multipliers r_i for $i = 2, 3, 4$ will reduce the resulting size of this quantity, as they are all strictly less than unity. Further reduction in the size of the remaining quantity in the decomposition of \mathcal{R}_0 depends on the terms σ , r_5 and r_6 . These remaining factors will lower the resulting threshold provided that the mosquitoes are biting a relatively small amount of humans per unit time and transmitting less than they are dying off. Additionally, the asymptomatic and symptomatic human hosts need to be transmitting at a sufficiently low rate. For this reason, we must introduce control measures which both reduce the various disease transmission probabilities involved and increase the vector death rate.

It is worth mentioning that setting the parameters τ and γ equal to zero obviously results in $\mathcal{R}_0 = 0$. However, these scenarios are not considered as the mosquito and human latent periods τ and γ are considered to be intrinsic properties of the vector and host, respectively. Moreover, these specific terms only appear in the factors $\sqrt{r_i}$ for $i = 2, 3$ which are strictly bounded above by unity. Additionally, we do not consider the bizarre cases that the human mortality rate $\xi_H = 0$ or mosquito recruitment rate $\Omega_M = 0$. Although both cases result in effectively

nullifying the threshold quantity \mathcal{R}_0 , humans are not immortal and the mosquito recruitment rate is usually relatively large. Letting this particular parameter value be equal to zero would imply the epidemiologically unreasonable scenario that there are no mosquitoes present in the region being considered. Neither do we consider the qualitative behavior of \mathcal{R}_0 if ξ_H is sufficiently large, as introducing a human transmission blocking control measure which also increases the human death rate of a given population is not an ethical control method. It is important to note that emphasis is made on the terms which are related to utilized control measures, i.e. the measures which have an effect on the mosquito death rate and the various transmission probabilities involved. Control measures will be formally introduced and properly covered in Section 4.2 below.

3.4. Endemic Equilibria and Bifurcation Analysis. An endemic occurs when disease persists in the population, mathematically this corresponds to all of the state variables being positive. For this reason, endemic equilibrium (EE) points are equilibrium points where the state variables are positive. Most epidemic models exhibit a dichotomy in terms of bifurcations that occur at the threshold $\mathcal{R}_0 = 1$, namely: super-critical (forward) and sub-critical (backward). These have drastically different epidemiological implications. A forward bifurcation happens when \mathcal{R}_0 crosses unity from below and, as a result, a small positive asymptotically stable super-threshold equilibria appears and the disease-free equilibrium losses its stability. Backward bifurcation happens when $\mathcal{R}_0 < 1$ and a small positive unstable sub-threshold equilibrium appears, while the disease-free equilibrium and a larger positive equilibrium are locally asymptotically stable.

From an epidemiological viewpoint, a forward bifurcation is more desirable as it results in the reproductive number being below unity to be sufficient to ensure that an epidemic does not occur. In the presence of a backward bifurcation, the reproductive number being below unity is no longer sufficient, as sub-threshold endemic equilibrium can arise in response to perturbations of specific parameters. In most cases, the parameters chosen are contact rates.

Due to the presence of the term $e^{-\varepsilon} = \sum_{n=0}^{\infty} \frac{(-1)^n}{n!} \left(\frac{E}{N_H} \right)^n$, one can not obtain a closed-form expression for the endemic equilibrium of system (4). However, we turn to a variant of the Center Manifold Theorem, introduced by Castillo-Chavez and Song [11], to show the existence of non-trivial equilibrium solutions of the SEYAR model (4) near the DFE. This section is focused on the nonlinear stability analysis corresponding to the SEYAR model. More precisely, the following lemma concerning its bifurcation behavior is proven.

Lemma 2. *(Bifurcation Analysis for the SEYAR Model) Let the positive quantities η_1 and η_2 be defined as follows:*

$$\begin{aligned} \eta_1 &:= Z_6 Q_2 + \frac{\tau^2 Z_1 Q_1^2 Q_4^2}{K_1 \xi_M} \left(1 + \frac{K_2}{K_4} + \frac{K_3}{K_5} + Q_0 \right) + \frac{\tau Z_2 K_2}{K_4 K_7} \left(\frac{\lambda_{RS} Q_0}{K_6} + 1 + Q_0 \right) + \frac{\tau Z_3 K_3}{K_5 K_7} \left(\frac{\lambda_{RS} Q_0}{K_6} + 1 + Q_0 \right) \\ &\quad + \frac{\tau Z_7 Q_4 Q_1 K_2}{\xi_M K_4} + \frac{\tau Z_5 Q_4 Q_1 K_3}{\xi_M K_5} + \frac{2\tau Z_2 K_2^2}{K_4^2 K_7} + \frac{2\tau Z_3 K_3^2}{K_5^2 K_7}, \\ \eta_2 &:= \frac{\tau Z_2 K_1 K_2}{K_4 K_6 K_7} + \frac{\tau Z_3 K_1 K_3}{K_5 K_6 K_7} + \frac{\tau Z_4 K_2 K_3}{K_4 K_5 K_7} + Z_6 Q_3, \end{aligned}$$

where the terms labeled K_i , Q_i and Z_i , for $i = 1, \dots, 7$ are defined in Section (7) below. If the parameter Λ is defined as

$$(9) \quad \Lambda := \frac{\eta_2}{\eta_1},$$

then the bifurcation for the SEYAR model (4) is sub-critical provided that $\Lambda > 1$ and super-critical provided $\Lambda < 1$.

As previously mentioned, lemma (2) is proven by making use of an application of the Center Manifold Theorem [11], adapted to the case of nonlinear dynamical systems. As in the case of most malaria models appearing throughout scientific literature, the type of bifurcation experienced by the system is completely determined by the sign of the a -term (22), appearing in Theorem (7.2). In the case of the SEYAR model (4) $a \propto (\eta_2 - \eta_1)$, resulting in a size constraint on Λ . In an epidemiological setting, it is desirable for the bifurcation, if it exists, to be super-critical, i.e. forward. Lemma (2) tells us that if one wants to avoid the case of a sub-critical bifurcation from occurring, we must demand the quantity $\Lambda < 1$ in addition with $\mathcal{R}_0 < 1$.

Remark 3.3. *(Verification of the Jacobian entries and explicit expression of the a -term) A verification of the entries of the Jacobian evaluated at the DFE along with an explicit expression of the number a in terms of the original model parameters is provided utilizing Maple software in the electronic supplementary material.*

4. PARAMETER ESTIMATION AND GENERALIZED CONTROL MEASURES

4.1. A Unified Formal Approach to Parameter Estimation. In order to use the *SEYAR* model (4) to obtain biologically meaningful numerical estimates, it is necessary to obtain values for the parameters appearing in Table 1. Provided these parameter values exist, they are usually difficult to obtain. The formulas appearing in this section provide relationships between the parameters in Table 1 and other well-known biological quantities measured in malaria epidemiology. These functional relationships enable a characterization of many of the static quantities used in malaria modeling and provide numerous ways to estimate them.

I *Probability of surviving the length of the Plasmodium incubation period* (\mathcal{P}): Due to equation (15) appearing in Section 7, if time is measured in days, then the probability of a mosquito surviving one day is $\nu(1) = e^{-\xi_M}$, so that the mosquito mortality rate is $\xi_M = -\ln \nu(1)$. Define τ to be the length of the *Plasmodium* incubation period, i.e. the duration of the intrinsic incubation period. Therefore, the probability of surviving the length of the *Plasmodium* incubation period is $\mathcal{P} := \nu(\tau) = e^{-\xi_M \tau}$. This quantity varies with respect to the parasite species and has temperature dependency.

II *Human Feeding Rate* (σ): The human feeding rate quantifies the average number of mosquito bites suffered by a human, per mosquito, per day. Define m_f to be the mosquito feeding rate, so that the reciprocal is then the time interval between blood meals, and let m_q denote the proportion of mosquito blood meals taken on humans. Then the expected number of bites on humans per mosquito, per day is given by the equation $\sigma = m_q m_f$.

III *Human Biting Rate* (*HBR*): The human biting rate quantifies the number of mosquito bites suffered by humans, per human, per day. Let m_e be the rate of mosquito emergence per human, per day, so that the equilibrium mosquito density per human is $m_0 = \frac{m_e}{\xi_M}$. The *HBR* is given by the product of the human feeding rate σ and the equilibrium mosquito density, i.e. $HBR = \sigma m_0$.

IV *Stability Index* (\mathcal{S}): A generic female *Anopheles* mosquito lives an average of $\frac{1}{\xi_M}$ days and bites a human once every σ days. The expected number of mosquito bites on humans over a mosquito's lifetime, called the stability index, is defined to be $\mathcal{S} := \frac{\sigma}{\xi_M}$. The mortality rate ξ_M is constant and the mosquitoes lifespan is given by an exponential distribution. As a result, \mathcal{S} can be understood as the approximate number of bites after a mosquito becomes infected.

V *Human Blood Index* (*HBI*): Following the terminology utilized in [57], a mosquito of age a is expected to have given $m_f a$ bites, of which $\sigma a = m_f m_q a$ are on humans. For a cohort of recently emerged mosquitoes, the proportion of surviving mosquitoes of age a that have ever bitten a human is $\eta_\sigma(a) = 1 - e^{-\sigma a}$. Thus, the proportion of mosquitoes in a population that has survived to age a and has bitten a human is $\eta_\sigma(a) \nu(a)$, so that after a normalization, it follows that the *HBI* is

$$HBI := \frac{\int_0^\infty \eta_\sigma(a) \nu(a) da}{\int_0^\infty \nu(a) da}.$$

Making use of the functional (10) defined in Lemma (4.1) below, we have $HBI = \mathcal{G}_\nu(\eta_\sigma(a))$. Therefore, by equation (11) with $\omega = 0$ and $\kappa = \sigma$, it follows that

$$HBI = \frac{\sigma}{\sigma + \xi_M}.$$

As pointed out in [57], the above quantity can be interpreted as a ratio of two waiting times. The numerator is the waiting time to the first human bite or death $\frac{1}{\sigma + \xi_M}$ and the denominator is the waiting time to the first human bite among surviving mosquitoes $\frac{1}{\sigma}$.

VI *Proportion of Infected Mosquitoes* (M^*): Denote $I^* = Y^* \cup A^*$ to be the portion of infected humans. The stars superscripts are meant to emphasize the fact that this is a static analysis and as a result, I^* is assumed to be constant. Furthermore, let $\beta_I := \beta_A + \beta_Y$ stand for the probability of disease transmission from an infected human to a susceptible mosquito. As a result, mosquitoes acquired infection at rate $\sigma \beta_I I^*$ and the quantity of surviving mosquitoes of age a that ever become infected is $\eta_{\sigma \beta_I I^*}(a) = 1 - e^{-\sigma \beta_I I^* a}$. The proportion of the mosquito cohort that is both alive and infected at age a is $\eta_{\sigma \beta_I I^*}(a) \nu(a)$. In the same manner as (V), $M^* = \mathcal{G}_\nu(\eta_{\sigma \beta_I I^*}(a))$. Therefore, by equation (11) with $\omega = 0$ and $\kappa = \sigma \beta_I I^*$ it follows that

$$M^* = \frac{\sigma \beta_I I^*}{\sigma \beta_I I^* + \xi_M}.$$

The quantity M^* can be viewed as the ratio of the waiting time to death or infection $\frac{1}{\sigma\beta_I I^* + \xi_M}$ and the waiting time to infection among surviving mosquitoes $\frac{1}{\sigma\beta_I I^*}$.

VII *Sporozoite Rate* (\mathcal{Z}): The infective state of the malaria parasite that is passed on to human hosts from the salivary glands of the *Anopheles* mosquito is called *Sporozoite* stage. A related concept is the sporozoite rate, which is the probability that an individual mosquito ever becomes infectious, or equivalently, the proportion of infectious mosquitoes. If τ is the length of the *Plasmodium* incubation period, then the proportion of mosquitoes of age a that are infectious is

$$\eta_{\sigma\beta_I I^*}^\tau(a) = \begin{cases} 1 - e^{-\sigma\beta_I I^*(a-\tau)} & \text{if } a > \tau, \\ 0 & \text{if } a \leq \tau. \end{cases}$$

Placing this together, the proportion of mosquitoes that is both infectious and alive at age a is $\eta_{\sigma\beta_I I^*}^\tau(a)\nu(a)$ and $\mathcal{Z} = \mathcal{G}_\nu(\eta_{\sigma\beta_I I^*}^\tau(a))$. Thus, by equation (11) with $\omega = \tau$ and $\kappa = \sigma\beta_I I^*$ it follows that

$$\mathcal{Z} = \frac{\sigma\beta_I I^*}{\sigma\beta_I I^* + \xi_M} e^{-\tau\xi_M}.$$

It is worth pointing out that \mathcal{Z} is simply the product of the probabilities of ever becoming infected and the incubation period, i.e. $\mathcal{Z} = M^*\mathcal{P}$.

VIII *Lifetime Transmission Potential* (β): The lifetime transmission potential is defined as the expected amount of new infections that would be generated by a newly emerged adult. If β_M denotes the transmission probability from an infectious mosquito to an susceptible human, then the total expected output from a mosquito population at age a is $\sigma\beta_M \eta_{\sigma\beta_I I^*}^\tau(a)\nu(a)$. Lifetime transmission potential is obtained by integrating over the positive real a axis

$$\beta = \sigma\beta_M \int_0^\infty \eta_{\sigma\beta_I I^*}^\tau(a)\nu(a)da.$$

By similar reasoning as above, we have that $\beta = \frac{\sigma\beta_M}{\xi_M} \mathcal{G}_\nu(\eta_{\sigma\beta_I I^*}^\tau(a))$. So that by equation (11) with $\omega = \tau$ and $\kappa = \sigma\beta_I I^*$ it follows that

$$\beta = \frac{\sigma^2 \beta_M \beta_I I^*}{\xi_M(\sigma\beta_I I^* + \xi_M)} e^{-\tau\xi_M}.$$

Therefore, β can be viewed as the product of the four quantities: (1) the probability that a mosquito becomes infected M^* , (2) the probability that an infected mosquito lives to become infectious \mathcal{P} , (3) the transmission efficiency β_M and the stability index \mathcal{S} .

IX *Entomological Inoculation Rate* (*EIR*): The *EIR* serves as a measure of human exposure to infectious mosquitoes. By definition, the *EIR* stands for the quantity of infectious bites received per human, per day. Mathematically, this is expressed as the product of the *HBR* σ and the Sporozoite Rate \mathcal{Z} . More specifically

$$\begin{aligned} EIR &= \sigma m_0 \mathcal{Z}, \\ &= \frac{m_0 \sigma^2 \beta_I I^*}{\sigma\beta_I I^* + \xi_M} e^{-\tau\xi_M}. \end{aligned}$$

X *Vectorial Capacity* (V_C): Vectorial Capacity quantifies the total number of potentially infectious bites that would eventually arise from all the mosquitoes biting a single perfectly infectious (i.e., all mosquito bites result in infection) human on a single day. More concisely, V_C is the expected number of humans infected, per human, per day, assuming ideal transmission efficiency, i.e. $\beta_I = \beta_M = 1$. The vectorial capacity V_C of a mosquito population can be obtained by taking the product of the following four quantities: (1) the vectorial competence b of the female *Anopheles* mosquito, which is its ability to transmit malaria. (2) the emergence rate of mosquitoes m_ϵ , (3) the squared stability index \mathcal{S}^2 (this quantity is squared owing to the fact that two bites are necessary for malaria transmission: the one that infects the definite host and the one that infects the indefinite), and (4) the probability of a mosquito surviving the *Plasmodium* incubation period \mathcal{P} . Taking these principles into account we arrive at the

following formula for V_C

$$\begin{aligned} V_C &:= b m_\epsilon \mathcal{S}^2 \mathcal{P}, \\ &= b m_0 \xi_M \left(\frac{\sigma}{\xi_M} \right)^2 e^{-\xi_M \tau}, \\ &= \frac{b m_0 \sigma^2 \nu \tau(1)}{-\ln \nu(1)}. \end{aligned}$$

XI *Individual Vectorial Capacity (V_I)*: Individual Vectorial Capacity quantifies the total number of potentially infectious bites emanating from a single mosquito after feeding on an infectious human host. For this reason, it is defined as the product of following three quantities: (1) the probability of a mosquito surviving the *Plasmodium* incubation period \mathcal{P} , (2) the stability index \mathcal{S} , and (3) the probability of disease transmission from an infected human to a susceptible mosquito β_M . Therefore, we arrive at the following formula for V_I :

$$\begin{aligned} V_I &:= \beta_M \mathcal{P} \mathcal{S}, \\ &= \frac{\sigma \beta_M e^{-\xi_M \tau}}{\xi_M}. \end{aligned}$$

Theorem 4.1. (*Functional Equation for the SEYAR Model*) Define the functional $\mathcal{G}_\nu(\cdot) : L^\infty(\mathbb{R}_+) \rightarrow \mathbb{R}_+$ by the following integral equation

$$(10) \quad \mathcal{G}_\nu(\varphi(a)) := \xi_M \int_0^\infty \varphi(a) \nu(a) da,$$

where $\nu(a) := e^{-a\xi_M}$. For exponential distributions of the form

$$\eta_\kappa^\omega(a) = \begin{cases} 1 - e^{-\kappa(a-\omega)} & \text{if } a > \omega, \\ 0 & \text{if } a \leq \omega, \end{cases}$$

it follows that

$$(11) \quad \mathcal{G}_\nu(\eta_\kappa^\omega(a)) = \frac{\kappa}{\kappa + \xi_M} e^{-\omega \xi_M},$$

in the sense of improper Riemann integrals.

Remark 4.1. The fact that $\int_0^\infty \nu(a) da = \xi_M^{-1}$ in combination with the discussion in item V of Section 4.1 involving weighted averages motivates the definition of the above functional (10).

4.2. Incorporating Generalized Control Measures. The entomological inoculation rate, discussed in Section 4.1, is a meaningful epidemiologic predictor that serves as a good measure of malaria intensity in a given region, [34]. In 2007, David L. Smith estimated the reproductive number for 121 African populations. On figure 2, found in [58, p. 0534] two numerical plots are displayed in which the reproductive number estimates are compared with the entomological inoculation rate of the populations under consideration. One plot corresponds to heterogeneous biting and transmission-blocking immunity taken into account in the parameter estimates and the other without. In both cases, the quantities where shown to be directly proportional, i.e. regions with a relatively large (small) *EIR* also have a relatively large (small) reproductive number. In other words, regions with relatively large *EIR* values of each region also have relatively large \mathcal{R}_0 values. In areas with large \mathcal{R}_0 , it is unlikely that one single control measure will be sufficient to stop the disease expansion [58].

Concerning protection obtained through vaccination, Figure 6 in [58, p. 0536] presents a numerical plot comparing the reproductive number \mathcal{R}_0 and the proportion of the population that must be neutralized through a vaccine, under ideal assumptions. In low transmission areas, malaria eradication seems to be a practical and achievable goal. However, in high transmission settings, the classic theory suggests that greater than 99% of hosts would need to be protected in order to sufficiently reduce transmission to reach a state of stability. The large range of \mathcal{R}_0 values across Africa attest to the immense challenge faced by malaria control programs.

In practice, vaccine-conveyed immunity is not one hundred percent. This fact is accounted for by the vaccine efficacy V_f , which denotes the percentage of protection each vaccinated individual has. If V_p denotes the proportion of the population that has been vaccinated, i.e. the vaccine coverage. The product $V_f V_p$ stands for the fraction of the population under consideration that is protected, so that the remaining proportion $(1 - V_f V_p)$ is not directly protected, with respect to vaccine-conveyed immunity. As a result, vaccination controls are

incorporated into the model by defining the weight $\bar{v} := (1 - V_f V_p)$. Therefore, the control-modified progression rates are given by the following equations

$$\begin{cases} \tilde{\lambda}_{EA} &:= \bar{v}\gamma u(\varepsilon), \\ \tilde{\lambda}_{EY} &:= \bar{v}\gamma(1 - u(\varepsilon)). \end{cases}$$

Insecticide-treated nets (ITNs) are the most prominent malaria preventive measure for large-scale deployment in highly endemic areas, such as sub-Saharan Africa, [39]. ITNs are nets coated with synthetic pyrethroid insecticides. Due to their high arthropod toxicity and low mammalian toxicity, such insecticides are well suited for this purpose. Many studies have shown them to both kill and repel mosquitoes. In a recent study, a regression analysis of the protective efficacy on the transmission intensity, as measured by the *EIR*, was performed at the following four different endemic regions of Africa: Burkina Faso, The Gambia, Ghana, and Kenya. It was noted that the protective efficacy was lower in areas with a higher *EIR*, which was consistent with the original hypothesis that relative impact is lower in areas with higher entomological inoculation rates, [39]. Moreover, in the case of homogeneous biting 99.95% ITN coverage was predicted to be necessary, [58].

Regarding the ITN coverage, let the symbol ρ_f denote the protective efficacy, i.e. the percentage reduction in malaria episodes due to bed net usage. Upon letting ρ_p be the proportion of ITN usage, i.e. the percentage decrease in transmission due to the employment of ITNs, then the reduction in mosquito to human transmission is captured by the multiplier $(1 - \rho_f \rho_p)$. Three separate scenarios are considered in which the population coverage of ITNs is assumed to be 33% (low), 66% (medium) and 99% (high). Additionally, let ξ_{ITN} denote the maximum ITN-induced death rate for the mosquito population. Following [3], it is assumed that ITN usage reduces the effective human to mosquito effective contact rates β_A and β_Y and increases the mosquito mortality rate ξ_M . Thus, the effects of ITN usage on the disease transmission dynamics of the *SEYAR* model (4) are accounted for by the following modification.

$$\begin{cases} \tilde{\beta}_A &:= (1 - \rho_f \rho_p)\beta_A, \\ \tilde{\beta}_Y &:= (1 - \rho_f \rho_p)\beta_Y, \\ \tilde{\xi}_M &:= \xi_M + \rho_f \rho_p \xi_{ITN}. \end{cases}$$

To obtain the modified system and the reproductive threshold, one needs to invoke the direct substitution where the tilde in each term being dropped corresponds to the system in the natural variables. One should note that this differs from the change of variable technique. Therefore, the resulting control-modified variant of the *SEYAR* model (4) expanded in the original model parameters is

$$\begin{cases} \dot{S} = \Omega_H + \lambda_{RS}R - \left(\sigma\beta_M \frac{M_L}{N_H} + \xi_H\right)S, \\ \dot{E} = \sigma\beta_M \frac{M_L}{N_H}S - (\gamma + \xi_H)E, \\ \dot{Y} = (1 - V_f V_p)\gamma(1 - u(\varepsilon))E - (\xi_H + \delta + \lambda_{YR})Y, \\ \dot{A} = (1 - V_f V_p)\gamma u(\varepsilon)E - (\lambda_{AR} + \xi_H)A, \\ \dot{R} = \lambda_{AR}A + \lambda_{YR}Y - (\lambda_{RS} + \xi_H)R, \\ \dot{M}_S = \Omega_M - \left(\xi_M + \rho_f \rho_p \xi_{ITN} + \sigma(1 - \rho_f \rho_p)\beta_Y \frac{Y}{N_H} + \sigma(1 - \rho_f \rho_p)\beta_A \frac{A}{N_H}\right)M_S, \\ \dot{M}_E = \sigma(1 - \rho_f \rho_p)\left(\beta_Y \frac{Y}{N_H} + \beta_A \frac{A}{N_H}\right)M_S - (\xi_M + \rho_f \rho_p \xi_{ITN} + \tau)M_E, \\ \dot{M}_I = \tau M_E - (\xi_M + \rho_f \rho_p \xi_{ITN})M_I. \end{cases}$$

Assuming that the initial exposed proportion is zero, i.e. $\varepsilon_0 = 0$, the corresponding vaccination control-modified reproductive threshold $\mathcal{R}_0^{\bar{v}}$ is given by the following formula

$$(12) \quad \mathcal{R}_0^{\bar{v}} = \sqrt{\frac{\sigma^2 \tau \gamma \Omega_M \xi_H \beta_M (1 - \rho_f \rho_p) \bar{v}}{(\xi_M + \rho_f \rho_p \xi_{ITN})^2 (\gamma + \xi_H) (\tau + \xi_M + \rho_f \rho_p \xi_{ITN}) \Omega_H}} \left(\frac{\beta_A u_{low}}{\lambda_{AR} + \xi_H} - \frac{\beta_Y (u_{low} - 1)}{\lambda_{YR} + \xi_H + \delta} \right).$$

Remark 4.2. It is worth emphasizing that the ITN vector $(\rho_f, \rho_p) \in [0, 1] \times [0, 1]$ is a fixed quantity and the only controls are the vaccination terms V_f, V_p . This avoids the issue of identifiability of the model parameters with respect to the control parametrization.

The incorporation of the vaccination controls into the system implicitly introduces a restriction on the control parameter domain of $\mathcal{R}_0^{\bar{v}}$. Let $\epsilon > 1$, then if one takes the control parameter domain to be the entire rectangle $[0, \epsilon) \times [0, \epsilon) \supset [0, 1) \times [0, 1)$, then $\mathcal{R}_0^{\bar{v}}$ may be nullified or complex valued. Let $\mathbb{C} := \{\bar{z} : \bar{z} = a + bi \text{ where } (a, b) \in$

$\mathbb{R} \times \mathbb{R}$ and $i = \sqrt{-1}$ } denote the field of complex numbers. Making use of the definitions of C_i for $i = 1, 2$, presented in Section (3.2), it follows that the vaccination control-modified reproductive threshold will not be equal to zero or complex valued provided that $\mathcal{R}_0^{\bar{v}}$ is restricted to the hyperbolic sub-domain \mathcal{H} , as described in the following theorem.

Theorem 4.2. (Hyperbolic Sub-domain for the Parameter Space of the SEYAR Model) Fix the vector $(\rho_f, \rho_p) \in [0, 1] \times [0, 1]$ and each C_i for $i = 1, 2$, as defined in Section (3.2), and define the following hyperbolic sub-domain of the rectangle $[0, 1] \times [0, 1]$

$$\mathcal{H} := \left\{ (V_f, V_p) \in [0, 1] \times [0, 1] : V_f \in \left(0, \frac{1}{V_p}\right) \right\}.$$

Then $\mathcal{R}_0^{\bar{v}} \notin \mathbb{C} - \{0\}$ if and only if $(V_f, V_p) \in \mathcal{H}$.

Although, it is epidemiologically unreasonable to consider a vaccine efficacy V_f or vaccine coverage V_p control measure which equals to or exceeds 100%, this formal analysis is presented to provide a solid mathematical foundation for the numerical implementation of the model. More generally, if we consider m transmission blocking human control measures, then the modification is given by

$$\begin{cases} \lambda_{EA}^c &:= \prod_{j=1}^m \left(1 - V_f^j V_p^j\right) \gamma u(\varepsilon), \\ \lambda_{EY}^c &:= \prod_{j=1}^m \left(1 - V_f^j V_p^j\right) \gamma (1 - u(\varepsilon)). \end{cases}$$

For the n vector controls we have

$$\begin{cases} \beta_A^c &:= \prod_{i=1}^n \left(1 - \rho_f^i \rho_p^i\right) \beta_A, \\ \beta_Y^c &:= \prod_{i=1}^n \left(1 - \rho_f^i \rho_p^i\right) \beta_Y, \\ \xi_M^c &:= \xi_M + \prod_{i=1}^k \rho_f^i \rho_p^i \|\xi_i\|_\infty, \end{cases}$$

where $(\rho_f^i, \rho_p^i) \in [0, 1] \times [0, 1]$ for $i = 1, \dots, n$ and each $\|\xi_i\|_\infty$ denotes the maximum, possibly unachievable, vector death rate increase corresponding to each i^{th} vector control method. It should be noted that it is assumed that $k \leq n$ vector control measures increase the mosquito death rate. Formally, one could induce a sub ordering on the vector transmission reduction factors and extract the k terms such that the death rate increases. However, this formality is implied and would be unnecessary. The system including generalized controls is obtained via the same substitution as in the motivational example discussed above. For convenience the generalized control-modified reproductive threshold is listed below in explicit form

$$(13) \quad \mathcal{R}_0^c = \sqrt{\frac{\sigma^2 \tau \gamma \Omega_M \xi_H \beta_M \prod_{i=1}^n \left(1 - \rho_f^i \rho_p^i\right) \prod_{j=1}^m \left(1 - V_f^j V_p^j\right) \left(\frac{\beta_A u_{\text{low}}}{\lambda_{AR} + \xi_H} - \frac{\beta_Y (u_{\text{low}} - 1)}{\lambda_{YR} + \xi_H + \delta}\right)}{\Omega_H (\gamma + \xi_H) \left(\xi_M + \prod_{i=1}^k \rho_f^i \rho_p^i \|\xi_i\|_\infty\right)^2 \left(\tau + \xi_M + \prod_{i=1}^k \rho_f^i \rho_p^i \|\xi_i\|_\infty\right)}},$$

where $V_f^j \in \left(0, \frac{1}{V_p^j}\right)$ for $j = 1, \dots, m$, so that $\mathcal{R}_0^c \notin \mathbb{C} - \{0\}$, as covered in Theorem 4.2 above.

4.3. SEYAR Model Including Relapse Rates. While in the *hepatocytes*, unlike *P. falciparum*, *P. vivax* and *P. Ovale* enter into an additional form called the *hypnozoite*. In the *hypnozoite* stage, the parasite is in a dormant state, resulting in no clinical symptoms displayed in the recovered patients after months or even years, until suddenly resurfacing. In order to properly account for such biological behavior, relapse rates are including into the SEYAR model. The asymptomatic and symptomatic human relapse rates are denoted by λ_{SA} and λ_{SY} , respectively. This slight adjustment yields the following *P. vivax* version of the SEYAR model (4). Listed below is the flow diagram, dynamical system and reproductive threshold corresponding to this model.

In Figure 1, the solid lines represent progression from one compartment to the next, while the dotted stand for the human-mosquito interaction. Humans enter the susceptible compartment either through birth or migration and then progress through each additional compartment subject to the rates described above. These assumptions give rise to the following relapse rate modified SEYAR model IVP (14) describing the dynamics of malaria disease

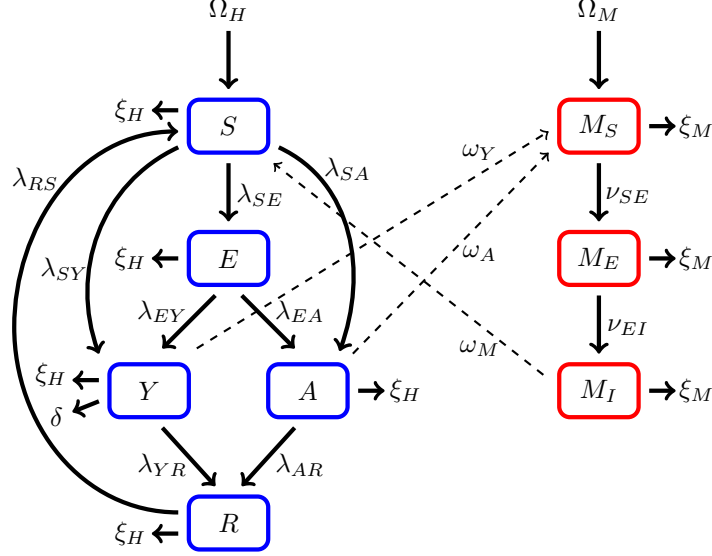


FIGURE 2. Schematic diagram of the SEYAR model including relapse rates

transmission in the human and mosquito populations

$$\left\{ \begin{array}{l} \dot{S} = \Omega_H + \lambda_{RS}R - \left(\sigma\beta_M \frac{M_I}{N_H} + \xi_H \right) S - (\lambda_{SA} + \lambda_{SY})S, \\ \dot{E} = \sigma\beta_M \frac{M_I}{N_H} S - (\gamma + \xi_H)E, \\ \dot{Y} = \gamma(1 - u(\varepsilon))E - (\xi_H + \delta + \lambda_{YR})Y + \lambda_{SY}S, \\ \dot{A} = \gamma u(\varepsilon)E - (\lambda_{AR} + \xi_H)A + \lambda_{SA}S, \\ \dot{R} = \lambda_{AR}A + \lambda_{YR}Y - (\lambda_{RS} + \xi_H)R, \\ \dot{M}_S = \Omega_M - \left(\xi_M + \sigma\beta_Y \frac{Y}{N_H} + \sigma\beta_A \frac{A}{N_H} \right) M_S, \\ \dot{M}_E = \sigma \left(\beta_Y \frac{Y}{N_H} + \beta_A \frac{A}{N_H} \right) M_S - (\xi_M + \tau) M_E, \\ \dot{M}_I = \tau M_E - \xi_M M_I, \\ (S_0, E_0, Y_0, A_0, R_0, M_{S_0}, M_{E_0}, M_{I_0})^T \in \mathbb{R}_+^8 \text{ such that } E_0 \leq \vartheta N_0, \end{array} \right.$$

where u and ϑ are defined by equations (2) and (3), respectively. The model parameters and initial data restrictions are the same as in the original model. Moreover, the results of the mathematical analysis concerning the issues of well-posedness and nonlinear stability are similar to that of the original model. For example, listed below is a lemma regarding the LAS of the DFE for the above model variation.

Lemma 3. (Local Asymptotic Stability of the DFE for the SEYAR Model Including Relapse Rates) Define the following quantity

$$(14) \quad \mathcal{R}_0 := \sqrt{\frac{\sigma^2 \tau \gamma \Omega_M \xi_H \beta_M}{\xi_M^2 (\gamma + \xi_H) (\tau + \xi_M) \Omega_H} \left(\frac{\beta_A U_{low}}{\lambda_{AR} + \xi_H} - \frac{\beta_Y (U_{low} - 1)}{\lambda_{YR} + \xi_H + \delta} \right)},$$

where $U_{low} := e^{\varepsilon_0} (u_{low} - u_{high}) + u_{high}$. Then, the DFE \mathbf{x}_{dfc} for the SEYAR model including relapse rates (14) is locally asymptotically stable provided that $\mathcal{R}_0 < 1$ and unstable if $\mathcal{R}_0 > 1$.

Therefore, the modified system has the same reproductive threshold as the original. This is due to the fact that the sub-matrices of the Jacobian F and V , resulting from the block matrix partitioning technique utilized in the next generation method, are unaffected by this minor modification. Therefore, the results regarding the LAS of the DFE corresponding to the new system are inherited from the original. Additionally, the control-modified

system is given by

$$\begin{cases} \dot{S} = \Omega_H + \lambda_{RS}R - \left(\sigma\beta_M \frac{M_L}{N_H} + \xi_H \right) S - (\lambda_{SA} + \lambda_{SY})S, \\ \dot{E} = \sigma\beta_M \frac{M_L}{N_H} S - (\gamma + \xi_H)E, \\ \dot{Y} = \prod_{j=1}^m \left(1 - V_f^j V_p^j \right) \gamma(1 - u(\varepsilon))E - (\xi_H + \delta + \lambda_{YR})Y + \lambda_{SY}S, \\ \dot{A} = \prod_{j=1}^m \left(1 - V_f^j V_p^j \right) \gamma u(\varepsilon)E - (\lambda_{AR} + \xi_H)A + \lambda_{SA}S, \\ \dot{R} = \lambda_{AR}A + \lambda_{YR}Y - (\lambda_{RS} + \xi_H)R, \\ \dot{M}_S = \Omega_M - \left(\xi_M + \prod_{i=1}^k \rho_f^i \rho_p^i \|\xi_i\|_\infty + \sigma \prod_{i=1}^n \left(1 - \rho_f^i \rho_p^i \right) \beta_Y \frac{Y}{N_H} + \sigma \prod_{i=1}^n \left(1 - \rho_f^i \rho_p^i \right) \beta_A \frac{A}{N_H} \right) M_S, \\ \dot{M}_E = \sigma \prod_{i=1}^n \left(1 - \rho_f^i \rho_p^i \right) \left(\beta_Y \frac{Y}{N_H} + \beta_A \frac{A}{N_H} \right) M_S - \left(\xi_M + \prod_{i=1}^k \rho_f^i \rho_p^i \|\xi_i\|_\infty + \tau \right) M_E, \\ \dot{M}_I = \tau M_E - \left(\xi_M + \prod_{i=1}^k \rho_f^i \rho_p^i \|\xi_i\|_\infty \right) M_I. \end{cases}$$

Remark 4.3. The above modification attests to the delicate relationship between the compartmentalized modeling of infectious diseases and the next generation approach. As we have seen in the above example, the reproductive threshold for a given compartmentalized model is not unique. Some of the most useful information one can obtain from such models resides in various threshold quantities. The reproductive threshold contains important information concerning the long-time behavior (stability) of the underlying model, not the local dynamics. Thus, it stands to reason that any two given compartmentalized epidemiological models may possess very different short-time (local) behavior, but can exhibit similar long-time (global) behavior. This troublesome fact suggests that good modeling lies in the delicate compromise between introducing terms which result in interesting local behavior that describe the disease dynamics accurately to some degree, while simultaneously resulting in the long-time behavior of the model under consideration containing new and useful information. For example, the modification introduced in this section which resulted in a variant of the SEYAR model including relapse rates had no affect on the long-time dynamics, as the reproductive threshold was identical to the original version. However, clearly the new terms incorporated into the system will result in different local behavior. This attest to the fact that good modeling does not just depend on adding more terms and, as a result, over complicating the model. Some of the most important and useful information to be extrapolated from such models depends on certain threshold quantities that can be invariant under a given modification. As we have seen in the above example, the most important information, i.e. the reproductive threshold was shown to be invariant under the modification concerning relapse rates. To have an affect on the reproductive threshold, one would have to go back to the original epidemiological assumptions on which the model was built, e.g. re define what the infected states are. For example, if the recovered class R was considered to be an infected state in the SEYAR model formulation, then the reproductive threshold would be different. Extreme care should be taken when deriving or altering such a model, so that the new modification brings new and useful information to the foreground while simultaneously not over complicating the situation for no additional gain.

5. SENSITIVITY ANALYSIS AND NUMERICAL RESULTS

5.1. Sensitivity Analysis. Errors are usually present in data collection and presumed parameter values. In this section, a sensitivity analysis is applied to classify the parameters which have the highest impact on the reproductive threshold \mathcal{R}_0 . This provides a way to determine which parameter values should be targeted by intervention strategies. A parameter with a relatively large sensitivity index should be estimated with precision, while a parameter with a relatively small sensitivity index does not require as much effort.

Let Θ be defined as in Section 3.3, then it is of trivial consequence that $\mathcal{R}_0 \in C^1(\Theta)$. Due to this fact and that we have an explicit expression for \mathcal{R}_0 of the SEYAR model (4), we arrive at the following definition.

Definition 2. (Sensitivity Index of the Reproductive Threshold [12]) Consider the reproductive threshold $\mathcal{R}_0 \in C^1(\Theta)$ given by equation (6) in Section 3.2 and let $\{e_i : 1 \leq i \leq 14\}$ be the canonical basis in \mathbb{R}^{14} . For $\tilde{\rho} \in \Theta$ define $\rho_i := \langle e_i, \tilde{\rho} \rangle$, where $\langle \cdot, \cdot \rangle$ denotes the inner product in 14-dimensional Euclidean space, then the normalized forward sensitivity index of \mathcal{R}_0 with respect to the parameter ρ_i is defined by the following differential equation

$$\Upsilon_{\rho_i}^{\mathcal{R}_0} := \frac{\partial \mathcal{R}_0}{\partial \rho_i} \times \frac{\rho_i}{\mathcal{R}_0}.$$

The normalized forward sensitivity index provides a way to quantify the relative change in the given expression when the parameter changes. The sensitivity index is well-defined provided that \mathcal{R}_0 is at least in C^1 with

respect to each parameter ρ_i . The analytic formulas for the sensitivity indices are complex and do not offer much qualitative insight, as a result we evaluate the indices at the parameter values corresponding to each location. Listed below are tables containing the sensitivity indices of \mathcal{R}_0 for the *SEYAR* model (4) evaluated at the parameter values given in Section 7.6. The parameters are ordered from the most sensitive to the least.

Parameter	Sensitivity Index
ξ_M	-1.27500
σ	+1
Ω_M	+0.5
β_M	+0.5
Ω_H	-0.49999
β_Y	+0.49369
U_{low}	-0.48739
λ_{YR}	-0.37495
ξ_H	+0.30742
τ	+0.27499
β_A	+0.00630
λ_{AR}	-0.00610
γ	+0.00027
δ	-0.00001

TABLE 2. Kaduna

Parameter	Sensitivity Index
ξ_M	-1.25000
σ	+1
Ω_M	+0.5
β_M	+0.5
Ω_H	-0.50000
β_Y	+0.493906
U_{low}	-0.487812
λ_{YR}	-0.389920
ξ_H	+0.332370
τ	+0.250000
β_A	+0.006093
λ_{AR}	-0.005935
γ	+0.001608
δ	-0.000007

TABLE 3. Namawala

Parameter	Sensitivity Index
ξ_M	-1.291666
σ	+1
Ω_M	+0.5
β_M	+0.5
Ω_H	-0.499999
β_Y	+0.493975
U_{low}	-0.487951
λ_{YR}	-0.395175
ξ_H	+0.341059
τ	+0.291666
β_A	+0.006024
λ_{AR}	-0.005877
γ	+0.001355
δ	-0.000006

TABLE 4. Butelgut

The sensitivity analysis conducted on the reproductive threshold of the model above shows that the most sensitive parameters are the mosquito mortality rate ξ_M and the man biting rate σ . Conversely, the least sensitive are the mean duration of the human latent period γ and disease-induced death rate for humans δ . The sensitivity indices listed in the above tables can be viewed as growth measurements of the reproductive threshold with respect to the parameter under consideration. Without loss of generality, focus is turned to the Kaduna location. Concerning Kaduna, an increase in ξ_M by 10% will result in a decrease in \mathcal{R}_0 by 12.75%. Similarly, an increase in σ by 10% will cause a 10% increase in \mathcal{R}_0 . Also, it is worth noting the asymptomatic recovery and effective contact rates λ_{AR} and β_A are relatively less sensitive than the symptomatic human related terms λ_{YR} and β_Y . Furthermore, an increase in Ω_M by 10% results in an increase of \mathcal{R}_0 by approximately 5% and a 10% decrease in Ω_H will cause a 5% increase in \mathcal{R}_0 . These numerical observations are consistent with the qualitative analysis presented in Section 3.3.

It should be noted that definition (2) is pointwise, thus the ordering of the hierarchy is dependent on the relative sizes of the parameter values. The hierarchy of sensitivity that the *SEYAR* model parameters obey is common among many compartmentalized homogeneous population malaria models appearing in literature, e.g. [12, 51]. The two most sensitive parameters correspond to the vector population. These parameters have the property that one is directly proportional to the reproductive number while one is inversely proportional. Increasing the mosquito death rate will also reduce the man biting rate, as the average mosquito life span is shortened. This is beneficial from a practical standpoint, as the parameter which is desirable to increase has the additional effect of decreasing the parameter that is desirable to decrease. Theoretically, this aids in the designing of programs for disease control, as it isolates the parameters that should be targeted for reduction by intervention strategies. Insecticide-treated bed nets and indoor residual spraying are among the most common methods used for such purposes. In Section 4.2 these control measures are incorporated into the model in a generalized setting.

Remark 5.1. (*Verification of the numerical quantities listed in the above tables*) A verification of the numerical entries in the tables displayed above is provided utilizing Maple software in the electronic supplementary material.

5.2. Numerical Results. Displayed below is a table containing numerical values for the following: (i) the parameter configuration space classification $C_1 - C_2$, introduced via definition (1) in Section 3.2, (ii) the *EIR* corresponding to each location, as discussed in Section 4.1, (iii) the reproductive threshold accounting for asymptomatic carriers \mathcal{R}_A , given by equation (6), and (iv) the reproductive threshold neglecting asymptomatic

carriers \mathcal{R}_Y , as discussed in Section 3.3. These numerical values correspond to the following three high transmission sites: Kaduna in Nigeria, Namawala in Tanzania, and Butelgut in Papua New Guinea. The parameter values associated with each site are listed in Section 7.6.

TABLE 5. *EIR* and Threshold Quantities

Site	Classification	<i>EIR</i>	\mathcal{R}_A	\mathcal{R}_Y
Kaduna	<i>A-dominant</i> /-6.00*	120 [‡]	393.05 [†]	390.56 ^{††}
Namawala	<i>A-dominant</i> /-6.24*	329 ^{‡‡}	68.38 [†]	67.96 ^{††}
Butelgut	<i>A-dominant</i> /-6.32*	517 [§]	81.12 [†]	80.63 ^{††}

* These quantities were calculated from definition (1) in Section 3.2.

‡ This value was taken from [55].

‡‡ This value was taken from [60].

§ This value was calculated in [34], using data obtained from the following sources [9, 31].

† These quantities were calculated from equation (6) assuming that the initial exposed proportion is zero, i.e. $\varepsilon_0 = 0$.

†† These quantities were calculated by setting the asymptomatic progression rates equal to zero.

One should observe that the size of the reproductive thresholds for the three sites under consideration are consistent with the sizes of the corresponding entomological inoculation rate values. Regions with a relatively large *EIR* value also have relatively large \mathcal{R}_0 values. As mentioned in Section 4.2, in areas with large reproductive thresholds it is unlikely that one single control measure will be sufficient to stop the disease expansion. Additionally the threshold quantities \mathcal{R}_A and \mathcal{R}_Y obey the theoretical estimate provided in Theorem (3.3). Therefore neglecting to account for asymptomatic carriers results in an underestimation of the reproductive threshold corresponding to each location. The theoretical estimate provided in Theorem (3.3) holds for all possible positive epidemiologically reasonable quantities. Furthermore, the numerical entries displayed in the tables of Section 5.1 and those listed in Table 5 are pointwise evaluations. As mentioned in Section 3.2, there have been reports which indicate that asymptomatic carriers in a given population may transmit the disease at a higher rate than the symptomatic. In this case, the sensitivity hierarchy will possess a different ordering and the size differences in the threshold quantities displayed above will be larger.

Remark 5.2. (*Verification of the numerical threshold quantities listed in Table 5*) A verification of the numerical threshold quantities presented in Table 5 is provided utilizing Maple software in the electronic supplementary material.

6. CONCLUSIONS AND DISCUSSIONS

This study clearly shows that the existence of asymptomatic individuals results in a strict underestimation of \mathcal{R}_0 , and provides the means to quantify this influence. It also provides the means to study NAI as the factor that drives asymptomaticity. As mentioned in [23], the exploration of NAI is key to the rational development and deployment of vaccines and other malaria control methods corresponding to any given population at risk. Therefore, it is a necessary foundation upon to build strategies of eradication by any means.

The *SEYAR* model (4) accounts for the impact that the exposure dependent naturally acquired immune proportion has on asymptomatic carriers and malaria disease transmission dynamics. Through making use of the IVP (1), the infected compartment I is effectively decomposed into two mutually disjoint sub-compartments accounting for symptomatic and asymptomatic individuals. This results in a model which does not fall into a sub-class of the type studied in [28]. Current asymptomatic models appearing in literature are formed by inserting a state invariant constant control parameter or a sum of transcendental expressions involving various state invariant immunity acquisition rates. The *SEYAR* model is derived by a separation through means of the NAI proportion of a population which depends on exposure through equation (2). After deriving the model and addressing the issues of well-posedness and stability analysis, a nonlinear stability analysis is performed in which the bifurcation behavior of the model is characterized. A sensitivity analysis is carried out and generalized control measures are introduced in the model. Moreover, numerical values of various quantities discussed throughout this work are provided for the following three high transmission sites: Kaduna in Nigeria,

Namawala in Tanzania, and Butelgut in Papua New Guinea. A brief summary of highlights drawn from the conclusions of this work is presented in the form of a list below.

- (1) In Section 3.1 it was shown that the *SEYAR* model (4) is mathematically and epidemiologically well-posed provided the initial data satisfied suitable regularity assumptions. Additionally, in theorem (3.2) a mathematically precise and epidemiologically reasonable lower bound for the feasible region of the model was provided.
- (2) In Lemma (1) of Section 3.2 the *SEYAR* model (4) was shown to satisfy the threshold condition. Moreover, \mathcal{R}_0 was decomposed into a product to properly analyze the size contribution of each factor involved. Provided that the mosquito mortality rate ξ_M can be made large enough so that the term C_0 comprised of fractional multipliers is sufficiently small, i.e. $C_0 < 1$, then the size of \mathcal{R}_0 is completely determined by the human-dependent factor r_6 , defined in remark (vi), which consists of a weighted difference of vital dynamics with the NAI proportion, recovery and death rates. Motivated by the monotonic behavior of \mathcal{R}_0 , a formal characterization of the parameter configuration space was introduced via definition (1).
- (3) In Section 3.3 an estimate is provided which characterizes the impact that the asymptomatic class has on the reproductive threshold. More precisely, it was shown that neglecting asymptomatic carriers results in an underestimation of the threshold.
- (4) In Section 3.4, use is made of Theorem (7.2) to show the existence of nontrivial sub-threshold equilibrium solutions near the DFE. More precisely, it was shown that the bifurcation experienced by the *SEYAR* model (4) is forward or backward depending on the size of an auxiliary threshold parameter Λ defined by (9). As it is desirable for no endemic equilibrium states to arise while $\mathcal{R}_0 < 1$, we impose the additional requirement that $\Lambda < 1$.
- (5) In Section 5.1, a sensitivity analysis is conducted on the reproductive number of the model for parameter configurations corresponding to high transmission settings. Additionally, tables are provided containing the sensitivity indices of \mathcal{R}_0 with respect to each parameter. An ordering of the parameters from the most sensitive to least revealed that the most sensitive parameters were the mosquito mortality rate ξ_M and man biting rate σ . The least sensitive are the human mean latent period γ and the disease-induced human death rate δ . Additionally, the asymptomatic recover and effective contact rates λ_{AR} and β_A were shown to be relatively less sensitive than the symptomatic human related terms λ_{YR} and β_Y .
- (6) In Section 5.2 numerical results corresponding to the three high transmission sites mentioned above are provided. The numerical values of the threshold quantities were shown to be consistent with the theory presented in Section 3.3. As the sites of interest are high transmission areas with relatively high entomological inoculation rates, the reproductive thresholds were shown to be comparably large.

As directions of future research, it will be interesting to apply the method of decomposing the infected compartment by means of the related rate IVP (1) in Section 2 to other infectious diseases where asymptomatic individuals play a fundamental role on the dynamical behavior. Additionally, it will be informative to consider extensions of the *SEYAR* model formed by incorporating the other kinds of immunity mentioned in the introduction. Furthermore, it will be beneficial to introduce additional control measures into the models, such as aerial fogging and a time-dependent treatment rate of symptomatic carriers. In conclusion, the *SEYAR* model (4) has provided us with a precise mathematical understanding of the relationship between the exposure dependent nature of NAI and asymptomatic malaria disease transmission dynamics.

ACKNOWLEDGMENTS

Research reported in this publication was supported by a National Institute of Allergy and Infectious Diseases cooperative agreement of the National Institutes of Health under award number U19AI089702-01.

7. APPENDIX

This section of the appendix contains formal proofs of the lemmas and theorems presented in Section 3. Listed below is an overview of the notation and mathematical framework utilized in the proofs. For an in-depth look into the function classes utilized in this work, and many other closely related topics in the field of harmonic analysis, the reader is referred to [27, 30].

7.1. Notation and Mathematical Framework. Firstly, let $\mathbb{R}_+ := \{x \in \mathbb{R} : x \geq 0\}$ be the space of non-negative real numbers and dt denote the Lebesgue measure for any complex-valued measurable function φ . The

$L^1(\mathbb{R}_+)$ norm of φ is defined as

$$\|\varphi\|_1 := \int_0^\infty |\varphi| dt.$$

Extensive use is made of the space of essentially bounded functions $L^\infty(\mathbb{R}_+)$ characterized by the following norm

$$\|\varphi\|_\infty = \text{ess sup}_{t \in \mathbb{R}_+} |\varphi| := \inf \{B > 0 : dt(\{t \geq 0 : |\varphi| > B\}) = 0\}.$$

Analogously to the case of the essential supremum, the essential infimum is defined as

$$\text{ess inf}_{t \in \mathbb{R}_+} \|\varphi\| := \sup \{B > 0 : dt(\{t \geq 0 : |\varphi| < B\}) = 0\}.$$

Some of the proofs require at least a bounded first derivative, however a general $\varphi \in C^1(\mathbb{R}_+)$ is not bounded. Due to this fact, we need to restrict our analysis to a smaller space possessing a higher degree of regularity. The most natural space to turn to is the sub-space denoted $C_b^1(\mathbb{R}_+) \subset C^1(\mathbb{R}_+)$. This is the Banach space of bounded continuous functions whose first derivative is also bounded, endowed with the norm

$$C_b^1(\mathbb{R}_+) := \{\varphi \in C^1(\mathbb{R}_+) : \|\varphi\|_{C_b^1} := \|\varphi\|_\infty + \|\dot{\varphi}\|_\infty < +\infty\}.$$

The convolution of two functions is defined as $\varphi_1 * \varphi_2(t) = \int_0^t \varphi_1(\tau) \varphi_2(t - \tau) d\tau$. Whenever $\varphi_1 * \varphi_2(t) \in L^1(\mathbb{R}_+)$ the integral is finite and, as a result, well-defined.

7.2. Survival Analysis. Let T be a non-negative continuous random variable, standing for survival time, with probability density function $z(t)$ and cumulative distribution function $Z(t) := P\{T < t\}$. Define the survival function to be

$$\begin{aligned} \nu(t) &:= P\{T \geq t\}, \\ &= 1 - Z(t), \\ &= \int_t^\infty z(x) dx. \end{aligned}$$

In the above, Z represents the probability that the event of interest has occurred by duration t . In the context of mosquito survivorship, the event of interest is death and the waiting time is survival time. As a result, T stands for the waiting time until death occurs. It then stands to reason to define the survival function ν as the complement of Z . It follows that ν gives the probability of being alive just before duration t , or in other words, the probability that death has not occurred by duration t . The probability of dying on or before $t + \Delta t$, given survival to age t is $P\{T < t + \Delta t | T \geq t\}$. An alternative characterization the distribution T is given in terms of the hazard function $\xi_M(t)$ (or force of mortality), which quantifies the instantaneous rate of occurrence of death

$$\xi_M(t) := \lim_{\Delta t \rightarrow 0^+} \frac{P\{T < t + \Delta t | T \geq t\}}{\Delta t}.$$

The mosquito mortality rate ξ_M was chosen for convenience and the derivation for the corresponding human rate is similar. The numerator is the conditional probability that death will occur on or before time $t + \Delta t$, provided that it has not previously occurred, and the denominator is an infinitesimal increment of time. A straightforward calculation yields

$$\begin{aligned} \xi_M(t) &:= \lim_{\Delta t \rightarrow 0^+} \frac{P\{T < t + \Delta t | T \geq t\}}{\Delta t}, \\ &= \lim_{\Delta t \rightarrow 0^+} \frac{P\{t \leq T < t + \Delta t\}}{P\{T \geq t\} \Delta t}, \\ &= \lim_{\Delta t \rightarrow 0^+} \frac{Z(t + \Delta t) - Z(t)}{\nu(t) \Delta t}, \\ &= \frac{z(t)}{\nu(t)}, \\ &= -\frac{d}{dt} \ln \nu(t). \end{aligned}$$

The above equation implies that the rate of occurrence of death at duration t is equivalent to the density of deaths at t , divided by the probability of surviving to that duration without dying. Upon integrating from 0 to t and imposing the boundary condition $\nu(0) = 1$, which makes sense, since death surely has not occurred by

time 0. Placing this together, we arrive at an explicit formula for the probability of being alive up to duration t which has functional dependence on the hazard function for all duration up to t :

$$\nu(t) := e^{-\int_0^t \xi_M(s)ds}.$$

The hazard function is constant, i.e. $\xi_M(t) \equiv \xi_M$, under the assumption of constant risk over time. Thus, the survival function corresponding to the mosquito population is

$$(15) \quad \nu(t) = e^{-\xi_M t}.$$

This is a temporally dependent exponential distribution with mosquito mortality parameter ξ_M . Additionally, the expected value of T is given by the integral equation

$$\mathbb{E}(T) := \int_0^\infty tz(t)dt.$$

By definition, we must have $\int_0^\infty z(t)dt = 1$. Weighting an average by a function which does not integrate to unity, i.e. $\int_0^\infty z(t)dt \neq 1$, is accomplished by forcing the weighting function to behave like a probability measure by the common normalization technique, similar to that used in V of Section 4.1. More precisely,

$$\tilde{\mathbb{E}}(T) := \frac{\int_0^\infty tz(t)dt}{\int_0^\infty z(t)dt}.$$

7.3. Proofs.

7.3.1. Proof of Theorem 3.1 (See page 5).

Proof. In view of the well-posedness of the SEYAR model (4), it follows that the continuous composition of functions $u(t) = (u \circ \varepsilon)(t)$ solves the IVP (1) for all $\varepsilon \in C^2(\mathbb{R}_+)$ in the solution space. By the non-negativity of ε , if the the initial data ε_0 is such that

$$e^{\varepsilon_0}(u_{low} - u_{high}) + u_{high} \geq 0,$$

then the solution $u \in C^2(\mathbb{R}_+)$ is non-negative for all $t \in \mathbb{R}_+$. The above inequality is satisfied provided $\varepsilon_0 \leq \vartheta$ for ϑ defined by equation (3) in Section 2. \square

7.4. Proofs.

7.4.1. Proof of Theorem 3.1 (See page 8).

Proof. The functions under consideration represent bounded, continuous, smoothly-varying, non-negative biological quantities. Consequently, it is reasonable to assume that $\mathbf{x} \in C_b^1(\mathbb{R}_+)$. This reasoning combined with the fact that the vector field $\Phi \in C^1$ is locally Lipschitz implies the existence of a unique solution \mathbf{x} . Moreover, the solution \mathbf{x} depends continuously on the initial data and model parameters and can be continued to a maximal time interval, cf. [56]. \square

7.4.2. Proof of Theorem 3.2 (See page 8).

Proof. The case for the mosquito population is trivial, viz.

$$\lim_{t \rightarrow +\infty} N_M(t) = \frac{\Omega_M}{\xi_M}.$$

For the human population, let $L_t = e^{\int_0^t \xi_H ds} = e^{\xi_H t}$, so that

$$\begin{aligned} (L_t \dot{N}_H) &= L_t \Omega_H - \delta L_t Y, \\ L_t N_H(t) &= N_H(0) + \int_0^t L_s \Omega_H ds - \delta \int_0^t L_s Y(s) ds, \\ &= N_H(0) + \Omega_H \left(\frac{e^{\xi_H t}}{\xi_H} - \frac{1}{\xi_H} \right) - \delta \int_0^t e^{\xi_H s} Y(s) ds. \end{aligned}$$

Therefore, the explicit solution is given by

$$N_H(t) = e^{-\xi_H t} N_H(0) + \frac{\Omega_H}{\xi_H} (1 - e^{-\xi_H t}) - \delta \int_0^t e^{-\xi_H(t-s)} Y(s) ds,$$

or in operator form

$$N_H(t) = L_{-t} N_H(0) + \frac{\Omega_H}{\xi_H} (1 - L_{-t}) - \delta L_{-t} * Y(t).$$

After passing to the limit, it follows that

$$(16) \quad \lim_{t \rightarrow +\infty} N_H(t) = \frac{\Omega_H}{\xi_H} - \delta \lim_{t \rightarrow +\infty} L_{-t} * Y(t).$$

In the absence of symptomatic infection, i.e. $Y = 0$, it follows that $L_{-t} * Y(t) = 0$, so that

$$\lim_{t \rightarrow +\infty} N_H(t) = \frac{\Omega_H}{\xi_H}.$$

As expected, N_H asymptotes to the equilibrium population density of the human population. If symptomatic infection occurs in the population, by Hölders inequality it follows that

$$\begin{aligned} L_{-t} * Y(t) &\leq \|Y\|_\infty \|L_{-(t-s)}\|_1, \\ &= \|Y\|_\infty \int_0^t e^{-\xi_H(t-s)} ds, \\ &= \|Y\|_\infty \left[\frac{1}{\xi_H} - \frac{e^{-\xi_H t}}{\xi_H} \right]. \end{aligned}$$

Where the right-hand side of the above inequality is finite due to the assumption that $Y \in C^2(\mathbb{R}_+) \cap C_b^1(\mathbb{R}_+) \subset L^\infty(\mathbb{R}_+)$. By letting $t \rightarrow +\infty$ we arrive at the following estimate for the forcing term

$$\lim_{t \rightarrow +\infty} L_{-t} * Y(t) \leq \frac{\|Y\|_\infty}{\xi_H}.$$

The above estimate in combination with (16) yields the following lower bound

$$\lim_{t \rightarrow +\infty} N_H(t) \geq \frac{\Omega_H}{\xi_H} - \delta \frac{\|Y\|_\infty}{\xi_H}.$$

Therefore,

$$\lim_{t \rightarrow +\infty} N_H(t) \in \left[\frac{\Omega_H - \delta \|Y\|_\infty}{\xi_H}, \frac{\Omega_H}{\xi_H} \right].$$

Furthermore, for system (5) it follows that

$$\dot{N}_H \leq \Omega_H - \xi_H N_H = \xi_H \left(\frac{\Omega_H}{\xi_H} - N_H \right).$$

Combining the above observation with a similar argument for N_M yields

$$(17) \quad \begin{cases} \dot{N}_H \leq 0, & \text{if } N_H \geq \frac{\Omega_H}{\xi_H}, \\ \dot{N}_M \leq 0, & \text{if } N_M \geq \frac{\Omega_M}{\xi_M}. \end{cases}$$

Inequalities (17) imply that if the solution leaves the region Γ , then its derivative will instantaneously become negative, forcing it back to Γ . Moreover, if $x_i(0) = 0$ for any $1 \leq i \leq 8$ in system (4), then it directly follows that $\dot{x}_i \geq 0$. Therefore, all trajectories tend to Γ and are forward invariant. Due to this fact it is sufficient to study the dynamics of the system on the smaller compact sub-space Γ . \square

7.4.3. Proof of Lemma 1 (See page 9).

Proof. Firstly, we order the compartments so that the first five correspond to infected individuals and denote $\mathbf{w} = (E, Y, A, M_E, M_I, R, S, M_S)^T$. The corresponding DFE is

$$\mathbf{w}_{dfe} = \left(0, 0, 0, 0, 0, 0, \frac{\Omega_H}{\xi_H}, \frac{\Omega_M}{\xi_M} \right)^T.$$

Following the next generation method, system (4) is rewritten in the following form

$$\dot{\mathbf{w}} = \Phi(\mathbf{w}) = \mathcal{F}(\mathbf{w}) - \mathcal{V}(\mathbf{w}),$$

where $\mathcal{F} := (\mathcal{F}_1, \dots, \mathcal{F}_8)^T$ and $\mathcal{V} := (\mathcal{V}_1, \dots, \mathcal{V}_8)^T$, or more explicitly

$$\begin{pmatrix} \dot{E} \\ \dot{Y} \\ \dot{A} \\ \dot{M}_E \\ \dot{M}_I \\ \dot{R} \\ \dot{S} \\ \dot{M}_S \end{pmatrix} = \begin{pmatrix} \sigma\beta_M \frac{M_I}{N_H} S \\ 0 \\ 0 \\ \frac{\sigma(\beta_Y Y + \beta_A A)}{N_H} M_S \\ 0 \\ 0 \\ 0 \\ 0 \end{pmatrix} - \begin{pmatrix} (\gamma + \xi_H)E \\ -\gamma(1 - u(\varepsilon))E + (\xi_H + \delta + \lambda_{YR})Y \\ -\gamma u(\varepsilon)E + (\lambda_{AR} + \xi_H)A \\ (\xi_M + \tau)M_E \\ -\tau M_E + \xi_M M_I \\ -\lambda_{AR}A - \lambda_{YR}Y + (\lambda_{RS} + \xi_H)R \\ -\Omega_H - \lambda_{RS}R + \left(\sigma\beta_M \frac{M_I}{N_H} + \xi_H\right)S \\ -\Omega_M + \left(\xi_M + \frac{\sigma(\beta_Y Y + \beta_A A)}{N_H}\right)M_S \end{pmatrix}.$$

In addition, the matrix \mathcal{V} admits the decomposition $\mathcal{V} = \mathcal{V}^- - \mathcal{V}^+$, where the component-wise definition is inherited. Biologically speaking: \mathcal{F}_i is the rate of appearance of new infections in compartment i , \mathcal{V}_i^+ stands for the rate of transfer of individuals into compartment i by any other means and \mathcal{V}_i^- is the rate of transfer of individuals out of compartment i . It is easy to see that $\mathcal{F}, \mathcal{V}^-, \mathcal{V}^+$ satisfy assumptions (i)-(v) in Theorem (7.1). As mentioned in the beginning of Section 3.1, to study the stability of the equilibrium points we assume that each of the above vector fields is at least twice-continuously differentiable. Define $U_{low} := e^{\varepsilon_0}(u_{low} - u_{high}) + u_{high}$ and let F and V be the following sub-matrices of the Jacobian of the above system, evaluated at the solution \mathbf{w}_{dfe}

$$F = \left(\frac{\partial \mathcal{F}_i}{\partial x_j} \Big|_{\mathbf{w}_{dfe}} \right)_{1 \leq i, j \leq 5} = \begin{pmatrix} 0 & 0 & 0 & 0 & \sigma\beta_M \\ 0 & 0 & 0 & 0 & 0 \\ 0 & 0 & 0 & 0 & 0 \\ 0 & \sigma\beta_Y \frac{\Omega_M}{\Omega_H} \frac{\xi_H}{\xi_M} & \sigma\beta_A \frac{\Omega_M}{\Omega_H} \frac{\xi_H}{\xi_M} & 0 & 0 \\ 0 & 0 & 0 & 0 & 0 \end{pmatrix}$$

and

$$V = \left(\frac{\partial \mathcal{V}_i}{\partial x_j} \Big|_{\mathbf{w}_{dfe}} \right)_{1 \leq i, j \leq 5} = \begin{pmatrix} (\gamma + \xi_H) & 0 & 0 & 0 & 0 \\ \gamma(U_{low} - 1) & (\xi_H + \delta + \lambda_{YR}) & 0 & 0 & 0 \\ -\gamma U_{low} & 0 & (\lambda_{AR} + \xi_H) & 0 & 0 \\ 0 & 0 & 0 & (\xi_M + \tau) & 0 \\ 0 & 0 & 0 & -\tau & \xi_M \end{pmatrix}.$$

A straight-forward calculation shows that

$$V^{-1} = \begin{pmatrix} (\gamma + \xi_H)^{-1} & 0 & 0 & 0 & 0 \\ -\frac{\gamma(U_{low} - 1)}{(\gamma + \xi_H)(\xi_H + \delta + \lambda_{YR})} & (\xi_H + \delta + \lambda_{YR})^{-1} & 0 & 0 & 0 \\ \frac{\gamma U_{low}}{(\gamma + \xi_H)(\lambda_{AR} + \xi_H)} & 0 & (\lambda_{AR} + \xi_H)^{-1} & 0 & 0 \\ 0 & 0 & 0 & (\xi_M + \tau)^{-1} & 0 \\ 0 & 0 & 0 & \frac{\tau}{\xi_M(\xi_M + \tau)} & \xi_M^{-1} \end{pmatrix}$$

and

$$FV^{-1} = \begin{pmatrix} 0 & 0 & 0 & \frac{\sigma\beta_M \tau}{\xi_M(\xi_M + \tau)} & \frac{\sigma\beta_M}{\xi_M} \\ 0 & 0 & 0 & 0 & 0 \\ 0 & 0 & 0 & 0 & 0 \\ \frac{\sigma\gamma\Omega_M \xi_H}{(\gamma + \xi_H)\Omega_H \xi_M} \left(\frac{\beta_A U_{low}}{\lambda_{AR} + \xi_H} - \frac{\beta_Y(U_{low} - 1)}{\xi_H + \delta + \lambda_{YR}} \right) & \frac{\sigma\beta_Y \Omega_M \xi_H}{(\xi_H + \delta + \lambda_{YR})\Omega_H \xi_M} & \frac{\sigma\beta_A \Omega_M \xi_H}{(\xi_H + \lambda_{AR})\Omega_H \xi_M} & 0 & 0 \\ 0 & 0 & 0 & 0 & 0 \end{pmatrix}.$$

Let \mathcal{I} denote the 5×5 identity matrix, so that the characteristic polynomial $P(\lambda)$ of the matrix FV^{-1} is given by

$$\begin{aligned} P(\lambda) &= \det(FV^{-1} - \lambda\mathcal{I}), \\ &= \lambda^3 \left(\lambda^2 - \left(\frac{\sigma^2\tau\gamma\Omega_M\xi_H\beta_M}{\xi_M^2(\gamma+\xi_H)(\tau+\xi_M)\Omega_H} \left(\frac{\beta_A U_{low}}{\lambda_{AR}+\xi_H} - \frac{\beta_Y(U_{low}-1)}{\lambda_{YR}+\xi_H+\delta} \right) \right) \right). \end{aligned}$$

The solution set is given by

$$\{\lambda_i\}_{1 \leq i \leq 5} = \left\{ 0, 0, 0, \pm \sqrt{\frac{\sigma^2\tau\gamma\Omega_M\xi_H\beta_M}{\xi_M^2(\gamma+\xi_H)(\tau+\xi_M)\Omega_H} \left(\frac{\beta_A U_{low}}{\lambda_{AR}+\xi_H} - \frac{\beta_Y(U_{low}-1)}{\lambda_{YR}+\xi_H+\delta} \right)} \right\}.$$

Therefore, the reproductive threshold for the SEYAR model (4) is given by

$$\begin{aligned} \mathcal{R}_0 &:= \rho(FV^{-1}), \\ &= \max_{1 \leq i \leq 5} \{\lambda_i\}, \\ &= \sqrt{\frac{\sigma^2\tau\gamma\Omega_M\xi_H\beta_M}{\xi_M^2(\gamma+\xi_H)(\tau+\xi_M)\Omega_H} \left(\frac{\beta_A U_{low}}{\lambda_{AR}+\xi_H} - \frac{\beta_Y(U_{low}-1)}{\lambda_{YR}+\xi_H+\delta} \right)}. \end{aligned}$$

The proof of the lemma regarding the local asymptotic stability (LAS) of the DFE \mathbf{w}_{dfe} corresponding to the SEYAR Model (4) is now complete after invoking Theorem (7.1) in Section 7.5. \square

7.4.4. Proof of Theorem 3.3 (See page 12).

Proof. Let Θ_0 , $\tilde{\Theta}_0$, \mathcal{R}_A and \mathcal{R}_Y be defined as in the statement of the theorem. Additionally, denote the following quantities $r_6^0 := r_6|_{\Theta_0}$, $C_1^0 := C_1|_{\Theta_0}$, $C_2^0 := C_2|_{\Theta_0}$ and $C_0^0 := C_0|_{\Theta_0} = C_0|_{\tilde{\Theta}_0}$, where the terms r_6 and C_i for $i = 0, 1, 2$ are defined as in Section 3.2. By the monotonicity of the square root function, it follows that

$$\begin{aligned} \mathcal{R}_A &:= \mathcal{R}_0|_{\Theta_0}, \\ &= C_0^0 \sqrt{r_6^0}, \\ &> C_0^0 \sqrt{r_6^0 - U_{low_0} C_1^0}, \\ &= C_0^0 \sqrt{(1 - U_{low_0}) C_2^0}, \\ &= \mathcal{R}_0|_{\tilde{\Theta}_0}, \\ &:= \mathcal{R}_Y. \end{aligned}$$

\square

7.4.5. Proof of Lemma 2 (See page 14).

Proof. If we consider the dynamical system $\dot{x} = g(x, \omega)$, where ω is a bifurcation parameter and the vector field g is C^2 in both x and ω , then the disease-free equilibrium can be viewed as the manifold $(\mathbf{x}_{dfe}; \omega)$ where the local stability of \mathbf{x}_{dfe} changes at the point $(\mathbf{x}_{dfe}; \omega^*)$. Now we shall investigate the existence and stability of non-trivial equilibrium states in a neighborhood of the bifurcation point. We focus on the disease-free equilibrium \mathbf{x}_{dfe} and study the occurrence of a transcritical bifurcation at $\mathcal{R}_0 = 1$. Since \mathcal{R}_0 consists of the square root of a complicated combination of parameters, it is not practical to use as a bifurcation parameter. However, observe that $\mathcal{R}_0 = 1$ if and only if

$$\begin{aligned} \beta_M &= \frac{\xi_M^2 \Omega_H (\gamma + \xi_H) (\tau + \xi_M) (\lambda_{AR} + \xi_H) (\lambda_{YR} + \xi_H + \delta)}{\sigma^2 \tau \xi_H \Omega_M (\gamma U_{low} \beta_A (\lambda_{YR} + \xi_H + \delta) - \gamma (U_{low} - 1) \beta_Y (\lambda_{AR} + \xi_H))}, \\ &:= \beta_M^*. \end{aligned}$$

In lieu of Lemma (1) it follows that \mathbf{x}_{dfe} is locally asymptotically stable when $\beta_M < \beta_M^*$ and unstable if $\beta_M > \beta_M^*$. Thus, the combination of parameters β_M^* is a bifurcation value. To simplify the notation, we rewrite

system (4) as $\dot{x} = g(x, \beta_M)$ where $\mathbf{x} = (S, E, Y, A, R, M_S, M_E, M_I)^T$ so that x_i is the i^{th} component of \mathbf{x} and $g = (g_1, g_2, g_3, g_4, g_5, g_6, g_7, g_8)^T$, or more explicitly

$$\begin{aligned}
 g_1 &= \Omega_H + \lambda_{RS}x_5 - \left(\sigma\beta_M \frac{x_8}{\sum_i^5 x_i} + \xi_H \right) x_1, \\
 g_2 &= \sigma\beta_M \frac{x_8}{\sum_i^5 x_i} x_1 - (\gamma + \xi_H) x_2, \\
 g_3 &= \gamma(1 - u(\varepsilon)) x_2 - (\xi_H + \delta + \lambda_{YR}) x_3, \\
 g_4 &= \gamma u(\varepsilon) x_2 - (\lambda_{AR} + \xi_H) x_4, \\
 g_5 &= \lambda_{AR} x_4 + \lambda_{YR} x_3 - (\lambda_{RS} + \xi_H) x_5, \\
 g_6 &= \Omega_M - \left(\xi_M + \sigma\beta_Y \frac{x_3}{\sum_i^5 x_i} + \sigma\beta_A \frac{x_4}{\sum_i^5 x_i} \right) x_6, \\
 g_7 &= \sigma \left(\beta_Y \frac{x_3}{\sum_i^5 x_i} + \beta_A \frac{x_4}{\sum_i^5 x_i} \right) x_6 - (\xi_M + \tau) x_7, \\
 g_8 &= \tau x_7 - \xi_M x_8.
 \end{aligned} \tag{18}$$

Denote $J(\mathbf{x}_{\text{dfe}}, \beta_M^*)$ to be the Jacobian of g evaluated at the DFE \mathbf{x}_{dfe} and threshold β_M^* , so that

$$J(\mathbf{x}_{\text{dfe}}, \beta_M^*) = \begin{pmatrix} -\xi_H & 0 & 0 & 0 & \epsilon & 0 & 0 & -\sigma\beta_M^* \\ 0 & -(\gamma + \xi_H) & 0 & 0 & 0 & 0 & 0 & \sigma\beta_M^* \\ 0 & \gamma(1 - U_{\text{low}}) & -(\delta + \lambda_{YR} + \xi_H) & 0 & 0 & 0 & 0 & 0 \\ 0 & \gamma U_{\text{low}} & 0 & -(\lambda_{AR} + \xi_H) & 0 & 0 & 0 & 0 \\ 0 & 0 & \lambda_{YR} & \lambda_{AR} & -(\lambda_{RS} + \xi_H) & 0 & 0 & 0 \\ 0 & 0 & -\frac{\sigma\beta_Y \xi_H \Omega_M}{\Omega_H \xi_M} & -\frac{\sigma\beta_A \xi_H \Omega_M}{\Omega_H \xi_M} & 0 & -\xi_M & 0 & 0 \\ 0 & 0 & \frac{\sigma\beta_Y \xi_H \Omega_M}{\Omega_H \xi_M} & \frac{\sigma\beta_A \xi_H \Omega_M}{\Omega_H \xi_M} & 0 & 0 & -(\tau + \xi_M) & 0 \\ 0 & 0 & 0 & 0 & 0 & 0 & \tau & -\xi_M \end{pmatrix}.$$

If we invoke the following positive change of variables

$$\begin{cases} K_1 = \gamma + \xi_H, \\ K_2 = \gamma(1 - U_{\text{low}}), \\ K_3 = \gamma U_{\text{low}}, \\ K_4 = \delta + \lambda_{YR} + \xi_H, \\ K_5 = \lambda_{AR} + \xi_H, \\ K_6 = \lambda_{RS} + \xi_H, \\ K_7 = \tau + \xi_M, \end{cases}$$

then β_H^* can be written as

$$\beta_M^* = \frac{\xi_M^2 \Omega_H K_1 K_4 K_5 K_7}{\sigma^2 \tau \xi_H \Omega_M (\beta_A K_3 K_4 + \beta_Y K_2 K_5)}.$$

As a result, $J(\mathbf{x}_{\text{dfe}}, \beta_M^*)$ can be written as

$$J(\mathbf{x}_{\text{dfe}}, \beta_M^*) = \begin{pmatrix} -\xi_H & 0 & 0 & 0 & \epsilon & 0 & 0 & -\frac{\xi_M^2 \Omega_H K_1 K_4 K_5 K_7}{\sigma \tau \xi_H \Omega_M (\beta_A K_3 K_4 + \beta_Y K_2 K_5)} \\ 0 & -K_1 & 0 & 0 & 0 & 0 & 0 & \frac{\xi_M^2 \Omega_H K_1 K_4 K_5 K_7}{\sigma \tau \xi_H \Omega_M (\beta_A K_3 K_4 + \beta_Y K_2 K_5)} \\ 0 & K_2 & -K_4 & 0 & 0 & 0 & 0 & 0 \\ 0 & K_3 & 0 & -K_5 & 0 & 0 & 0 & 0 \\ 0 & 0 & \lambda_{YR} & \lambda_{AR} & -K_6 & 0 & 0 & 0 \\ 0 & 0 & -\frac{\sigma\beta_Y \xi_H \Omega_M}{\Omega_H \xi_M} & -\frac{\sigma\beta_A \xi_H \Omega_M}{\Omega_H \xi_M} & 0 & -\xi_M & 0 & 0 \\ 0 & 0 & \frac{\sigma\beta_Y \xi_H \Omega_M}{\Omega_H \xi_M} & \frac{\sigma\beta_A \xi_H \Omega_M}{\Omega_H \xi_M} & 0 & 0 & -K_7 & 0 \\ 0 & 0 & 0 & 0 & 0 & 0 & \tau & -\xi_M \end{pmatrix}.$$

Due to the equivalency of the two conditions $\mathcal{R}_0 = 1$ and $\beta_M = \beta_M^*$, it follows that $J(\mathbf{x}_{\text{dfe}}, \beta_M^*)$ contains information of the linearized system evaluated at the disease-free equilibrium and threshold value. Utilizing the machinery covered in Section 7.5 below, the Jacobian evaluated at the threshold value, i.e. $J(\mathbf{x}_{\text{dfe}}, \beta_M^*)$ has a zero simple eigenvalue with all others having negative real parts. Therefore, the hypothesis of Theorem (7.2) is satisfied. We proceed by calculating the a and b terms (22) and (23) appearing in Theorem (7.2). In observance

of the conclusions in the theorem, it follows that the *SEYAR* model (4) will undergo a super-critical bifurcation if $a > 0$ and $b > 0$ and a sub-critical bifurcation if $a < 0$ and $b > 0$. The main ingredients in calculating a and b are the generalized right and left eigenvectors of the matrix $J(\mathbf{x}_{df}, \beta_M^*)$ and their corresponding non-zero Hessian entries, evaluated at the DFE \mathbf{x}_{df} . In this fashion we let $w = (w_1, w_2, w_3, w_4, w_5, w_6, w_7, w_8)$ and $v^T = (v_1, v_2, v_3, v_4, v_5, v_6, v_7, v_8)^T$ be right and left generalized eigenvectors of $J(\mathbf{x}_{df}, \beta_M^*)$, respectively. Since J is not symmetric, the left and right generalized eigenspaces are not equivalent. Solving the equations $Jw = 0$ and $(v^T J)^T = J^T v = 0$, where $D_i \in \mathbb{R}_{>0}$ for $i = 1, 2$, yields

$$\begin{pmatrix} w_1 \\ w_2 \\ w_3 \\ w_4 \\ w_5 \\ w_6 \\ w_7 \\ w_8 \end{pmatrix} = D_1 \begin{pmatrix} \frac{\epsilon \lambda_{AR} K_3 K_4 + \epsilon \lambda_{YR} K_2 K_5 - K_1 K_6 K_4 K_5}{K_6^2 K_4 K_5} \\ 1 \\ \frac{K_2}{K_4} \\ \frac{K_4}{K_3} \\ \frac{\lambda_{YR} K_2 K_5 + \lambda_{AR} K_3 K_4}{K_4 K_5 K_6} \\ \frac{\sigma \xi_H \Omega_M (\beta_Y K_2 K_5 + \beta_A K_3 K_4)}{\Omega_H \xi_M^2 K_4 K_5} \\ \frac{\sigma \xi_H \Omega_M (\beta_A K_3 K_4 + \beta_Y K_2 K_5)}{\xi_M \Omega_H K_4 K_5 K_7} \\ \frac{\sigma \tau \xi_H \Omega_M (\beta_A K_3 K_4 + \beta_Y K_2 K_5)}{\xi_M^2 \Omega_H K_4 K_5 K_7} \end{pmatrix} \quad \text{and} \quad \begin{pmatrix} v_1 \\ v_2 \\ v_3 \\ v_4 \\ v_5 \\ v_6 \\ v_7 \\ v_8 \end{pmatrix} = D_2 \begin{pmatrix} 0 \\ \frac{\sigma \tau \xi_H \Omega_M (\beta_A K_3 K_4 + \beta_Y K_2 K_5)}{\xi_M \Omega_H K_1 K_4 K_5 K_7} \\ \frac{\sigma \tau \beta_Y \xi_H \Omega_M}{\Omega_H \xi_M K_4 K_7} \\ \frac{\sigma \tau \beta_A \xi_H \Omega_M}{\Omega_H \xi_M K_5 K_7} \\ 0 \\ 0 \\ \frac{\tau}{K_7} \\ 1 \end{pmatrix}.$$

For system (18), the non-zero partial derivatives of g evaluated at \mathbf{x}_{df} are

$$\begin{aligned} \frac{\partial^2 g_1}{\partial x_8 \partial x_2} &= \frac{\partial^2 g_1}{\partial x_8 \partial x_3} = \frac{\partial^2 g_1}{\partial x_8 \partial x_4} = \frac{\partial^2 g_1}{\partial x_8 \partial x_5} = \frac{\sigma \beta_M \xi_H}{\Omega_H}, \\ \frac{\partial^2 g_2}{\partial x_8 \partial x_2} &= \frac{\partial^2 g_2}{\partial x_8 \partial x_3} = \frac{\partial^2 g_2}{\partial x_8 \partial x_4} = \frac{\partial^2 g_2}{\partial x_8 \partial x_5} = -\frac{\sigma \beta_M \xi_H}{\Omega_H}, \\ \frac{\partial^2 g_3}{\partial x_2 \partial x_2} &= \frac{2\gamma \xi_H e^{\varepsilon_0}}{\Omega_H} (u_{low} - u_{high}), \quad \frac{\partial^2 g_4}{\partial x_2 \partial x_2} = \frac{2\gamma \xi_H e^{\varepsilon_0}}{\Omega_H} (u_{high} - u_{low}), \\ \frac{\partial^2 g_6}{\partial x_3 \partial x_1} &= \frac{\partial^2 g_6}{\partial x_3 \partial x_2} = \frac{\partial^2 g_6}{\partial x_3 \partial x_5} = \frac{\sigma \beta_Y \xi_H^2 \Omega_M}{\Omega_H^2 \xi_M}, \\ \frac{\partial^2 g_6}{\partial x_4 \partial x_1} &= \frac{\partial^2 g_6}{\partial x_4 \partial x_2} = \frac{\partial^2 g_6}{\partial x_4 \partial x_5} = \frac{\sigma \beta_A \xi_H^2 \Omega_M}{\Omega_H^2 \xi_M}, \\ \frac{\partial^2 g_6}{\partial x_3 \partial x_3} &= 2 \frac{\partial^2 g_6}{\partial x_3 \partial x_1}, \quad \frac{\partial^2 g_6}{\partial x_4 \partial x_4} = 2 \frac{\partial^2 g_6}{\partial x_4 \partial x_1}, \\ \frac{\partial^2 g_6}{\partial x_6 \partial x_3} &= -\frac{\sigma \beta_Y \xi_H}{\Omega_H}, \quad \frac{\partial^2 g_6}{\partial x_6 \partial x_4} = -\frac{\sigma \beta_A \xi_H}{\Omega_H}, \\ \frac{\partial^2 g_6}{\partial x_3 \partial x_4} &= \frac{\sigma \xi_H^2 \Omega_M (\beta_Y + \beta_A)}{\xi_M \Omega_H^2}, \\ \frac{\partial^2 g_7}{\partial x_3 \partial x_1} &= \frac{\partial^2 g_7}{\partial x_3 \partial x_2} = \frac{\partial^2 g_7}{\partial x_3 \partial x_5} = -\frac{\sigma \beta_Y \xi_H^2 \Omega_M}{\Omega_H^2 \xi_M}, \\ \frac{\partial^2 g_7}{\partial x_4 \partial x_1} &= \frac{\partial^2 g_7}{\partial x_4 \partial x_2} = \frac{\partial^2 g_7}{\partial x_4 \partial x_5} = -\frac{\sigma \beta_A \xi_H^2 \Omega_M}{\Omega_H^2 \xi_M}, \\ \frac{\partial^2 g_7}{\partial x_3 \partial x_3} &= 2 \frac{\partial^2 g_7}{\partial x_3 \partial x_1}, \quad \frac{\partial^2 g_7}{\partial x_4 \partial x_4} = 2 \frac{\partial^2 g_7}{\partial x_4 \partial x_1}, \\ \frac{\partial^2 g_7}{\partial x_6 \partial x_3} &= \frac{\sigma \beta_Y \xi_H}{\Omega_H}, \quad \frac{\partial^2 g_7}{\partial x_6 \partial x_4} = \frac{\sigma \beta_A \xi_H}{\Omega_H}, \\ \frac{\partial^2 g_7}{\partial x_3 \partial x_4} &= -\frac{\sigma \xi_H^2 \Omega_M (\beta_Y + \beta_A)}{\xi_M \Omega_H^2}, \\ \frac{\partial^2 g_1}{\partial x_8 \partial \beta_H} &= -\sigma, \quad \frac{\partial^2 g_2}{\partial x_8 \partial \beta_H} = \sigma. \end{aligned}$$

Due to the fact that the parameter β_M only appears in system (18) twice, the calculation of the b term is less involved. Indeed, for b we have

$$\begin{aligned}
 (19) \quad b &= \sum_{i,k=1}^8 v_k w_i \frac{\partial^2 g_k}{\partial x_i \partial \beta_H} (\mathbf{x}_{dfe}, \beta_M^*) , \\
 &= v_1 w_8 \frac{\partial^2 g_1}{\partial x_8 \partial \beta_M} (\mathbf{x}_{dfe}, \beta_M^*) + v_2 w_8 \frac{\partial^2 g_2}{\partial x_8 \partial \beta_M} (\mathbf{x}_{dfe}, \beta_M^*) , \\
 &= \sigma v_2 w_8 , \\
 &= \frac{\sigma^2 \tau \xi_H \Omega_M (\beta_A K_3 K_4 + \beta_Y K_2 K_5)}{\xi_M \Omega_H K_1 K_4 K_5 K_7} v_8 w_8 , \\
 &= \frac{\sigma^3 \tau^2 \xi_H^2 \Omega_M^2 (\beta_A K_3 K_4 + \beta_Y K_2 K_5)^2}{\xi_M^3 \Omega_H^2 K_1 K_4^2 K_5^2 K_7^2} w_2 v_8 , \\
 &= \frac{\sigma^3 \tau^2 \xi_H^2 \Omega_M^2 (\beta_A K_3 K_4 + \beta_Y K_2 K_5)^2}{\xi_M^3 \Omega_H^2 K_1 K_4^2 K_5^2 K_7^2} D_1 D_2 , \\
 &> 0 .
 \end{aligned}$$

Since $D_i \in \mathbb{R}_{>0}$ for $i = 1, 2$, it follows that b is always positive, hence the bifurcation behavior of system (18) is completely determined by the sign of a . To simplify the pending calculation we invoke the following change of variables

$$\begin{cases} Z_1 = \frac{\sigma \beta_M \xi_H}{\Omega_H}, \\ Z_2 = \frac{\sigma \beta_Y \xi_H^2 \Omega_M}{\Omega_H^2 \xi_M}, \\ Z_3 = \frac{\sigma \beta_A \xi_H \Omega_M}{\Omega_H^2 \xi_M}, \\ Z_4 = \frac{\sigma \xi_H^2 \Omega_M (\beta_Y + \beta_A)}{\xi_M \Omega_H^2}, \\ Z_5 = \frac{\sigma \beta_A \xi_H}{\Omega_H}, \\ Z_6 = \frac{2\gamma \xi_H e^{\varepsilon_0}}{\Omega_H} (u_{high} - u_{low}), \\ Z_7 = \frac{\sigma \beta_Y \xi_H}{\Omega_H}, \\ Q_0 = \frac{\lambda_{YR} K_2 K_5 + \lambda_{AR} K_3 K_4}{K_4 K_5 K_6}, \\ Q_1 = \frac{\beta_Y K_2 K_5 + \beta_A K_3 K_4}{K_4 K_5 K_7}, \\ Q_2 = \frac{\sigma \tau \xi_H \Omega_M \beta_Y}{\Omega_H \xi_M K_4 K_7}, \\ Q_3 = \frac{\sigma \tau \xi_H \Omega_M \beta_A}{\Omega_H \xi_M K_5 K_7}, \\ Q_4 = \frac{\sigma \xi_H \Omega_M}{\Omega_H \xi_M}, \end{cases}$$

so that the generalized eigenvectors can be written as:

$$\begin{pmatrix} w_1 \\ w_2 \\ w_3 \\ w_4 \\ w_5 \\ w_6 \\ w_7 \\ w_8 \end{pmatrix} = D_1 \begin{pmatrix} \frac{\lambda_{RS} Q_0 - K_1}{K_6} \\ 1 \\ \frac{K_2}{K_4} \\ \frac{K_3}{K_5} \\ Q_0 \\ -\frac{Q_4 Q_1 K_7}{\xi_M} \\ Q_4 Q_1 \\ \frac{\tau Q_4 Q_1}{\xi_M} \end{pmatrix} \quad \text{and} \quad \begin{pmatrix} v_1 \\ v_2 \\ v_3 \\ v_4 \\ v_5 \\ v_6 \\ v_7 \\ v_8 \end{pmatrix} = D_2 \begin{pmatrix} 0 \\ \frac{\tau Q_4 Q_1}{K_1} \\ Q_2 \\ Q_3 \\ 0 \\ 0 \\ \frac{\tau}{K_7} \\ 1 \end{pmatrix} .$$

In view of the relatively strong regularity assumptions mentioned in the beginning of Section 3.1 and natural symmetry of the system, it follows that $\frac{\partial^2 g_k}{\partial x_i \partial x_j} v_k w_i w_j = \frac{\partial^2 g_k}{\partial x_j \partial x_i} v_k w_j w_i$ for all $1 \leq i, j \leq 8$. Furthermore, $\frac{\partial^2 g_k}{\partial x_i \partial x_j} v_k w_i w_j = 0$ for $k = 1, 5, 6, 8$, since $\frac{\partial^2 g_k}{\partial x_i \partial x_j} = 0$ for all $1 \leq i, j \leq 8$ and $v_k = 0$ for $k = 1, 5, 6$. As a result,

the terms that contribute to the sum correspond to $k = 2, 3, 4, 7$. Thus, a can be written as

$$\begin{aligned}
 (20) \quad a &= \sum_{i,j,k=1}^8 v_k w_i w_j \frac{\partial^2 g_k}{\partial x_i \partial x_j} (\mathbf{x}_{dfe}, \beta_M^*) , \\
 &= 2 \left[v_2 w_8 w_2 \frac{\partial^2 g_2}{\partial x_8 \partial x_2} (\mathbf{x}_{dfe}, \beta_M^*) + v_2 w_8 w_3 \frac{\partial^2 g_2}{\partial x_8 \partial x_3} (\mathbf{x}_{dfe}, \beta_M^*) + v_2 w_8 w_4 \frac{\partial^2 g_2}{\partial x_8 \partial x_4} (\mathbf{x}_{dfe}, \beta_M^*) \right. \\
 &\quad + v_2 w_8 w_5 \frac{\partial^2 g_2}{\partial x_8 \partial x_5} (\mathbf{x}_{dfe}, \beta_M^*) + v_3 w_2^2 \frac{\partial^2 g_3}{\partial x_2 \partial x_2} (\mathbf{x}_{dfe}, \beta_M^*) + v_4 w_2^2 \frac{\partial^2 g_4}{\partial x_2 \partial x_2} (\mathbf{x}_{dfe}, \beta_M^*) \\
 &\quad + v_7 w_3 w_1 \frac{\partial^2 g_7}{\partial x_3 \partial x_1} (\mathbf{x}_{dfe}, \beta_M^*) + v_7 w_3 w_2 \frac{\partial^2 g_7}{\partial x_3 \partial x_2} (\mathbf{x}_{dfe}, \beta_M^*) + v_7 w_3 w_5 \frac{\partial^2 g_7}{\partial x_3 \partial x_5} (\mathbf{x}_{dfe}, \beta_M^*) \\
 &\quad + v_7 w_4 w_1 \frac{\partial^2 g_7}{\partial x_4 \partial x_1} (\mathbf{x}_{dfe}, \beta_M^*) + v_7 w_4 w_2 \frac{\partial^2 g_7}{\partial x_4 \partial x_2} (\mathbf{x}_{dfe}, \beta_M^*) + v_7 w_4 w_5 \frac{\partial^2 g_7}{\partial x_4 \partial x_5} (\mathbf{x}_{dfe}, \beta_M^*) \\
 &\quad + v_7 w_3^2 \frac{\partial^2 g_7}{\partial x_3 \partial x_3} (\mathbf{x}_{dfe}, \beta_M^*) + v_7 w_4^2 \frac{\partial^2 g_7}{\partial x_4 \partial x_4} (\mathbf{x}_{dfe}, \beta_M^*) + v_7 w_6 w_3 \frac{\partial^2 g_7}{\partial x_6 \partial x_3} (\mathbf{x}_{dfe}, \beta_M^*) \\
 &\quad \left. + v_7 w_6 w_4 \frac{\partial^2 g_7}{\partial x_6 \partial x_4} (\mathbf{x}_{dfe}, \beta_M^*) + v_7 w_3 w_4 \frac{\partial^2 g_7}{\partial x_3 \partial x_4} (\mathbf{x}_{dfe}, \beta_M^*) \right] , \\
 &= 2 \left[-Z_1 v_2 w_8 w_2 - Z_1 v_2 w_8 w_3 - Z_1 v_2 w_8 w_4 - Z_1 v_2 w_8 w_5 - Z_6 v_3 w_2^2 + Z_6 v_4 w_2^2 - Z_2 v_7 w_3 w_1 - Z_2 v_7 w_3 w_2 - Z_2 v_7 w_3 w_5 \right. \\
 &\quad \left. - Z_3 v_7 w_4 w_1 - Z_3 v_7 w_4 w_2 - Z_3 v_7 w_4 w_5 - 2Z_2 v_7 w_3^2 - 2Z_3 v_7 w_4^2 + Z_7 v_7 w_6 w_3 + Z_5 v_7 w_6 w_4 + Z_4 v_7 w_3 w_4 \right] , \\
 &= 2 \left[Z_7 v_7 w_6 w_3 + Z_5 v_7 w_6 w_4 + Z_4 v_7 w_3 w_4 + Z_6 v_4 w_2^2 - \left(Z_1 v_2 w_8 w_2 + Z_1 v_2 w_8 w_3 + Z_1 v_2 w_8 w_4 + Z_1 v_2 w_8 w_5 + Z_6 v_3 w_2^2 \right. \right. \\
 &\quad \left. \left. + Z_2 v_7 w_3 w_1 + Z_2 v_7 w_3 w_2 + Z_2 v_7 w_3 w_5 + Z_3 v_7 w_4 w_1 + Z_3 v_7 w_4 w_2 + Z_3 v_7 w_4 w_5 + 2Z_2 v_7 w_3^2 + 2Z_3 v_7 w_4^2 \right) \right] .
 \end{aligned}$$

Upon grouping positive terms and simplifying, the right-hand side of the above expression can be written as:

$$\begin{aligned}
 &= 2D_1^2 D_2 \left[-\frac{\tau Z_7 Q_4 Q_1 K_2}{\xi_M K_4} - \frac{\tau Z_5 Q_4 Q_1 K_3}{\xi_M K_5} + \frac{\tau Z_4 K_2 K_3}{K_4 K_5 K_7} + Z_6 Q_3 - \left(Z_6 Q_2 + \frac{\tau^2 Z_1 Q_1^2 Q_4^2}{K_1 \xi_M} \left(1 + \frac{K_2}{K_4} + \frac{K_3}{K_5} + Q_0 \right) \right. \right. \\
 &\quad \left. \left. + \frac{\tau Z_2 K_2}{K_4 K_7} \left(\frac{\lambda_{RS} Q_0 - K_1}{K_6} + 1 + Q_0 \right) + \frac{\tau Z_3 K_3}{K_5 K_7} \left(\frac{\lambda_{RS} Q_0 - K_1}{K_6} + 1 + Q_0 \right) + \frac{2\tau Z_2 K_2^2}{K_4^2 K_7} + \frac{2\tau Z_3 K_3^2}{K_5^2 K_7} \right) \right] , \\
 &= 2D_1^2 D_2 \left[\frac{\tau Z_2 K_1 K_2}{K_4 K_6 K_7} + \frac{\tau Z_3 K_1 K_3}{K_5 K_6 K_7} + \frac{\tau Z_4 K_2 K_3}{K_4 K_5 K_7} + Z_6 Q_3 - \left(Z_6 Q_2 + \frac{\tau^2 Z_1 Q_1^2 Q_4^2}{K_1 \xi_M} \left(1 + \frac{K_2}{K_4} + \frac{K_3}{K_5} + Q_0 \right) \right. \right. \\
 &\quad \left. \left. + \frac{\tau Z_2 K_2}{K_4 K_7} \left(\frac{\lambda_{RS} Q_0}{K_6} + 1 + Q_0 \right) + \frac{\tau Z_3 K_3}{K_5 K_7} \left(\frac{\lambda_{RS} Q_0}{K_6} + 1 + Q_0 \right) + \frac{\tau Z_7 Q_4 Q_1 K_2}{\xi_M K_4} + \frac{\tau Z_5 Q_4 Q_1 K_3}{\xi_M K_5} + \frac{2\tau Z_2 K_2^2}{K_4^2 K_7} + \frac{2\tau Z_3 K_3^2}{K_5^2 K_7} \right) \right] , \\
 &:= 2D_1^2 D_2 (\eta_2 - \eta_1) , \\
 &= 2D_1^2 D_2 \left(\frac{\eta_2}{\eta_1} - 1 \right) \eta_1 .
 \end{aligned}$$

Since $(D_i, \eta_i) \in \mathbb{R}_{>0} \times \mathbb{R}_{>0}$ for $i = 1, 2$, it follows that the sign of a is completely dependent on the size of the quantity $\frac{\eta_2}{\eta_1}$. Therefore, define

$$\Lambda := \frac{\eta_2}{\eta_1}$$

to arrive at the following dichotomy

$$\begin{cases} a < 0 \iff \Lambda < 1, \\ a > 0 \iff \Lambda > 1. \end{cases}$$

This completes the proof concerning the bifurcation analysis of model (4). \square

7.4.6. Proof of Theorem 4.1 (See page 17).

Proof.

$$\begin{aligned} \mathcal{G}_\nu(\eta_\kappa^\omega(a)) &= \xi_M \int_0^\infty \eta_\kappa^\omega(a) \nu(a) da, \\ &= \xi_M \int_\omega^\infty \eta_\kappa^\omega(a) \nu(a) da, \\ &= \xi_M \lim_{\zeta \rightarrow +\infty} \int_\omega^\zeta e^{-a\xi_M} - e^{-a(\kappa+\xi_M)+\kappa\omega} da, \\ &= \xi_M \lim_{\zeta \rightarrow +\infty} \left[\frac{e^{-a(\kappa+\xi_M)+\kappa\omega}}{\kappa + \xi_M} - \frac{e^{-a\xi_M}}{\xi_M} \Big|_{[\omega, \zeta]} \right], \\ &= \xi_M \lim_{\zeta \rightarrow +\infty} \left[\frac{e^{-\zeta(\kappa+\xi_M)+\kappa\omega}}{\kappa + \xi_M} - \frac{e^{-\zeta\xi_M}}{\xi_M} + e^{-\omega\xi_M} \left(\frac{1}{\xi_M} - \frac{1}{\kappa + \xi_M} \right) \right], \\ &= \xi_M e^{-\omega\xi_M} \left(\frac{1}{\xi_M} - \frac{1}{\kappa + \xi_M} \right), \\ &= \frac{\kappa}{\kappa + \xi_M} e^{-\omega\xi_M}. \end{aligned}$$

\square

7.4.7. Proof of Theorem 4.2 (See page 19).

Proof. Fix the vector $(\rho_f, \rho_p) \in [0, 1] \times [0, 1)$ and each C_i for $i = 1, 2$, as defined in Section (3.2). It follows that the sign of the term under the square root of \mathcal{R}_0^v , as defined by equation (12) in Section (4.2), is determined by the sign of the following expression

$$((C_1 - C_2)U_{low} + C_2)(1 - \rho_f \rho_p)(1 - V_f V_p).$$

Thus, the control-modified reproductive threshold will not be nullified or complex-valued provided the vaccination terms satisfy the following hyperbolic inequality $V_f V_p < 1$. Therefore, $\mathcal{R}_0^v \notin \mathbb{C} - \{0\}$ if and only if $(V_f, V_p) \in \mathcal{H}$, where \mathcal{H} is defined as in the statement of Lemma (4.2). \square

7.4.8. Proof of Lemma 3 (See page 20).

Proof. A straight-forward calculation shows that sub-matrices F and V of the Jacobian evaluated at the DFE \mathbf{w}_{dfe} corresponding to the dynamical system (14) are given by

$$F = \left(\frac{\partial \mathcal{F}_i}{\partial x_j} \Big|_{\mathbf{w}_{dfe}} \right)_{1 \leq i, j \leq 5} = \begin{pmatrix} 0 & 0 & 0 & 0 & \sigma\beta_M \\ 0 & 0 & 0 & 0 & 0 \\ 0 & 0 & 0 & 0 & 0 \\ 0 & \sigma\beta_Y \frac{\Omega_M}{\Omega_H} \frac{\xi_H}{\xi_M} & \sigma\beta_A \frac{\Omega_M}{\Omega_H} \frac{\xi_H}{\xi_M} & 0 & 0 \\ 0 & 0 & 0 & 0 & 0 \end{pmatrix}$$

and

$$V = \left(\frac{\partial \mathcal{V}_i}{\partial x_j} \Big|_{\mathbf{w}_{dfe}} \right)_{1 \leq i, j \leq 5} = \begin{pmatrix} (\gamma + \xi_H) & 0 & 0 & 0 & 0 \\ \gamma(U_{low} - 1) & (\xi_H + \delta + \lambda_{YR}) & 0 & 0 & 0 \\ -\gamma U_{low} & 0 & (\lambda_{AR} + \xi_H) & 0 & 0 \\ 0 & 0 & 0 & (\xi_M + \tau) & 0 \\ 0 & 0 & 0 & -\tau & \xi_M \end{pmatrix}.$$

The reproductive threshold $\mathcal{R}_0 := \rho(FV^{-1})$ for any given compartmentalized infectious disease model is completely determined by the matrices F and V . Therefore, it is of trivial consequence that the models (4) and (14) possess identical reproductive thresholds, given by (6) arising from Lemma (1). \square

7.5. Summary of Stability Theorems. The goal of this section of the appendix is to provide the reader with a brief collection and overview of the theorems that are widely used in determining the stability of the equilibrium points for nonlinear dynamical systems. The first theorem will be needed in order to determine the local asymptotic stability of the DFE corresponding to the *SEYAR* model, while the second is used to investigate the existence of non-trivial sub-threshold equilibrium states of the model. In the setting of dynamical systems one cannot usually pinpoint a solution exactly, but only approximately. As a result, an equilibrium point must be stable to be physically meaningful. A stable equilibrium point of a system is a solution \mathbf{x}^* with the property that if for every open ball $B(\mathbf{x}^*, \epsilon)$ of radius ϵ , centered at \mathbf{x}^* , there is a $\delta < \epsilon$, such that if every solution \mathbf{x} with initial data $\mathbf{x}(0) \in B(\mathbf{x}^*, \delta)$, remains in $B(\mathbf{x}^*, \epsilon)$ for $t > 0$. In other words, if the initial data starts in $B(\mathbf{x}^*, \delta)$, then the flow map $\phi(t, \mathbf{x})$ of the model remains in $B(\mathbf{x}^*, \epsilon)$ for eternity. An equilibrium point \mathbf{x}^* is said to be asymptotically stable, if in addition to the above, there is a $\delta > 0$ such that

$$\lim_{t \rightarrow +\infty} \mathbf{x}(t) = \mathbf{x}^*.$$

Provided an epidemiological model can be grouped into n homogeneous compartments, the local asymptotic stability of the equilibrium states can be established by utilizing the next generation method, appearing in [63]. By making use of the Center Manifold Theorem [33], Van den Driessche and Watmough provided a simple prescription for determining the local asymptotic stability of DFE points of a given system. This criterion is given in terms of the reproductive number \mathcal{R}_0 of the system which acts as a threshold value. This effectively relates \mathcal{R}_0 to the DFE of the system. As a result, this has proven to be very useful in disease control. To cast the above discussion into a mathematical framework, we let $\mathbf{x} = (x_1, \dots, x_k)^T \in \mathbb{R}_+^k$ and define the space of disease free states for the compartmental model to be $X := \{x \in \mathbb{R}_+^k : x_i = 0 \text{ for } i = 1, \dots, m, m < n\}$. Then for $\Phi \in C^2(\mathbb{R}^k)$, we form the following dynamical system

$$(21) \quad \dot{\mathbf{x}}(t) = \Phi(\mathbf{x}(t)) = \mathcal{F}(\mathbf{x}(t)) - \mathcal{V}(\mathbf{x}(t)),$$

where $\mathcal{V} = \mathcal{V}^- - \mathcal{V}^+$.

Theorem 7.1. (Van den Driessche and Watmough [63]) Define $\mathcal{R}_0 = \rho(FV^{-1})$ and consider the disease transmission model given by (21) such that Φ satisfies the follow criteria:

- i If $\mathbf{x} \geq 0$, then so are \mathcal{F} , \mathcal{V}^+ , and \mathcal{V}^- ,
- ii If $\mathbf{x} = 0$, then $\mathcal{V}^- = 0$,
- iii If $i > m$, then $\mathcal{F}_i = 0$,
- iv If $\mathbf{x} \in X$, then $\mathcal{F}_i = \mathcal{V}^+ = 0$, for all $0 \leq i \leq m$,
- v If $\mathcal{F}(\mathbf{x}) = 0$, then all eigenvalues of $D\Phi(\mathbf{x}^*)$ have negative real parts.

If \mathbf{x}^* is a DFE for (21), then \mathbf{x}^* is locally asymptotically stable provided $\mathcal{R}_0 < 1$ and unstable if $\mathcal{R}_0 > 1$.

The above theorem is proved by making use of the following lemma.

Lemma 4. If \mathbf{x}^* is a DFE of system (21) and Φ satisfies assumptions (i)-(v), then the derivatives $D\mathcal{F}(\mathbf{x}^*)$ and $D\mathcal{V}(\mathbf{x}^*)$ can be partitioned as follows:

$$D\mathcal{F}(\mathbf{x}^*) = \begin{pmatrix} F & 0 \\ 0 & 0 \end{pmatrix} \quad \text{and} \quad D\mathcal{V}(\mathbf{x}^*) = \begin{pmatrix} V & 0 \\ J_3 & J_4 \end{pmatrix}.$$

Where F and V are defined as:

$$F = \left(\frac{\partial \mathcal{F}_i}{\partial x_j} \Big|_{\mathbf{x}^*} \right)_{1 \leq i, j \leq m} \quad \text{and} \quad V = \left(\frac{\partial \mathcal{V}_i}{\partial x_j} \Big|_{\mathbf{x}^*} \right)_{1 \leq i, j \leq m}.$$

Remark 7.1. In the above matrix partitioning, F is non-negative, V is an invertible M -matrix and J_3, J_4 are sub-matrices of the Jacobian associated with various transmission terms. This theorem provides a convenient epidemiological interpretation of the reproductive threshold \mathcal{R}_0 corresponding to a given dynamical system in the SIR family. Additionally, due to the partitioning of the Jacobian mentioned above, the stability of the system is determined by $\det(FV^{-1} - \lambda\mathcal{I})$, where \mathcal{I} is the identity matrix. If the matrix F containing transmission probabilities and contact rates is set to zero, then all eigenvalues of $-V$ have negative real part. As a result, the stability, or lack of, experienced by the system in question depends on the entries of F . Due to this reason, the bifurcation parameters are chosen from the entries of F . In the case that the transmission probabilities are relatively high, an endemic could occur and additional non-trivial equilibrium can arise. Regarding the *SEYAR* model, besides the man-biting rate σ , the only possible parameters are the transmission probabilities β_Y, β_A .

and β_M . From a epidemiological perspective, we have more control over the mosquito to human transmission probability β_M . Due to this reason, β_M is chosen as the parameter for the bifurcation analysis. One could perform a similar analysis for β_Y and β_A , however all of the transmission probabilities involved are related through the reproductive number \mathcal{R}_0 of the model. As a result, the analysis would be similar.

Let $s(A)$ and $\rho(A)$ stand for the spectral abscissa and radius, respectively. The proof of Theorem 7.1 hinges on M-matrix theory. A matrix B is said to have the Z-sign pattern provided all of its off diagonal entries are non-positive. If $B = s\mathcal{I} - P$, where $P \geq 0$. If $s > \rho(P)$, then B is a non-singular M-matrix, if $s = \rho(P)$, then B is a singular M-matrix. This observation is then combined with a linear algebra lemma, which we restate below for convenience of the reader. To this end, they make use of the following argument: define $J_1 := F - V$, then V is a non-singular M-matrix and F is non-negative. It follows that $-J_1 := V - F$ has the Z-sign pattern. By the non-negativity of FV^{-1} , it is a direct consequence that $-J_1V^{-1} := \mathcal{I} - FV^{-1}$ also has the Z-sign pattern. Now we apply Lemma 5 with $H = V$ and $-J_1 := V - F$, to conclude that $-J_1$ is a non-singular M-matrix if and only if $\mathcal{I} - FV^{-1}$. Also, since all of its eigenvalues have magnitude bounded above by $\rho(FV^{-1})$, we have that $\mathcal{I} - FV^{-1}$ is a non-singular M-matrix if and only if $\rho(FV^{-1}) < 1$. Therefore, $s(J_1) < 0$ if and only if $\mathcal{R}_0 < 1$. Through making use of a similar argument in combination with Lemma 6 of Appendix A, found in [63], they arrive at the following trichotomy, establishing \mathcal{R}_0 as a threshold parameter

$$\begin{cases} s(J_1) < 0 \iff \mathcal{R}_0 < 1, \\ s(J_1) = 0 \iff \mathcal{R}_0 = 1, \\ s(J_1) > 0 \iff \mathcal{R}_0 > 1. \end{cases}$$

Lemma 5. *Let H be a non-singular M-matrix and assume that B and BH^{-1} have the Z sign pattern. Then B is a non-singular M-matrix if and only if BH^{-1} is a non-singular M-matrix.*

In Section (3.4) use is made of the following variant of the Center Manifold Theorem specifically adapted to the case of bifurcation analysis for nonlinear systems. The utility of this theorem resides in the classification of the bifurcation due to the sign of the parameters a and b , defined below.

Theorem 7.2. *(Castillo-Chavez and Song [11]) Consider the following dynamical system with real parameter ω*

$$\dot{x} = f(x, \omega), \quad f : \mathbb{R}^n \times \mathbb{R} \rightarrow \mathbb{R}, \quad \text{and} \quad f \in C^2(\mathbb{R}^n \times \mathbb{R}).$$

Without loss of generality, we assume that $x = 0$ is an equilibrium point for the above system for all ω , i.e. $f(0, \omega) \equiv 0$ for all ω . Provided that the following assumptions are satisfied:

I $A = D_x f(0, 0) = \left(\frac{\partial f_i}{\partial x_j}(0, 0) \right)$ is the linearization matrix of the system around the equilibrium point 0 with ω evaluated at 0. Zero is a simple eigenvalue of A and all remaining eigenvalues have negative real part. Non trivial null space of dimension one.

II The matrix A has a right eigenvector w and left eigenvector v corresponding to the zero eigenvalue.

Let f_k denote the k^{th} component of f and

$$(22) \quad a = \sum_{i,j,k=1}^n v_k w_i w_j \frac{\partial^2 f_k}{\partial x_i \partial x_j}(0, 0),$$

$$(23) \quad b = \sum_{i,k=1}^n v_k w_i \frac{\partial^2 f_k}{\partial x_i \partial \omega}(0, 0).$$

Then the local dynamics around the equilibrium point 0 are completely determined by the signs of a and b . More precisely,

- i $a > 0, b > 0$. When $\omega < 0$ such that $|\omega| \ll 1$, 0 is locally asymptotically stable and there exists a positive unstable equilibrium; when $0 < \omega \ll 1$, 0 is unstable and there exists a negative locally asymptotically stable equilibrium.
- ii $a < 0, b < 0$. When $\omega < 0$ such that $|\omega| \ll 1$, 0 is unstable; when $0 < \omega \ll 1$, 0 is locally asymptotically stable and there exists a positive unstable equilibrium.
- iii $a > 0, b < 0$. When $\omega < 0$ such that $|\omega| \ll 1$, 0 is unstable and there exists a locally asymptotically stable negative equilibrium; when $0 < \omega \ll 1$, 0 is stable and a positive unstable equilibrium exists.

iv $a < 0$, $b > 0$. When ω changes sign, 0 changes its stability from stable to unstable. As a result, a negative unstable equilibrium becomes positive and locally asymptotically stable. In particular, if $a > 0$ and $b > 0$, then a backward bifurcation occurs at $\omega = 0$.

Remark 7.2. *It is worth mentioning that the a and b terms appearing in the above theorem depend on generalized eigenvectors, i.e. zero entries are allowed. In the proof of Theorem (7.2), the a and b terms arise from a differential equation obtained from a parameterization of a one-dimensional center manifold $c(t)$, given by*

$$\dot{c} = \frac{a}{2}c^2 + b\omega c.$$

Observe how a transcritical bifurcation occurs in the above equation at $\omega = 0$ and can be classified according the signs of the a and b terms, defined above. These terms depend on the Kronecker product of generalized eigenvectors and entries of the Hessian evaluated at the DFE. As pointed out in Castillo-Chavez and Song [11], negative components of the generalized eigenvectors are permitted through a modification of Theorem (7.2). The essence of the argument hinges on the fact that the theorem can still be applied, one only has to compare the negative entries of the eigenvectors with their corresponding entries of the non-negative equilibrium of interest. Therefore, one has to consider the original parameterization of the center manifold, prior to the coordinate change where the DFE is assumed to be zero. Notice how the negative entries in the generalized eigenvectors calculated in Section 3.4 correspond to the positive entries of the DFE of interest.

7.6. Parameter Values. Presented below are tables of numerical rates corresponding to the following three high transmission sites: Kaduna in Nigeria, Namawala in Tanzania and Butelgut in Papua New Guinea. The data has been collected from multiple sources, all of which are noted in the footnotes. Although the source of the data is heterogeneous, care has been taken to introduce as much accuracy as possible. As mentioned in [34], all of the sites mentioned above are areas of intense *P. falciparum* transmission. Due to the additional prevalence of *P. vivax* in Butelgut, the corresponding data represents combined estimates of both species, [34]. The data for the other sites exclusively corresponds to the *P. falciparum* species. There are a variety of vector species that inhabit these sites. The data listed here corresponds to the dominant vector species of the area being considered. The dominant vector species of each site is listed in the footnotes. Furthermore, as mentioned in Section 2 and reported in [37], the parasites carried by asymptomatic human hosts can be more infectious than those of symptomatic. For the parameter values displayed in Section 7.6, we invoke the assumption that the asymptomatic carriers corresponding to each site transmit at a lower rate than that of the symptomatic and that asymptomatic individuals recover faster than symptomatic, i.e. $\beta_A < \beta_Y$ and $\lambda_{AR} > \lambda_{YR}$.

Table 6 below contains demographic data for the countries that each site is contained in. These numerical values are used to calculate the recruitment rates of the human populations Ω_H corresponding to each region under consideration. These quantities in combination with the parameter values listed in the subsequent tables, appearing on the following pages, will be used to calculate the reproductive thresholds associated with each location and the various quantities covered in Sections 3.2 and 3.3.

TABLE 6. Human Population Data

Country	Life expectancy	Birth rate	Migration rate	Source
Nigeria	53.02	37.64	-0.22	[1]
Tanzania	61.71	36.39	-0.54	[1]
Papua New Guinea	67.03	24.38	0.00	[1]

The human population data displayed in table 6 is from the Central Intelligence Agency (CIA). Denote Ω_{LE} , Ω_{BR} and Ω_{MR} to be the life expectancy, birth rate and migration rate of the population under consideration. Life expectancy is measured in years. The birth rate entries appearing in column 3 of the above table are crude birth rates. The Crude birth rate measures the average quantity of live births during a year, per 1,000 people and is given in units of total births per 1,000 people per year. The migration rates are net migration rates, which measure the difference of immigrants and emigrants in a given population over the span of a year and are given in units of humans per year, per 1,000 people.

TABLE 7. Kaduna

Parameter	Description	Dimension	Value	Source
Ω_H	Recruitment rate of humans	humans \times time $^{-1}$	1.02×10^{-4}	[1] [†]
Ω_M	Recruitment rate of mosquitoes	mosquitoes \times time $^{-1}$	1505.82	[34] [‡]
ξ_H	Natural mortality rate of human	time $^{-1}$	0.019	[1] ^{††}
ξ_M	Natural mortality rate of mosquito	time $^{-1}$	0.11	[12, 47] ^{‡‡}
β_A	Probability of disease transmission from asymptomatic human to a susceptible mosquito	time $^{-1}$	0.048	assumed [§]
β_Y	Probability of disease transmission from symptomatic human to a susceptible mosquito	time $^{-1}$	0.48	[12] ^{§§}
β_M	Probability of disease transmission from infected mosquito to susceptible human	time $^{-1}$	0.032	[34] ^{§§§}
γ	The intermediate host mean latent period	time $^{-1}$	0.11	[12] [*]
τ	The definitive host mean latent period	time $^{-1}$	0.09	[17, 34] ^{**}
δ	Disease-induced death rate for humans	time $^{-1}$	1.66×10^{-6}	[26] ^{***}
σ	Biting rate of mosquito	time $^{-1}$	0.42	[34] [#]
λ_{AR}	Asymptomatic human recovery rate	time $^{-1}$	0.6	assumed [¶]
λ_{YR}	Symptomatic human recovery rate	time $^{-1}$	0.06	assumed ^{¶¶}
λ_{RS}	Temporary immunity loss rate in humans	time $^{-1}$	5.48×10^{-4}	[12]
u_{low}	The lower NAI protected threshold	n/a	0.5	assumed

[†] The human recruitment rate is obtained from the entries in the first row of Table 6 and the weighted sum formula $\Omega_H = (\Omega_{BR} + \Omega_{MR})/365.25/1,000 = (37.64 - 0.22)/365.25/1,000 \approx 1.02 \times 10^{-4}$.

[‡] The daily vector emergence rate is measured in units of new adult female mosquitoes per day. Thus, it is given by dividing the entry in row six column four of Table 3 in [34, p. 541] by the normalizing quantity 365.25, i.e. $\Omega_M = (0.55 \times 10^6)/365.25 \approx 1505.82$.

^{††} The average natural human mortality rate is calculated by dividing the entry listed in row one column two of Table 6 into unity, i.e. $\xi_H = 1/\Omega_{LE} = 1/53.02 \approx 0.019$.

^{‡‡} The dominant vector species of Kaduna at the time the field measurements were taken was *An. gambiae*, [55]. Let Ω_L stand for the average *An. gambiae* life expectancy, which is dependent upon the region under consideration. The data provided in [47] and appearing in row nine column one of Table A.3 in [12, p. 19] corresponds to *An. gambiae* activity in Nigeria. Due to this, we select the entry contained in row one column nine, so that $\Omega_L = 9$. Therefore, the average daily *An. gambiae* mosquito mortality rate is $\xi_M = 1/\Omega_L = 1/9 \approx 0.11$.

[§] The assumption is made that the probability of transmission from asymptomatic humans to susceptible mosquitoes is one-tenth the transmission probability corresponding to symptomatic humans, i.e. $\beta_A = 0.048$.

^{§§} We adopt the convention utilized in [12], where an estimate of 0.48 will be used for high transmission areas and an estimate of 0.24 will be used for low. Kaduna is a high transmission area, thus we let $\beta_Y = 0.48$. An alternate choice would be to choose the average value of the parameters corresponding to the dominant species of parasite. The average value of the parameters appearing in rows one through five in column one of Table A.6 in [12, p. 21] is approximately 0.36. The origin of the parameters used in this calculation is [7, 24, 62].

^{§§§} The effective daily vector to human contact rate is obtained by dividing the value in row two column four of Table 3 in [34, p. 541] by Ω_L . Thus, $\beta_M = 0.29/\Omega_L = 0.29/9 \approx 0.032$.

^{*} The human latent period $\tilde{\gamma}$, measure in days, corresponding to *P. falciparum* infection is taken from row three column one in Table A.7 in [12, p. 21]. The range 9 – 10 is given. The average value is then chosen, i.e. $\tilde{\gamma} \approx 9.5$. It follows that the average duration of the intermediate host latent period is $\gamma = 1/\tilde{\gamma} = 1/9.5 \approx 0.11$. The parameter source is [46].

^{**} Let $\tilde{\tau}$ denote the *Plasmodium* incubation period, i.e. the number of days required for parasite development. Thus, by using the entry in row eight column three of Table 2 in [34, p. 539], it follows that the average duration of the definitive host latent period is $\tau = 1/\tilde{\tau} = 1/11.6 \approx 0.09$. Technically, this parameter was calculated from the mean and median temperatures listed in the original source [17].

^{***} The malaria death rates are taken from [26] and are given in units of per 100,000 people per year. As in the case of the human demographic data listed in Table 6, these rates correspond to the overall country that the region is contained in. Using the data provided in [26], it follows that $\delta = 60.46/365.25/100,000 \approx 1.66 \times 10^{-6}$.

[#] The average man biting rate is estimated by dividing the entry in row one column four of Table 3 in [34, p. 541] by Ω_L . More precisely, we have that $\sigma = 3.8/9 \approx 0.42$.

^{¶, ¶¶} Asymptomatic carriers transmit malaria to a lesser extent than symptomatic carriers and recover faster. Due to this we assume that the recovery rate λ_{YR} for symptomatic individuals is one-tenth the rate λ_{AR} of asymptomatic individuals. Let the quantity $1/\lambda$ denote the average duration of the human infectious period, provided that the individual has had no treatment. If Ω_I stands for the average duration of the *P. falciparum* infectious period in humans. We select the average of the entries appearing in row four column one of Table A.9 in [12, p. 21], so that $\Omega_I = 18$. Therefore, $\lambda_{YR} \approx \lambda = 1/\Omega_I = 1/18 \approx 0.06$ and it follows that $\lambda_{AR} = 0.6$. The original source of the parameter value is [5].

^{||} The temporary immunity loss rate λ_{RS} is such that $1/\lambda_{RS}$ is equal to the average duration of the human immune period. As in [12], we assume that the immune period lasts for an average of 5 years in areas of high transmission and 1 year in areas of low transmission. For Kaduna it follows that $\lambda_{RS} = 1/(5)365.25 \approx 5.48 \times 10^{-4}$.

^{|||} This baseline assumption is due to the fact that the population under consideration is *A-dominant*.

TABLE 8. Namawala

Parameter	Description	Dimension	Value	Source
Ω_H	Recruitment rate of humans	humans \times time $^{-1}$	9.82×10^{-5}	[1] [†]
Ω_M	Recruitment rate of mosquitoes	mosquitoes \times time $^{-1}$	4928.13	[34] [‡]
ξ_H	Natural mortality rate of human	time $^{-1}$	0.016	[1] ^{††}
ξ_M	Natural mortality rate of mosquito	time $^{-1}$	0.09	[12, 47] ^{‡‡}
β_A	Probability of disease transmission from asymptomatic human to a susceptible mosquito	time $^{-1}$	0.048	assumed [§]
β_Y	Probability of disease transmission from symptomatic human to a susceptible mosquito	time $^{-1}$	0.48	[12] ^{§§}
β_M	Probability of disease transmission from infected mosquito to susceptible human	time $^{-1}$	0.002	[34] ^{§§§}
γ	The intermediate host mean latent period	time $^{-1}$	0.11	[12] [*]
τ	The definitive host mean latent period	time $^{-1}$	0.09	[17, 34] ^{**}
δ	Disease-induced death rate for humans	time $^{-1}$	1.16×10^{-6}	[26] ^{***}
σ	Biting rate of mosquito	time $^{-1}$	0.13	[34] [#]
λ_{AR}	Asymptomatic human recovery rate	time $^{-1}$	0.6	assumed [¶]
λ_{YR}	Symptomatic human recovery rate	time $^{-1}$	0.06	assumed ^{¶¶}
λ_{RS}	Temporary immunity loss rate in humans	time $^{-1}$	5.48×10^{-4}	[12]
u_{low}	The lower NAI protected threshold	n/a	0.5	assumed

[†] From Table 6, it follows that $\Omega_H = (36.39 - 0.54)/365.25/1,000 \approx 9.82 \times 10^{-5}$.

[‡] By utilizing the data provided in Table 3 in [34, p. 541], it follows that $\Omega_M = (1.8 \times 10^6)/365.25 \approx 4928.13$.

^{††} The average natural human mortality rate is calculated in a similar fashion, as in the case of Kaduna, by utilizing the data provided in Table 6.

^{‡‡} The dominant vector species of Namawala at the time the field measurements were taken was *An. gambiae*, [60]. The data provided in [29] and appearing in row six column one of Table A.3 in [12, p. 19] corresponds to *An. gambiae* activity in Tanzania. Using this data, it follows that $\Omega_L = 11.26$. Therefore, the average daily *An. gambiae* mosquito mortality rate is $\xi_M = 1/11.26 \approx 0.09$.

[§] As previously mentioned, the asymptomatic human to susceptible mosquito transmission probability is assumed to be $\beta_A = 0.048$.

^{§§} Since Namawala is a high transmission area, we let $\beta_Y = 0.48$.

^{§§§} By dividing the value in row two column five of Table 3 in [34, p. 541] by Ω_L , it follows that $\beta_M = 0.017/11.26 \approx 0.002$.

^{*} The average duration of the intermediate host latent period is taken to be $\gamma = 1/\tilde{\gamma} = 1/9.5 \approx 0.11$. The parameter value $\tilde{\gamma}$ is taken from row three column one in Table A.7 in [12, p. 21]. The average value is then chosen, i.e. $\gamma \approx 9.5$. The original parameter source is [46].

^{**} By using the entry in row eight column four of Table 2 in [34, p. 539], it follows that the average duration of the definitive host latent period is $\tau = 1/11.6 \approx 0.09$

^{***} By the data provided in [26], it follows that $\delta = 42.42/365.25/100,000 \approx 1.16 \times 10^{-6}$.

[#] By using the data in row one column five of Table 3 in [34, p. 541], we have that $\sigma = 1.5/11.26 \approx 0.13$.

[¶] As in the previous table, the recovery rate pertaining to asymptomatic individuals is assumed to be $\lambda_{AR} = 0.6$.

^{¶¶} The average of the entries appearing in row four column one of Table A.9 in [12, p. 21] is selected, so that $\Omega_I = 18$. Therefore, $\lambda_{YR} \approx \lambda = 1/\Omega_I = 1/18 \approx 0.06$. The original source of the parameter value is [5].

^{||} As Namawala is a high transmission area, the temporary immunity loss rate is taken to be $\lambda_{RS} = 1/(5)365.25 \approx 5.48 \times 10^{-4}$.

^{|||} This baseline assumption is due to the fact that the population under consideration is *A-dominant*.

TABLE 9. Butelgut

Parameter	Description	Dimension	Value	Source
Ω_H	Recruitment rate of humans	humans \times time $^{-1}$	6.67×10^{-5}	[1] [†]
Ω_M	Recruitment rate of mosquitoes	mosquitoes \times time $^{-1}$	4106.78	[34] [‡]
ξ_H	Natural mortality rate of human	time $^{-1}$	0.015	[1] ^{††}
ξ_M	Natural mortality rate of mosquito	time $^{-1}$	0.14	[12, 47] ^{‡‡}
β_A	Probability of disease transmission from asymptomatic human to a susceptible mosquito	time $^{-1}$	0.048	assumed [§]
β_Y	Probability of disease transmission from symptomatic human to a susceptible mosquito	time $^{-1}$	0.48	[12] ^{§§}
β_M	Probability of disease transmission from infected mosquito to susceptible human	time $^{-1}$	0.006	[34] ^{§§§}
γ	The intermediate host mean latent period	time $^{-1}$	0.11	[12] [*]
τ	The definitive host mean latent period	time $^{-1}$	0.1	[17, 34] ^{**}
δ	Disease-induced death rate for humans	time $^{-1}$	1.03×10^{-6}	[26] ^{***}
σ	Biting rate of mosquito	time $^{-1}$	0.14	[34] [#]
λ_{AR}	Asymptomatic human recovery rate	time $^{-1}$	0.6	assumed [¶]
λ_{YR}	Symptomatic human recovery rate	time $^{-1}$	0.06	assumed ^{¶¶}
λ_{RS}	Temporary immunity loss rate in humans	time $^{-1}$	5.48×10^{-4}	[12]
u_{low}	The lower NAI protected threshold	n/a	0.5	assumed

[†] From Table 6, it follows that $\Omega_H = (24.38 - 0.00)/365.25/1,000 \approx 6.67 \times 10^{-5}$.

[‡] By utilizing the data provided in Table 3 in [34, p. 541], it follows that $\Omega_M = (1.5 \times 10^6)/365.25 \approx 4106.78$.

^{††} Similarly, the average natural human mortality rate is calculated by utilizing the data provided in Table 6.

^{‡‡} The dominant vector species of Butelgut at the time the field measurements were taken was *An. punctulatus*, [9]. The data provided in [49] and appearing in row thirteen column one of Table A.3 in [12, p. 19] corresponds to *An. punctulatus* activity in Papua New Guinea. Using this data, it follows that $\Omega_L = 7.1$. Therefore, the average daily *An. punctulatus* mosquito mortality rate is $\xi_M = 1/7.1 \approx 0.14$.

[§] As previously demonstrated, the asymptomatic human to susceptible mosquito transmission probability is assumed to be $\beta_A = 0.048$.

^{§§} Since Butelgut is a high transmission area, we let $\beta_Y = 0.48$.

^{§§§} By dividing the value in row two column six of Table 3 in [34, p. 541] by Ω_L , it follows that $\beta_M = 0.042/7.1 \approx 0.006$.

^{*} The average duration of the intermediate host latent period is taken to be $\gamma = 1/\tilde{\gamma} = 1/9.5 \approx 0.11$. The parameter value $\tilde{\gamma}$ is taken from row three column one in Table A.7 in [12, p. 21]. The average value is then chosen, i.e. $\gamma \approx 9.5$. The original parameter source is [46].

^{**} By using the entry in row eight column five of Table 2 in [34, p. 539], it follows that the average duration of the definitive host latent period is $\tau = 1/9.6 \approx 0.1$.

^{***} By the data provided in [26], it follows that $\delta = 37.57/365.25/100,000 \approx 1.03 \times 10^{-6}$.

[#] By using the data in row one column six of Table 3 in [34, p. 541], we have that $\sigma = 0.99/\Omega_L = 0.99/7.1 \approx 0.14$.

[¶] Due to similar reasoning as above, the recovery rate pertaining to asymptomatic individuals is assumed to be $\lambda_{AR} = 0.6$.

^{¶¶} The average of the entries appearing in row four column one of Table A.9 in [12, p. 21] is selected, so that $\Omega_I = 18$. Therefore, $\lambda_{YR} \approx \lambda = 1/\Omega_I = 1/18 \approx 0.06$. The original source of the parameter value is [5].

^{||} As Butelgut is a high transmission area, the temporary immunity loss rate is taken to be $\lambda_{RS} = 1/(5)365.25 \approx 5.48 \times 10^{-4}$.

^{|||} This baseline assumption is due to the fact that the population under consideration is *A-dominant*.

REFERENCES

- [1] Central Intelligence Agency. *The World Factbook 2014-15*. Government Printing Office, 2015.
- [2] Ricardo Águas, Lisa J White, Robert W Snow, and M Gabriela M Gomes. Prospects for malaria eradication in sub-saharan africa. *PLoS One*, 3(3):e1767, 2008.
- [3] Folashade B Agusto, Sara Y Del Valle, Kbenesh W Blayneh, Calistus N Ngonghala, Maria J Goncalves, Nianpeng Li, Ruijun Zhao, and Hongfei Gong. The impact of bed-net use on malaria prevalence. *Journal of theoretical biology*, 320:58–65, 2013.
- [4] Fabiana P Alves, Rui R Durlacher, Maria J Menezes, Henrique Krieger, Luiz H Pereira Silva, and Erney P Camargo. High prevalence of asymptomatic plasmodium vivax and plasmodium falciparum infections in native amazonian populations. *The American Journal of Tropical Medicine and Hygiene*, 66(6):641–648, 2002.
- [5] PB Bloland and HA Williams. Roundtable on the demography of forced migration, and joseph l. mailman school of public health. program on forced migration and health. *Malaria control during mass population movements and natural disasters*, 2002.
- [6] J Teun Bousema, Louis C Gouagna, Chris J Drakeley, Annemieke M Meutstege, Bernard A Okech, Ikupa NJ Akim, John C Beier, John I Githure, and Robert W Sauerwein. Plasmodium falciparum gametocyte carriage in asymptomatic children in western kenya. *Malaria journal*, 3(1):18, 2004.
- [7] Mark F Boyd. Epidemiology: factors related to the definitive host. *Malariaiology*, 1:608–697, 1949.
- [8] Leonard Jan Bruce-Chwatt et al. *Essential malariology*. William Heinemann Medical Books Ltd., 1980.
- [9] TR Burkot, PM Graves, R Paru, RA Wirtz, and PF Heywood. Human malaria transmission studies in the anopheles punctulatus complex in papua new guinea: Sporozoite rates, inoculation rates, and sporozoite densities. *The American journal of tropical medicine and hygiene*, 39(2):135–144, 1988.
- [10] Richard Carter and Kamini N Mendis. Evolutionary and historical aspects of the burden of malaria. *Clinical microbiology reviews*, 15(4):564–594, 2002.
- [11] Carlos Castillo-Chavez and Baojun Song. Dynamical models of tuberculosis and their applications. *Mathematical biosciences and engineering*, 1(2):361–404, 2004.
- [12] Nakul Chitnis, James M Hyman, and Jim M Cushing. Determining important parameters in the spread of malaria through the sensitivity analysis of a mathematical model. *Bulletin of mathematical biology*, 70(5):1272–1296, 2008.
- [13] Vivian L Clark and James A Kruse. Clinical methods: the history, physical, and laboratory examinations. *JAMA*, 264(21):2808–2809, 1990.
- [14] William E Collins. Plasmodium knowlesi: A malaria parasite of monkeys and humans*. *Annual review of entomology*, 57:107–121, 2012.
- [15] José Rodrigues Coura, Martha Suárez-Mutis, and Simone Ladeia-Andrade. A new challenge for malaria control in brazil: asymptomatic plasmodium infection-a review. *Memórias do Instituto Oswaldo Cruz*, 101(3):229–237, 2006.
- [16] Alan F Cowman, Drew Berry, and Jake Baum. The cellular and molecular basis for malaria parasite invasion of the human red blood cell. *The Journal of cell biology*, 198(6):961–971, 2012.
- [17] MH Craig, RW Snow, and D Le Sueur. A climate-based distribution model of malaria transmission in sub-saharan africa. *Parasitology today*, 15(3):105–111, 1999.
- [18] Zulma Milena Cucunubá, Ángela Patricia Guerra, Sonia Judith Rahirant, Jorge Alonso Rivera, Liliana Jazmín Cortés, and Rubén Santiago Nicholls. Asymptomatic plasmodium spp. infection in tierralta, colombia. *Memórias do Instituto Oswaldo Cruz*, 103(7):668–673, 2008.
- [19] Matthias P Dal-Bianco, Kai B Köster, Ulrich D Kombila, Jürgen FJ Kun, Martin P Grobusch, Ghyslain Mombo Ngoma, Pierre B Matsiegui, Christian Supan, Carmen L Ospina Salazar, Michel A Missinou, et al. High prevalence of asymptomatic plasmodium falciparum infection in gabonese adults. *The American journal of tropical medicine and hygiene*, 77(5):939–942, 2007.
- [20] Peter H David, Marcel Hommel, Louis H Miller, Iroka J Udeinya, and Lynette D Oligino. Parasite sequestration in plasmodium falciparum malaria: spleen and antibody modulation of cytoadherence of infected erythrocytes. *Proceedings of the National Academy of Sciences*, 80(16):5075–5079, 1983.
- [21] Ana Lucia SS de Andrade, Celina MT Martelli, Renato M Oliveira, Jorge R Arias, Fabio Zicker, and Lorin Pang. High prevalence of asymptomatic malaria in gold mining areas in brazil. *Clinical Infectious Diseases*, 20(2):475–475, 1995.

- [22] Alberto d'Onofrio. Stability properties of pulse vaccination strategy in seir epidemic model. *Mathematical biosciences*, 179(1):57–72, 2002.
- [23] Denise L Doolan, Carlota Dobaño, and J Kevin Baird. Acquired immunity to malaria. *Clinical microbiology reviews*, 22(1):13–36, 2009.
- [24] CC Draper. Observations on the infectiousness of gametocytes in hyperendemic malaria. *Transactions of the Royal Society of Tropical Medicine and Hygiene*, 47(2):160–165, 1953.
- [25] RA Eke, LN Chigbu, and W Nwachukwu. High prevalence of asymptomatic plasmodium infection in a suburb of aba town, nigeria. *Ann Afr Med*, 5(1):42–5, 2006.
- [26] World Life Expectancy. Malaria death rate per 100,000, 2016. URL <http://www.worldlifeexpectancy.com/cause-of-death/malaria/by-country/>.
- [27] Raymond C Fabec and Gestur Ólafsson. *Non-Commutative Harmonic Analysis*. 2014.
- [28] João AN Filipe, Eleanor M Riley, Christopher J Drakeley, Colin J Sutherland, and Azra C Ghani. Determination of the processes driving the acquisition of immunity to malaria using a mathematical transmission model. 2007.
- [29] Michael T Gillies and Tony J Wilkes. A study of the age-composition of populations of anopheles gambiae giles and a. funestus giles in north-eastern tanzania. *Bulletin of entomological research*, 56(02):237–262, 1965.
- [30] Loukas Grafakos. *Classical fourier analysis*, volume 2. Springer, 2008.
- [31] PM Graves, TR Burkot, AJ Saul, RJ Hayes, and R Carter. Estimation of anopheline survival rate, vectorial capacity and mosquito infection probability from malaria vector infection rates in villages near madang, papua new guinea. *Journal of Applied Ecology*, pages 134–147, 1990.
- [32] Sydney Price James et al. Malaria at home and abroad. *Malaria at Home and Abroad.*, 1920.
- [33] Guckenheimer John and Holmes Philip. Nonlinear oscillations, dynamical systems, and bifurcations of vector fields. *Applied mathematical sciences*, 42, 1997.
- [34] Gerry F Killeen, F Ellis McKenzie, Brian D Foy, Catherine Schieffelin, Peter F Billingsley, and John C Beier. A simplified model for predicting malaria entomologic inoculation rates based on entomologic and parasitologic parameters relevant to control. *The American journal of tropical medicine and hygiene*, 62 (5):535–544, 2000.
- [35] R Koch. Dritter bericht über die tätigkeit der malaria-expedition (schluss aus no. 17.). *DMW-Deutsche Medizinische Wochenschrift*, 26(18):296–297, 1900.
- [36] Robert Koch. Dritter bericht über die tätigkeit der malariaexpedition. 2010.
- [37] Dolie D Laishram, Patrick L Sutton, Nutan Nanda, Vijay L Sharma, Ranbir C Sobti, Jane M Carlton, and Hema Joshi. The complexities of malaria disease manifestations with a focus on asymptomatic malaria. *Malaria journal*, 11(1):1, 2012.
- [38] Dolie D Laishram, Patrick L Sutton, Nutan Nanda, Vijay L Sharma, Ranbir C Sobti, Jane M Carlton, Hema Joshi, et al. The complexities of malaria disease manifestations with a focus on asymptomatic malaria. *Malar J*, 11(1):29, 2012.
- [39] Christian Lengeler et al. Insecticide-treated bed nets and curtains for preventing malaria. *Cochrane Database Syst Rev*, 2(2), 2004.
- [40] Michael Y Li and James S Muldowney. Global stability for the seir model in epidemiology. *Mathematical biosciences*, 125(2):155–164, 1995.
- [41] Michael Y Li, John R Graef, Liancheng Wang, and János Karsai. Global dynamics of a seir model with varying total population size. *Mathematical biosciences*, 160(2):191–213, 1999.
- [42] Kim A Lindblade, Laura Steinhardt, Aaron Samuels, S Patrick Kachur, and Laurence Slutsker. The silent threat: asymptomatic parasitemia and malaria transmission. 2013.
- [43] George Macdonald et al. The epidemiology and control of malaria. *The Epidemiology and Control of Malaria.*, 1957.
- [44] GG MacPherson, MJ Warrell, NJ White, SORNCHAI Looareesuwan, and DA Warrell. Human cerebral malaria. a quantitative ultrastructural analysis of parasitized erythrocyte sequestration. *The American journal of pathology*, 119(3):385, 1985.
- [45] Sandip Mandal, Ram Rup Sarkar, and Somdatta Sinha. Mathematical models of malaria-a review. *Malar J*, 10(202):10–1186, 2011.
- [46] L Molineaux and G Gramiccia. The garki projectworld health organization, 1980.
- [47] L Molineaux, GR Shidrawi, JL Clarke, JR Boulzaguet, and TS Ashkar. Assessment of insecticidal impact on the malaria mosquito's vectorial capacity, from data on the man-biting rate and age-composition. *Bulletin*

of the World Health Organization, 57(2):265, 1979.

[48] World Health Organization. *World Malaria Report 2015*. World Health Organization, 2015.

[49] W Peters and HA Standfast. Part ii. holoendemic malaria—the entomological picture. *Transactions of the Royal Society of Tropical Medicine and Hygiene*, 54(3):249–254, 1960.

[50] T Ponnudurai, AHW Lensen, GJA Van Gemert, MG Bolmer, and JHE Th Meuwissen. Feeding behaviour and sporozoite ejection by infected anopheles stephensi. *Transactions of the Royal Society of Tropical Medicine and Hygiene*, 85(2):175–180, 1991.

[51] Pariyaporn Roop-O, Wirawan Chinviriyasit, and Settapat Chinviriyasit. The effect of incidence function in backward bifurcation for malaria model with temporary immunity. *Mathematical biosciences*, 265:47–64, 2015.

[52] Ronald Rosenberg and Jarasporn Rungsiwongse. The number of sporozoites produced by individual malaria oocysts. *The American journal of tropical medicine and hygiene*, 45(5):574–577, 1991.

[53] Robert Sallares. *Malaria and Rome: A History of Malaria in Ancient Italy*. OUP Oxford, 2002.

[54] E Sergent and L Parrot. L’immunité, la prémunition et la résistance innée. *Archives de l’institut Pasteur d’Algérie*, 13:279–319, 1935.

[55] MW Service. Some basic entomological factors concerned with the transmission and control of malaria in northern nigeria. *Transactions of the Royal Society of Tropical Medicine and Hygiene*, 59(3):291–296, 1965.

[56] Stephen Smale, Morris W Hirsch, and Robert L Devaney. *Differential equations, dynamical systems, and an introduction to chaos*, volume 60. Academic Press, 2003.

[57] David L Smith and F Ellis McKenzie. Statics and dynamics of malaria infection in anopheles mosquitoes. *Malaria Journal*, 3(1):13, 2004.

[58] David L Smith, F Ellis McKenzie, Robert W Snow, and Simon I Hay. Revisiting the basic reproductive number for malaria and its implications for malaria control. *PLoS Biol*, 5(3):e42, 2007.

[59] Hal L Smith, Liancheng Wang, and Michael Y Li. Global dynamics of an seir epidemic model with vertical transmission. *SIAM Journal on Applied Mathematics*, 62(1):58–69, 2001.

[60] T Smith, JD Charlwood, J Kihonda, S Mwankusye, P Billingsley, J Meuwissen, E Lyimo, W Takken, T Teuscher, and Marcel Tanner. Absence of seasonal variation in malaria parasitaemia in an area of intense seasonal transmission. *Acta tropica*, 54(1):55–72, 1993.

[61] T Staalsoe and L Hviid. The role of variant-specific immunity in asymptomatic malaria infections: Maintaining. *Parasitology Today*, 14(5):177, 1998.

[62] RC Thomson et al. The malarial infectivity of an african village population to mosquitoes (anopheles gambiae). a random xeno-diagnostic survey. *American Journal of Tropical Medicine and Hygiene*, 6(6): 971–979, 1957.

[63] Pauline Van den Driessche and James Watmough. Reproduction numbers and sub-threshold endemic equilibria for compartmental models of disease transmission. *Mathematical biosciences*, 180(1):29–48, 2002.

[64] Joseph M Vinetz and Robert H Gilman. Plasmodium vivax and p. falciparum infections among parasitemic individuals within populations of indigenous amer-indians in the western brazilian amazon region. a high rate of asymptomatic p. falciparum prevalence has been well known to occur in areas of high malaria transmission in africa. *Am. J. Trop. Med. Hyg*, 66(6):639–640, 2002.

DEPARTMENT OF MATHEMATICS, UNIVERSITY OF GEORGIA, ATHENS, GA 30602

DEPARTMENT OF MATHEMATICS, UNIVERSITY OF GEORGIA, ATHENS, GA 30602